Molecular chaperones in the assembly of α-Synuclein and Parkinson's Disease

Samantha Pemberton

UNIVERSITÉ PARIS-SUD 11

ÉCOLE DOCTORALE :

INNOVATION THÉRAPEUTIQUE : DU FONDAMENTAL A L'APPLIQUÉ

PÔLE : INGÉNIERIE DES PROTÉINES ET CIBLES THÉRAPEUTIQUES

DISCIPLINE :

4101459 STRUCTURE, FONCTION ET INGÉNIERIE DES PROTÉINES

ANNÉE 2011 SÉRIE DOCTORAT N° 11136

THÈSE DE DOCTORAT

soutenue le 09/12/2011

par

Samantha PEMBERTON

Molecular chaperones in the assembly of α-Synuclein and Parkinson's Disease

Directeur de thèse : Ronald MELKI Directeur de Recherche, CNRS

Composition du jury :

Président du jury :	Herman VAN TILBEURGH	Enseignant-Chercheur, Université Paris Sud
Rapporteurs :	Ellen NOLLEN	Directeur de Recherche
	Luc BUÉE	Directeur de Recherche, Inserm
Examinateurs :	Anja BÖCKMANN	Directeur de Recherche, CNRS

Les chaperons moléculaires dans l'assemblage de l'α-Synucléine et la maladie de Parkinson

La formation et le dépôt de fibres d'α-Synucléine dans le cerveau humain sont à l'origine de la maladie de Parkinson. Cette thèse documente le rôle de deux chaperons moléculaires dans l'assemblage en fibres de l'α-Syn : Hsc70 (protéine de choc thermique constitutivement exprimée chez l'Homme) et Ssa1p (son équivalent chez la levure). Le but était d'élargir le catalogue d'effets connus des chaperons moléculaires sur α-Syn, pour éventuellement ouvrir la voie à des applications thérapeutiques. Nous avons montré que Hsc70 inhibe l'assemblage de l'α-Syn en fibres, en se liant avec une forte affinité à la forme soluble de l'α-Syn. Hsc70 se lie préférentiellement aux fibres de l'α-Syn, et cette liaison a un effet cytoprotecteur puisqu'elle rend les fibres moins toxiques pour les cellules de mammifères en culture. Pareillement à Hsc70, Ssa1p inhibe l'assemblage de l'α-Syn en fibres, et a une plus forte affinité pour les fibres que pour la forme soluble de l'α-Syn. En revanche, la liaison de Ssa1p aux fibres de l'α-Syn n'a pas d'effet cytoprotecteur, sûrement due aux différences entre les séquences du site de liaison aux peptides des deux chaperons moléculaires, qui fait que Ssa1p a une affinité plus faible que Hsc70 pour les fibres d'α-Syn. Nous avons fixé le complexe entre Ssa1p et α-Syn avec des agents pontants, pour ensuite établir une carte du site d'interaction entre les deux protéines en utilisant la spectrométrie de masse. Ceci est indispensable si un « mini » Ssa1p, constitué des éléments nécessaires et suffisants sera utilisé comme agent thérapeutique pour réduire la toxicité des fibres d'α-Syn.

Mot clés: chaperons moléculaires; co-chaperons; protéine de choc thermique; maladie de Parkinson; assemblage des protéines; repliement des protéines; α-Synucléine; fibres; Hsc70; oligomères; Ssa1p.

Molecular chaperones in the assembly of α-Synuclein and Parkinson's disease

The formation and deposition of α-Synuclein fibrils in the human brain is at the origin of Parkinson's disease. The objective of my thesis was to document the role of two molecular chaperones on the assembly of α-Syn into fibrils: Hsc70, a constitutively expressed human heat shock protein, and Ssa1p, its yeast equivalent. The aim was to expand the catalogue of known effects of molecular chaperones on the PD implicated protein, which could have therapeutic significance. We showed that Hsc70 inhibits the assembly of α-Syn into fibrils, by binding with high affinity to the soluble form of α-Syn. We documented that Hsc70 binds preferentially to α-Syn fibrils and that this binding has a cytoprotective effect, as it renders the fibrils less toxic to cultured mammalian cells. Similarly to Hsc70, Ssa1p inhibits the assembly of α-Syn into fibrils, and has a higher affinity for fibrils than for the soluble form of α-Syn. On the other hand, binding of Ssa1p to α-Syn fibrils does not have a cytoprotective effect, almost certainly due to differences in the amino acid sequences of the peptide binding sites of the two molecular chaperones, which mean that Ssa1p has a lower affinity than Hsc70 for α-Syn fibrils. We stabilized the complex between Ssa1p and α-Syn using chemical cross-linkers, to then map the interaction site between the two proteins. This is indispensable if a "mini" Ssa1p, comprised of only what is necessary and sufficient of Ssa1p, is to be used as a therapeutic agent to decrease the toxicity of α-Syn fibrils. A therapeutic agent based on exogenous protein Ssa1p is less likely to trigger an autoimmune response than for example the endogenous protein Hsc70.

Key words : Molecular chaperones; Co-chaperones; Heat shock protein; Parkinson's disease; Protein assembly; Protein folding; α-Synuclein; Fibrils; Hsc70; Oligomers; Ssa1p.

To Emily

"Live! Live the wonderful life that is in you! Let nothing be lost upon you.
Be always searching for new sensations. Be afraid of nothing."

— Oscar Wilde

Acknowledgements

*« **La plus grave maladie du cerveau, c'est de réfléchir** »*

-Les Shadoks

Firstly I would like to thank my examiners Ellen Nollen, Luc Buée and Anja Böckmann for taking the time to read this thesis and judge its suitability.

*Ronald: I count myself lucky to have been one of your students. It has been a pleasure. Thank you **so** much for your time, inspiration, advice, ideas, help, support, for nudging me in the right direction – the list could go on – but most of all for making these three years joyful ones with your unique sense of humour.*

To past and present members of Équipe 05 with whom I have laughed over many, many cups of Earl Grey over the last three years; Karine, Virginie, Mehdi, Luc, Elodie, Yannick, Laura, Kika, Céline and Jonathan, to name but a few. 10 o'clock tea-time was a vital part of my day; indeed I was lucky to join a team in France with such a tradition! Thank you for all your help in the laboratory and for answering my silly questions, but thank you also for being guinea-pigs to my "first attempt" sponge/ cheese/ cupcakes at various celebratory "pots", and for devouring with gusto. Amongst the good memories lurks a bad one, but at least you will all check hotel beds thoroughly before going to sleep now!!

A big thank you to my parents and to my sisters Melanie and Charlie for the continual invaluable support sent across the Channel via Skype, and for coming to visit in Paris.

*MERCI to all my Parisian friends, most especially Julien, my coloc' Julie and Aurelie, for emptying my scientific mind at the weekends and filling it with laughter and **unforgettable** memories. Julien, I couldn't have done it without you, your encouraging "non-pep talks" helped me through some tough times and gave me confidence in myself, not to mention your perfect English and French correction skills! ;) Special thanks to Tak' One members Romain H, Romain P, Séb and Paul for making me a rock star for one night: ♬Branchez la guitare♬ !!*

Enfin, merci à toi Piou (et toute ta grande famille y compris Louise et César), tu m'as aidée à tenir le coup. Merci de m'avoir coachée, supportée, soutenue et de m'avoir changé les idées à ton façon.

Last but not least, Emily, sorely missed but still an inspiration.

TABLE OF CONTENTS

List of Figures

List of Tables

List of Abbreviations

Aβ	Amyloid beta
AD	Alzheimer's disease
α-Syn	α-Synuclein
BSE	Bovine spongiform encephalopathy (or "mad cow" disease)
CD	Circular dichroism
CJD	Creutzfeldt-Jakob disease
CF	Cystic Fibrosis
CFTR	Cystic Fibrosis transmembrane conductance regulator
CLIPS	Chaperones linked to protein synthesis
DLB	Dementia with Lewy bodies
FFI	Fatal familial insomnia
GSS	Gerstmann-Sträussler-Scheinker syndrome
Hip	Hsp70-interacting protein
Hsc	Constitutive heat shock protein
Hsp	Heat shock protein
LB	Lewy body
LN	Lewy neurite
LUV	Large unilamellar vesicles
NAC	Non amyloid component
NBD	Nucleotide binding domain (of Hsp70s)
NEF	Nucleotide exchange factor
PBD	Peptide binding domain (of Hsp70s)
PD	Parkinson's Disease
PolyQ	Polyglutamine
ROS	Reactive oxygen species
SN	*Substantia nigra*
ThioT	Thioflavin T
vCJD	New variant CJD
WT	Wildtype

Résumé

L'α-Synucléine (α-Syn) est la protéine principalement incriminée dans la maladie de Parkinson. Une forme agrégée fibrillaire de cette protéine est le constituant principal des corps de Lewy, retrouvés dans le cerveau des patients atteints de la maladie de Parkinson. Les corps de Lewy renferment également des chaperons moléculaires, généralement impliqués dans le repliement des protéines. Les chaperons moléculaires jouent un rôle crucial dans les situations de stress. Ils sont appelés de ce fait protéines de stress ou de choc thermiques (HSPs), et sont classés en fonction de leur poids moléculaire (e.g. Hsp40, Hsp60, Hsp70, Hsp90, Hsp100 et les « petites » Hsps de moins de 35 kilodaltons). La présence de HSPs dans les corps de Lewy suggère qu'elles jouent un rôle important dans la progression de la maladie de Parkinson. Ce rôle a ainsi été examiné pour plusieurs chaperons moléculaires. Hsp70 inhibe l'assemblage de l'αSyn en fibres et diminue la toxicité associée à l'α-Syn *in vitro* et *in vivo.* Hsp90 semble avoir un effet inverse à celui de Hsp70 car elle favorise la formation de fibres d'αSyn dans de conditions physiologiques *in vitro*. À ce jour, Hsp104, un chaperon de la levure sans homologue connu chez l'Homme, est le seul chaperon moléculaire connu qui semblerait capable de désassembler des fibres d'α-Syn. Enfin, les petits chaperons moléculaires Hsp27 et αB-crystallin ont des effets protecteurs puisque le premier diminue la mort cellulaire induite par l'αSyn *in vivo*, alors que le deuxième inhibe fortement l'assemblage de l'αSyn *in vitro*.

L'objectif de ma thèse était de documenter le rôle de deux autres chaperons moléculaires dans l'assemblage en fibres de l'αSyn : Hsc70 (protéine de choc thermique constitutivement exprimée chez l'Homme) et Ssa1p (son équivalent chez la levure). Le but était d'élargir le « catalogue » d'effets connus des chaperons moléculaires sur cette protéine impliquée dans la maladie de Parkinson, et aussi d'ouvrir la voie à des applications thérapeutiques. Nous voulions non seulement documenter l'effet de Hsc70 et Ssa1p sur l'assemblage de l'α-Syn, mais aussi caractériser l'interaction de l'α-Syn avec ces chaperons moléculaires à l'échelle moléculaire.

J'ai montré que Hsc70 inhibe l'assemblage de l'α-Syn en fibres, en se liant avec une forte affinité à la forme soluble de l'α-Syn. Cet effet a été suivi par la fixation d'un fluorophore extrinsèque spécifique des fibres (thioflavin T), par microscopie électronique et par la mesure de la résistance des assemblages de l'α-Syn au détergent (SDS). Nous avons constaté que Hsc70 se lie préférentiellement aux fibres de l'α-Syn, avec une constante de dissociation cinq fois plus forte pour les fibres que pour la forme soluble. La liaison de Hsc70 aux fibres a un effet cytoprotecteur puisqu'elle rend les fibres moins toxiques pour cellules de mammifères en culture. Des expériences d'ultracentrifugation analytique réalisées en mélangeant l'α-Syn et l'Hsc70 révèlent la formation d'un complexe spécifique entre α-Syn et Hsc70. Ce travail a été publié dans la revue « The Journal of Biological Chemistry » (Pemberton, Madiona et al., 2011), et élaboré avec un addendum dans la revue « Communicative and Integrative Biology » (Pemberton, 2012).

J'ai ensuite cherché à caractériser l'interaction de l'α-Syn avec Ssa1p. Pareillement à Hsc70, Ssa1p inhibe l'assemblage de l'α-Syn en fibres, et a une plus forte affinité pour les fibres que pour la forme soluble de l'α-Syn. En revanche, la liaison de Ssa1p aux fibres d'α-Syn n'a pas d'effet cytoprotecteur. Cette particularité est sûrement due aux différences observées entre les séquences du site de liaison aux peptides des deux chaperons moléculaires, qui fait que Ssa1p a une affinité plus faible que Hsc70 pour les fibres d'α-Syn. Nous avons fixé le complexe entre Ssa1p et α-Syn à l'aide d'agents pontants, pour ensuite utiliser la spectrométrie de masse pour établir une carte du site d'interaction entre les deux protéines. Celle-ci est une phase indispensable pour permettre une utilisation thérapeutique d'un « minichaperon », constitué des éléments nécessaire et suffisant de Ssa1p, après modification pour améliorer l'affinité de Ssa1p pour les fibres d'α-Syn, pour réduire la toxicité des fibres d'α-Syn. Basé sur une protéine exogène – Ssa1p – le minichaperon présenterait moins de risque de développer une réaction auto-immune comme par exemple pour la protéine endogène Hsc70.

Enfin, j'ai contribué à un travail publié dans la revue « FEBS Journal » (Redeker, Bonnefoy et al., 2010), ayant pour but de caractériser l'interaction de Ssa1p avec Ure2p, une

protéine prion de levure. Pour ce travail, j'ai exprimé, produit, et purifié la protéine Ssa1 utilisé dans ces études.

Ce travail de thèse pourrait être poursuivi par des études structurales sur l'interaction de l'α-Syn soluble avec Hsc70 (par spectrométrie de masse supramoléculaire), et de l'α-Syn fibrillaire avec Hsc70 (par la spectrométrie de résonance magnétique de l'état solide). Ces travaux permettront d'élargir nos connaissances sur les mécanismes d'inhibition de l'agrégation de l'α-Syn et de « pacification » des fibres d'α-Syn par les chaperons moléculaires, et leur conséquence sur la maladie de Parkinson.

Introduction

Proteinopathies

What are the proteinopathies?

The proteinopathies are a family of human diseases caused by toxic, aggregation-prone proteins and characterized by the presence of protein aggregates in affected cells. There is a wide range of neurological disorders which result from specific protein accumulation, for example Alzheimer's disease (AD), the most common adult-onset neurodegenerative disease. A comprehensive list of aggregation prone proteins involved in neurological human proteinopathies is presented in Table 1, together with the diseases they are responsible for.

Table 1. Neurological human proteinopathies, adapted from (Walker and LeVine, 2000).

Aggregation prone protein	**Disease**
α-Synuclein (α-Syn)	Parkinson's disease Alzheimer's disease Diffuse Lewy Body disease Incidental Lewy body disease Multiple System Atrophy Amyotrophic Lateral Sclerosis
β-amyloid (Aβ)	Alzheimer's disease Cerebral Aβ Angiopathy
Superoxide dismutase 1 (SOD-1)	Familial ALS
Tau protein	Alzheimer's disease Frontotemporal dementia-chromosome 17 Progressive Supranuclear Palsy Familial Multiple System Tauopathy Corticobasal degeneration Pick's disease Postencephalitic parkinsonism Parkinsonism-dementia complex of Guam
Polyglutamine inserts (expanded CAG repeats)	Huntington disease Spinocerebellar ataxia type 1, 3 and 7 Dentatorubropallidoluysian atrophy Spinal and bulbar muscular atrophy
Prion protein	Creutzfeldt-Jakob disease Gerstmann-Sträussler-Scheinker disease Kuru Fatal familial insomnia
ABri	Familial British Dementia
ADan	Familial Danish Dementia
cystatin C	Familial Cerebral Haemorrhage with Amyloidosis (Icelandic)
neuroserpin	Familial Encephalopathy with Neuroserpin Inclusion Bodies
transthyretin	Familial Amyloidotic Neuropathy

In addition to the neurological proteinopathies, there are numerous systemic proteinopathies such as Type II diabetes and Cystic Fibrosis (CF), caused by the aggregation of misfolded Islet amyloid polypeptide (IAPP) and Cystic Fibrosis transmembrane conductance regulator (CFTR) respectively.

Physiological loss- or toxic gain-of-function?

The aggregation of CFTR is triggered by an inherited missense mutation, and is an example of a proteinopathy whereby the protein aggregates are not toxic, but mean that there is less functional protein available for normal activity. CFTR is expressed in airway epithelial cells where it acts as a phosphorylation-regulated chloride ion channel and a regulator of channels and transporters. More specifically, activation of CFTR leads to the concomitant inhibition of the epithelial sodium ion channel, which does not happen when CFTR is absent or dysfunctional (Stutts, Canessa et al., 1995; Mall, Bleich et al., 1998). It is thought that the loss of chloride secretion and the increase in sodium ion absorption reduce the thickness of the airway surface liquid which overlies the airway epithelia, impairing mucociliary clearance (Matsui, Grubb et al., 1998). Alongside this, reduced amounts of CFTR might affect the physical properties of secreted mucus (Quinton, 2008), and prevent the secretion of anti-microbial factors by submucosal glands (Wine and Joo, 2004). All of these features contribute to the deposition of thick, dehydrated mucus which is the perfect environment for persistent bacterial growth, triggering chronic inflammation and ultimately leading to organ failure in the CF lung.

Other proteinopathies result from a toxic gain-of-function mechanism where the non-native oligomers and/ or thread-like structures called fibrils are toxic to cells. Experimentally, a number of mechanisms describing how these aberrant aggregates perturb cellular homeostasis have been defined, and are summarized in Fig. 1. Protein aggregates may wreak havoc within cells by sequestering normal cellular proteins, either indirectly due to their ‘sticky’ nature, or as in polyglutamine (polyQ) diseases, where aggregates sequester DNA binding proteins, thus altering gene transcription. As well as this, aggregates could be

toxic to cells because they induce apoptosis, for instance by activating the caspase 3 pathway, as seen in polyQ diseases and AD. Aggregates could disturb normal synaptic function if they are present in cellular processes, by literally blocking the way. Finally, protein aggregation may provoke oxidative stress within cells, which in turn encourages protein aggregation, resulting in a distressing vicious cycle (Wolozin and Behl, 2000; Taylor, Hardy et al., 2002; Selkoe, 2003).

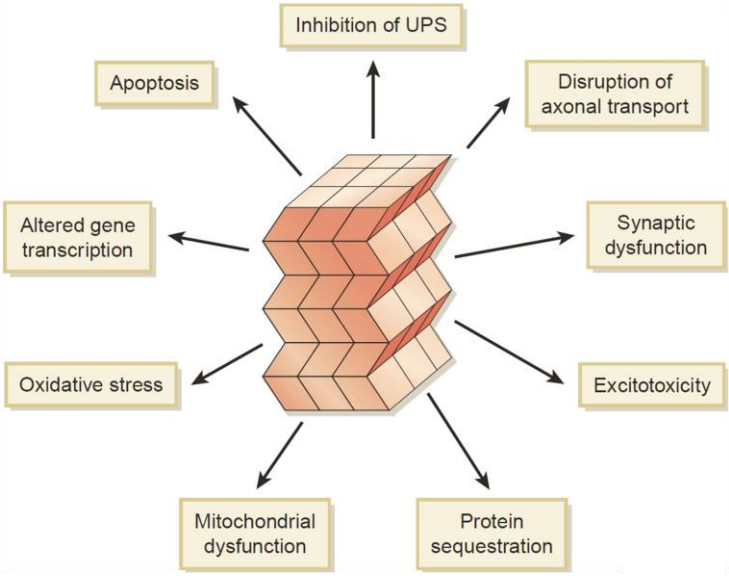

Figure 1. Potential mechanisms of toxicity of misfolded or aggregated proteins (depicted schematically in centre). Figure from (Forman, Trojanowski et al., 2004).

It is more than likely a combination of a loss of physiological function of the disease-implicated protein, and a gain of toxic function of its protein aggregates, that contribute to the pathological mechanisms of proteinopathies.

General mechanism of protein aggregation

There are a vast number of devastating proteinopathic disorders, each characterized by the specific implicating protein (for example α-Syn or CFTR) and the cellular location of this protein (synaptic terminals vs. airway epithelia, respectively). However, the general mechanism at the origin of most neurological and systemic proteinopathies is believed to be the same, and is summarized in Fig. 2. During the protein biosynthetic pathway, or when

proteins unfold from their native states, distinct folding intermediates arise. Some of these folding intermediates are able to self-associate into non-native oligomers, which are then able to elongate rapidly by interacting through two interfaces at any one time with two different neighbouring molecules (i.e. longitudinally as shown in Fig. 2, and laterally). As monomers are incorporated, the oligomers become more and more stable, allowing aggregates to build up. Growth is unlimited, because as one monomer is incorporated, a new binding site for yet another monomer is created. If the growing oligomer were to break, for instance as a result of Brownian movement (Brown, 1828), severing, or disaggregating factors, new stable nuclei would be generated which in effect would amplify the aggregation process as the number of possible monomer binding sites would increase (Brundin, Melki et al., 2010).

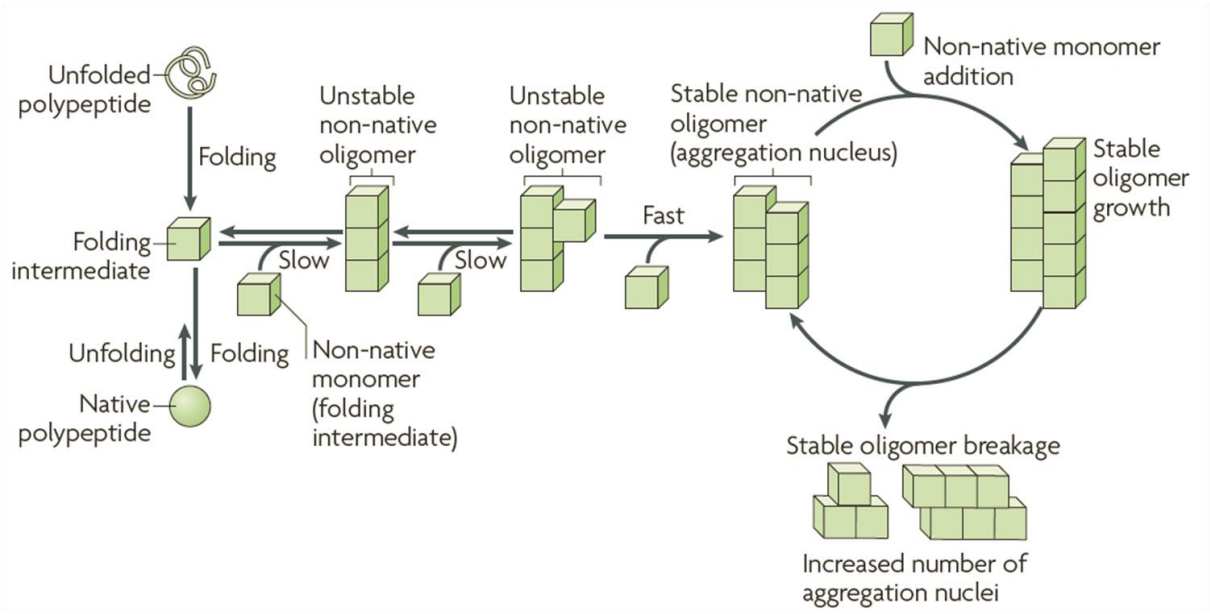

<u>Figure 2.</u> Basic mechanisms of protein aggregation. Figure from (Brundin, Melki et al., 2010).

Four of the proteinopathies mentioned in Table 1, Creutzfeldt-Jakob disease (CJD), Gerstmann-Sträussler-Scheinker syndrome (GSS), Kuru and Fatal familial insomnia (FFI) are prion disorders. But what is a prion and are *all* proteinopathies prion-like disorders?

Prions

What is a prion?

A prion is defined as being an infectious protein (**Pro**teinaceous **In**fectious), thus named by Stanley B. Prusiner in the spring of 1982 (Prusiner, 1982) and for which he was presented with the 1997 Nobel Prize in Physiology or Medicine. It is an endogenous protein capable of populating conformational intermediates that have a propensity to assemble into highly ordered assemblies. These intermediates recruit the normal, cellular form of the prion protein, PrP^{C}, stimulate its conversion to the disease-causing isoform, PrP^{Sc}, and can grow indefinitely (Fig. 3). PrP^{C} are rich in α-helical content (40 %) with little β-sheet structure (3 %) whereas PrP^{Sc} have less α-helical content (30 %) and are rich in β-sheets (45 %) (Colby and Prusiner, 2011).

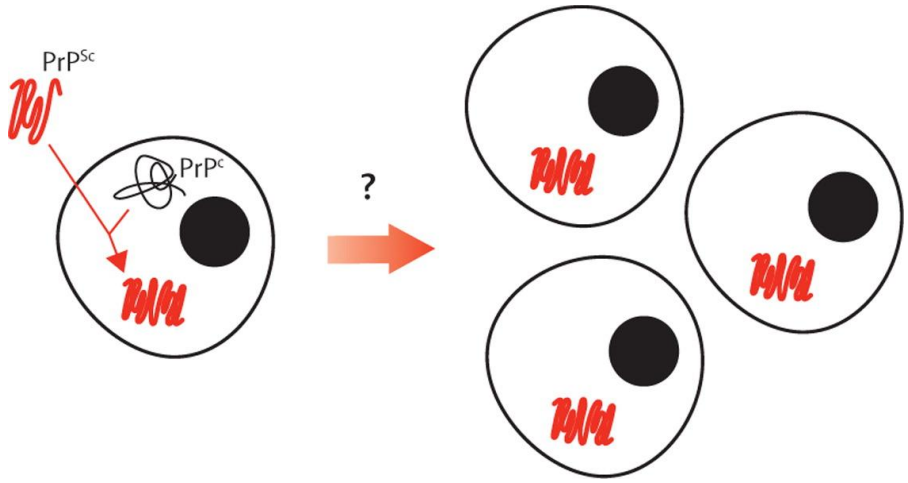

Figure 3. Model of templating and cell-to-cell transfer of prion proteins. Exogenous PrP^{Sc} (red), acting as a seed, recruits intracellular PrP^{C} (black) and converts its three-dimensional structure into an elongated PrP^{Sc}, thus extending the amyloid aggregate. The aggregates transfer intercellularly via an unknown mechanism. Figure from (Angot, Steiner et al., 2010).

History of the prion

Prion diseases (also known as Transmissible Spongiform Encephalopathies, TSEs) date back to the eighteenth century, when the first description of prion disease was reported in 1732 in a flock of sheep in Great Britain, and referred to as ‘rickets’ or ‘shakings’. Nearly a

century later, in 1821, the term ‘scrapie' was first used by Tessier to describe this sheep-afflicting illness, as the sheep would compulsively scrape their fleeces against rocks, trees and fences to relieve itching (Fig. 4).

Figure 4. Poll Dorset sheep with severe clinical signs of scrapie. Image from (Baylis, 2008).

In 1883, a Vet in Haute-Garonne, France, reported the behaviour of a cow to be like that of a scrapie infected sheep, possibly the first reporting of Bovine Spongiform Encephalopathy (BSE):

> *“I made a comparative analysis of the two afflictions and I found such a close a resemblance between them that I don't hesitate to affirm that I was dealing with the pruritic form of scrapie. In the species [cattle], the condition appeared to me to be hopeless; I also believed any medication was useless, and I advised the owner to butcher the steer that was sold for cheap [low class] meat” (Sarradet, 1883).*

In 1913, Hans Gerhard Creutzfeldt, a clinician trained in neuropathology and assistant to Alois Alzheimer, studied the case of a 22-year-old woman, Bertha Elschker, hospitalised with a rapidly deteriorating mental and neurological disorder. His report was not published until 1920, after World War One (Creutzfeldt, 1989). Upon publication, Alfons Jakob realised its importance, and soon after reported four more cases, of a “neuropathological syndrome associated with many disorders, rather than a disease” (Jakob, 1921). At the time no connection had been made between scrapie in sheep, goats and cows,

and what was witnessed by Creutzfeldt and Jakob. Had prion disease already crossed the species barrier from ovine to bovine to humans before science caught up and realised that it was a mistake to sell infected steer for cheap beef?

In 1936, Cuillé and Chelle showed that scrapie was caused by a non-conventional infectious agent localised in the brain and bone marrow. Most importantly they showed that upon injection of this agent, the disease could be transferred from one sheep to another (Cuillé, 1936), and then from sheep to goats in 1938 (Cuillé and Chelles, 1939).

In 1956, Gajdusek and Zigas went to investigate a disease affecting the Fore tribe of Papua New Guinea, which they had named “Kuru”, derived from the Fore word "kuria/ guria", 'to shake', and which affected eight times more women than men. Here, Gajdusek discovered the same cerebral lesions as those reported for scrapie, by Besnoit and Morel in 1898 (Besnoit C., 1898). Gajdusek concluded that Kuru was transmitted by the ritualistic consumption of deceased relatives, which was practiced by the Fore, and resulted in approximately 1,000 deaths in the first five years (1957–1961). Women were more affected than men as the cannibalism rituals reserved the brain tissue for the women, with muscles allotted to the men. Since the prohibition of cannibalism in the 1950’s, incidence of the disease declined steadily, but due to a long incubation period of more than 50 years, it lingered into the present century (Alpers, 2008). Gajdusek was awarded the 1976 Nobel Prize in Physiology or Medicine for demonstrating the infectious spread of a non-inflammatory degenerative disease in humans, after successfully transmitting Kuru to primates (Gajdusek, Gibbs et al., 1967), soon to be repeated with CJD (Gibbs, Gajdusek et al., 1968). In 1966, an important discovery showed that the infectious agent was resistant to ionisation and ultra-violet rays, suggesting the absence of DNA and RNA (Alper *et al,* 1966, 1967). Griffith then hypothesised that the infectious agent was purely proteinaceous (Griffith, 1967), and led to Prusiner’s proposition of the “prion” in 1982.

The first case of BSE was suspected in Great Britain in 1987 (Wells, Scott et al., 1987). By 1993, around 1000 new cases were being reported each week, leading to a full scale epidemic with around 50 % of all British cattle affected. Although not proven, it was

presumed that BSE (or “mad cow disease”) originated from the scrapie agent as a result of sheep offal being included in protein supplements fed to cattle (Brown, Will et al., 2001). It was not until a new variant of CJD (vCJD) affecting a younger human generation (average age 27 vs. 63 for sporadic CJD cases) appeared in 1994 that the real ‘prion panic’ began. The culprit? Contaminated beef which had found its way into the human food chain (Will, Ironside et al., 1996). To date, vCJD is responsible for 219 deaths worldwide with 175 in the UK alone (see the National Creutzfeldt–Jakob Disease Surveillance Unit website for vCJD data to March 2011).

Are all proteinopathies prion diseases?

In recent years, there has been significant growth in evidence, and subsequent discussion suggesting that proteinopathies other than the four caused by prion proteins (CJD, GSS, Kuru and FFI) in men, are in fact prion disorders. The distinguishing characteristic of prions is the manner in which they propagate within an infected organism, but also between individuals and animals. It has been shown that the proteins responsible for Parkinson’s, Alzheimer’s, and Huntington’s diseases and Amyotrophic Lateral Sclerosis (α-Synuclein (α-Syn), amyloid-beta (Aβ) and Tau, polyglutamine containing huntingtin (Htt), and superoxide dismutase 1 (SOD-1) respectively) do propagate between cells within an organism, thus sharing a common feature with prion proteins (Aguzzi and Rajendran, 2009; Angot and Brundin, 2009; Krammer, Schatzl et al., 2009; Olanow and Prusiner, 2009; Ren, Lauckner et al., 2009; Angot, Steiner et al., 2010; Brundin, Melki et al., 2010; Frost and Diamond, 2010; Hansen, Angot et al., 2010; Herrera, Tenreiro et al., 2011; Mougenot, Nicot et al., 2011; Munch and Bertolotti, 2011; Munch, O'Brien et al., 2011). The proteinopathy-causing proteins outlined in Table 1 are consequently classified as “prion-like” or prionoids (Aguzzi and Rajendran, 2009).

It remains to be seen whether these prion-like proteins are transmissible from one individual or animal to another, as seen for Kuru or scrapie, BSE and CJD. The only way to find out once and for all if α-Syn *et cetera* are also real prions would be to repeat the work of

Gajdusek and Gibbs with the proteinopathies in question. Alternatively, Parkinson-infected brains for dinner, anyone?

Parkinson's Disease

Parkinson's disease (PD) is the second most prevalent neurodegenerative disorder after AD. The disease occurs sporadically or idiopathically in the majority of cases (95 %), with a mean onset age of 70 years old (Tanner, 2003), and affecting approximately 1 % of 65 to 70 year olds, and 4 to 5 % of 85 year olds (Fahn, 2003). Sporadic PD has been associated with environmental risk factors such as pesticides and herbicides (Uversky, Li et al., 2001; Manning-Bog, McCormack et al., 2002; Uversky, Li et al., 2002), heavy metals (Riederer, Sofic et al., 1989; Zayed, Ducic et al., 1990; Dexter, Carayon et al., 1991; Hirsch, Brandel et al., 1991; Rybicki, Johnson et al., 1993; Altschuler, 1999; Gorell, Johnson et al., 1999; Gorell, Rybicki et al., 1999), and organic solvents (Seidler, Hellenbrand et al., 1996; Davis and Adair, 1999; Hageman, van der Hoek et al., 1999).

The other 5 % of PD patients have a genetically-linked form of the disease and mostly develop early-onset PD, with diagnosis generally before the age of 50 (Mizuno, Hattori et al., 2001; Van Den Eeden, Tanner et al., 2003). For example, several mutations in a gene called *PARK2* have been linked to autosomal-recessive PD with a mean onset age of around 28 years old (Kitada, Asakawa et al., 1998).

PD is a slow, progressive disorder that affects neuronal cells in the *substantia nigra* (SN, literally translating as 'black substance' due to its appearance) *pars compacta* of the brain, and whose symptoms are apparent after more than 70% of dopaminergic terminals and/ or neurons have been lost from this region. The SN contains around 400,000 neurons which project to the striatum (the output of which governs locomotor behaviour) and are responsible for producing the neurotransmitter dopamine. These neurons begin to pigment at birth and are fully pigmented at the age of 18 (melanoneuron cells). In an unaffected individual, the "normal" rate of nigral cell loss is around 2,400 per year. There is therefore a possibility that if an unaffected individual lived to approximately 120 years old, they would

develop PD. PD patients loose these cells at an accelerated rate. Although the cause and the pathway leading to nigral cell death are currently unknown, their progressive degeneration leads to a loss of connection with the striatum, and an overall decrease in the production of dopamine, which in turn could be responsible for the classical motor dysfunctions of PD: uncontrollable tremor, bradykinesia (slow movement) and rigidity, classically illustrated by Gowers in 1886 (Fig. 5).

Figure 5. Illustration of Parkinson's disease. Figure from (Gowers, 1886).

Treatment of PD motor symptoms with dopamine agonists is already well established, although there are still many problems with severe adverse-effects of the drugs used to date (Bonuccelli, Del Dotto et al., 2009). Although motor dysfunctions define the disease, and in 70 % of cases resting tremor is the first symptom of PD, various non-motor features are also seen, including autonomic dysfunction, cognitive and psychiatric changes, sensory symptoms, and sleep disturbances (Dickson, Fujishiro et al., 2009).

Pathological markers of Parkinson's disease: Lewy bodies

As well as the presentation of the classical motor symptoms, a neuropathological hallmark of Parkinson's disease is the presence of distinctive inclusion bodies that were first described by the neuropathologist Friedrich Lewy in 1912 (Lewy, 1912). They present in the form of granular aggregations and spherical pale bodies and/ or Lewy bodies (LBs, Fig. 6) in the somata of involved nerve cells (namely in surviving SN melanoneurons), and as spindle-like or thread-like Lewy neurites (LNs, Fig. 7) within cellular processes. LBs and LNs however are not only found within the SN, but can be seen in the cortex, amygdala, locus ceruleus, vagal nucleus, and the peripheral autonomic nervous system (Dickson, Fujishiro et al., 2009). The presence of inclusions in these non-motor areas could explain many of the non-motor symptoms of PD previously mentioned.

LBs and LNs are composed of aggregates of normal, misfolded and truncated proteins. The major constituent present is fibrillar α-Syn, the aggregation prone protein implicated in PD, as well as several other neurodegenerative diseases (Table 1). These diseases are united by the pathological presence of intracellular inclusions containing fibrillar α-Syn as the major component, and thus termed synucleinopathies. Other than fibrillar α-Syn, numerous other proteins are present, for instance ubiquitin (Kuzuhara, Mori et al., 1988), neurofilaments (Galvin, Lee et al., 1997), proteasome subunits (Ii, Ito et al., 1997) and molecular chaperones (Auluck, Chan et al., 2002).

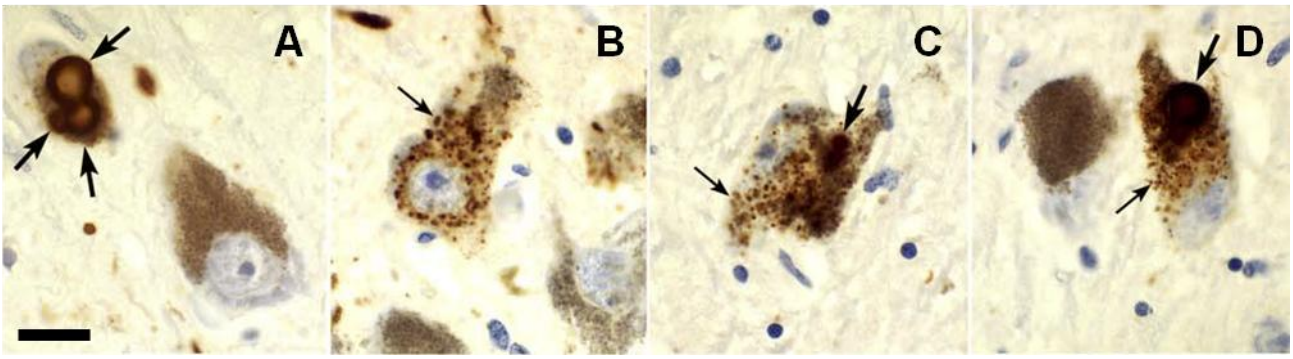

Figure 6. Dopaminergic melanoneurons in the substantia nigra, pars compacta. A, multiple LBs (arrows) fill a nerve cell directly next to a healthy melanoneuron. B-D, particulate α-Syn

(small arrows) aggregates to form LBs (larger arrows). In D, there is a normal melanoneuron without α-Syn (left) comparable with an unhealthy melanoneuron on the right. Bar (20 µm) in A applies to all. Figure adapted from (Braak, Ghebremedhin et al., 2004).

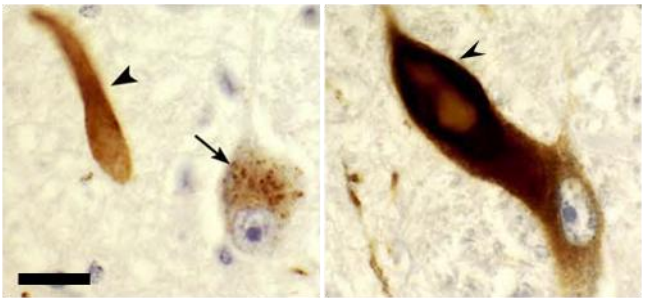

Figure 7. LNs seen in cholinergic neurons of the motor nucleus of the vagal nerve (arrow heads). α-Syn aggregates (arrow). Bar, 20 µm. Figure adapted from (Braak, Ghebremedhin et al., 2004).

Propagation of the pathological signs of Parkinson's disease

Braak and colleagues have long since described that α-Syn pathology spreads throughout the nervous system in a defined manner (Braak, Del Tredici et al., 2002; Braak, Del Tredici et al., 2003; Braak, Ghebremedhin et al., 2004). In 2007, they developed their findings and proposed the 'dual-hit hypothesis', suggesting that an unknown pathogen gains access to the brain in two ways: through the nose and the gut, i.e. through inhalation and swallowing. The pathogenic agent subsequently invades the brain by means of anterograde movement along unmyelinated axons from the olfactory epithelium to the temporal lobe, while simultaneously crossing the stomach wall to invade the distal fibers of the vagus nerve, then ascending in a retrograde direction to the vagal dorsal motor nucleus in the medulla (Fig. 8) (Hawkes, Del Tredici et al., 2007; Hawkes, Del Tredici et al., 2009). Supporting this hypothesis, LBs and LNs have been detected in cells of the olfactory bulb (Daniel and Hawkes, 1992; Braak, Del Tredici et al., 2003), along the olfactory pathway (Ubeda-Banon, Saiz-Sanchez et al., 2010) and in enteric nerve cell plexa of PD patients (Braak, de Vos et al., 2006). As well as this, a mouse model, where rotenone, a pesticide linked to PD (Gorell,

Johnson et al., 1998; Hatcher, Pennell et al., 2008; Elbaz, Clavel et al., 2009) which inhibits complex I of the mitochondrial respiratory chain, was administered intragastrically, and the mice subsequently showed aspects of the Braak staging of propagation (Pan-Montojo, Anichtchik et al., 2010).

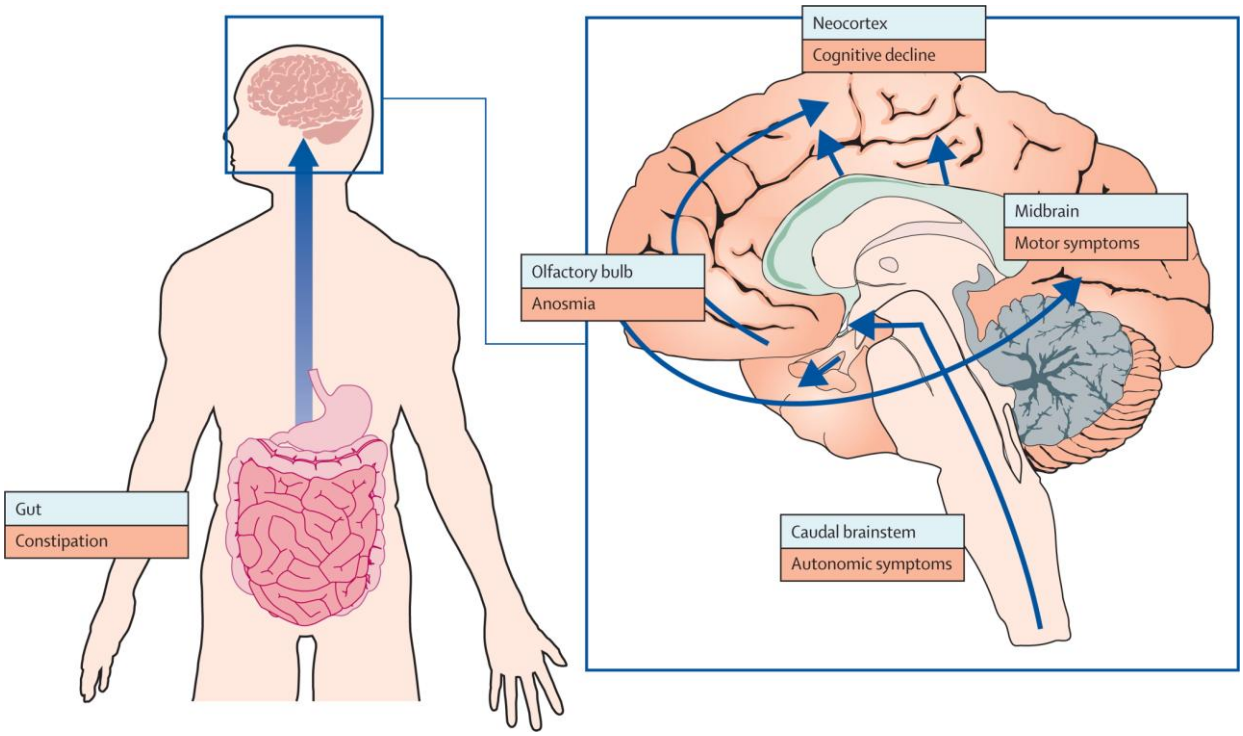

Figure 8. Dual-hit hypothesis of propagation of synucleinopathy during PD. An unknown pathogen gains access to the brain via the nose or the gut and then propagates to the caudal brainstem and the temporal lobe. Lewy body pathology then ascends to midbrain structures and cortical areas. Blue arrows depict the proposed ascending progression of PD pathology. Boxes indicate affected systems and main associated symptoms. Figure from (Angot, Steiner et al., 2010).

Considering that pathology spreads in a defined manner, the distribution of LBs and LNs within the brain is used to define the progression of PD, which has been divided into six neuropathological stages, as outlined in Table 2 overleaf (Braak, Ghebremedhin et al., 2004).

Table 2. Relation of Braak staging, with the anatomical region where LBs and LNs are found, and clinical features in PD.

Braak stage	Anatomical region	Clinical feature
1	Olfactory bulb, Medulla	Hyposmia; autonomic (orthostatic hypotension, impotence, urinary frequency, constipation)
2	Pons	Depression
3	Midbrain (Substantia nigra)	Motor symptoms : uncontrollable tremor, bradykinesia, rigidity
4	Basal forebrain	Dementia
5	Frontal cortex	Dementia
6	Parietal cortex	Dementia

α-Synuclein: the major constituent of LBs and LNs

Soluble α-Synuclein

α-Syn is a small, highly conserved abundant protein which accounts for approximately 1 % of the total protein in soluble cytosolic brain fractions (Iwai, Masliah et al., 1995).

α-Syn is comprised of 140 amino acids, with no tryptophan or cysteine residues, and its primary sequence can be divided up into three regions as shown in Fig. 9. There are three missense mutations in the α-Syn gene; alanine-30-proline (A30P), glutamic acid-46-lysine (E46K), and alanine-53-threonine (A53T). These mutations directly implicate α-Syn in PD as they all give rise to early-onset PD (Li, Uversky et al., 2001; Fredenburg, Rospigliosi et al., 2007). The three regions of α-Syn are:

1. The N terminal region (residues 1-60), includes the site of the three familial PD mutations (represented by green arrows). It also contains four 11-residue imperfect repeats with a conserved motif (KTKEGV, represented by red bands), which are similar to those found in apolipoproteins, which form amphipathic α-helices upon lipid binding (Segrest, Jones et al., 1992).
2. The central region, from 61 to 95, contains the highly aggregation-prone non-amyloid component (NAC) sequence, and two more imperfect repeats.

3. The C terminal region from 96 to 140 (in grey), is highly acidic and enriched with proline residues.

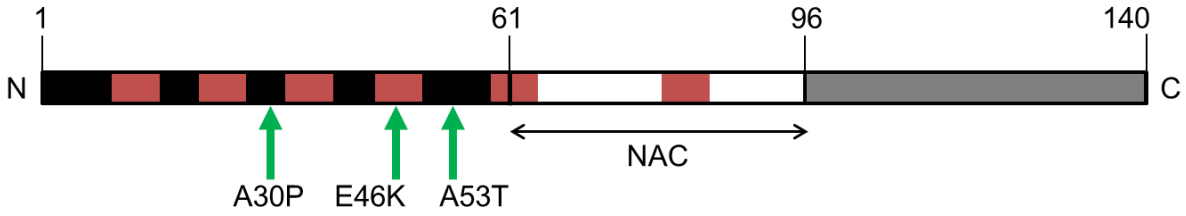

Figure 9. Primary structure of α-Syn. N-terminal region in black. Imperfect repeats with conserved sequence KTKEGV shown in red. NAC region in white (61-95). Acidic C-terminal region in grey (95-140) (Uversky and Eliezer, 2009).

When soluble and isolated in solution, recombinant α-Syn is a natively unfolded or intrinsically disordered protein, which lacks secondary structure as indicated not only by circular dichroism (CD) (Fig. 10) but also by Fourier-transform infrared spectroscopy (FTIR) (Uversky, Li et al., 2001) and nuclear magnetic resonance (NMR) (Morar, Olteanu et al., 2001).

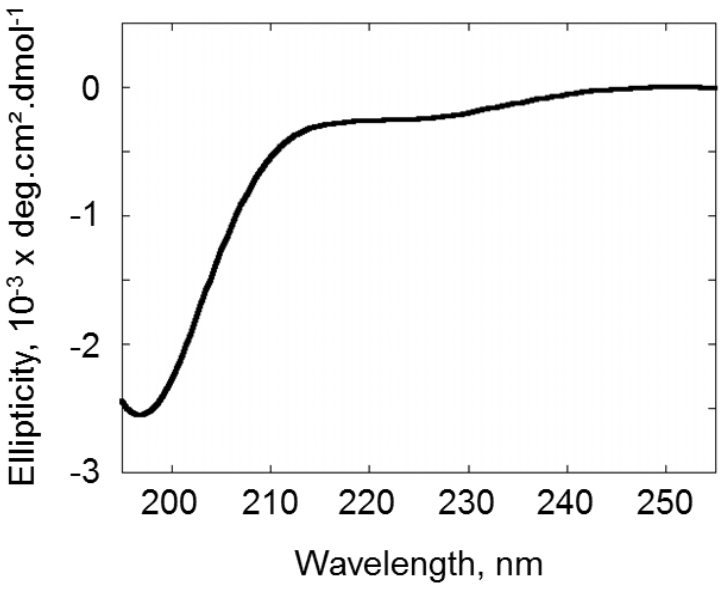

Figure 10. Far-UV circular dichroism spectra of soluble α-Syn (100 μM) displaying patterns typical of an intrinsically unstructured protein with a minimum at 196 nm and a lack of bands in the 210-230 nm region.

Although recombinant α-Syn is intrinsically disordered in solution, in the presence of negatively charged membranes and upon association, it undergoes a conformational change from a random coil to an α-helical structure (Davidson, Jonas et al., 1998; Jo, McLaurin et al., 2000). There is on-going debate as to the form of the membrane-bound helical α-Syn; bent or extended (Chandra, Chen et al., 2003; Jao, Der-Sarkissian et al., 2004; Borbat, Ramlall et al., 2006; Georgieva, Ramlall et al., 2008; Jao, Hegde et al., 2008) with the difference seemingly related to the curvature of the target membrane being bound by α-Syn (Trexler and Rhoades, 2009). This difference could explain the range of cellular functions that soluble α-Syn has been proposed to be a part of.

It was very recently suggested that although α-Syn has long been defined as a natively unfolded monomer which acquires α-helical structure upon binding to lipid membranes, this definition is probably wrong, and a consequence of the preparation and use of recombinant α-Syn protein. Bartels *et al* describe that endogenous α-Syn, isolated and analysed under non-denaturing conditions from various human cells, exists in large part as a helically folded tetramer of about 58 kDa (Bartels, Choi et al., 2011).

Cellular function of soluble α-Syn

The precise cellular function of soluble α-Syn remains elusive, but there is much speculation on its possible role. Knowing that α-Syn binds to plasma membranes and vesicles as previously mentioned, and that it is present in a high concentration at presynaptic terminals, there is evidence that it plays an important role in this region (Jakes, Spillantini et al., 1994). At the presynaptic terminal, α-Syn is thought to be in equilibrium between free and plasma membrane or vesicle bound states (McLean, Kawamata et al., 2000), with about 15 % membrane bound (Lee, Choi et al., 2002). Based on its association with vesicles and plasma membranes, soluble α-Syn may regulate vesicle uptake and release, amongst other functions at the presynaptic terminal (Norris, Giasson et al., 2004; Burre, Sharma et al., 2010). In accordance with this hypothesis, the phenotype of knock-out α-Syn mice also suggests that α-Syn is involved with synaptic transmission, more specifically as a negative

regulator of dopamine transmission (Abeliovich, Schmitz et al., 2000). Most recently, it has been suggested that α-Syn is a cellular ferrireductase (Davies, Moualla et al., 2011).

Assembly of α-Syn

In vitro at physiological temperature and under agitation, recombinant α-Syn readily progresses from soluble to fibrillar structures like those found within LBs and LNs and which can be observed using an electron microscope (inset, Fig. 11). These structures bind to thioflavin T (thioT), a widely used fluorescent dye that fluoresces upon binding to fibrillar species (Wolfe, Calabrese et al., 2010), and allows the progression from soluble to fibrillar α-Syn to be followed *in vitro* using a spectrofluorimeter (Fig. 11).

The assembly follows a Sigmoidal curve, with a lag phase; the rate limiting step of assembly where stable α-Syn nuclei form (phase 1, Fig. 11), followed by a period of rapid growth (phase 2, Fig. 11) in which the extremities of the fibrils elongate as α-Syn monomers are incorporated, and finally reaching the steady state (phase 3, Fig. 11) when there are no more monomers remaining to elongate the fibrils. Assembly is concentration dependent; at 100 μM α-Syn, the steady state of assembly is reached in approximately 350 min, whereas at 50 μM, the time taken to reach the steady state is increased to around 600 min.

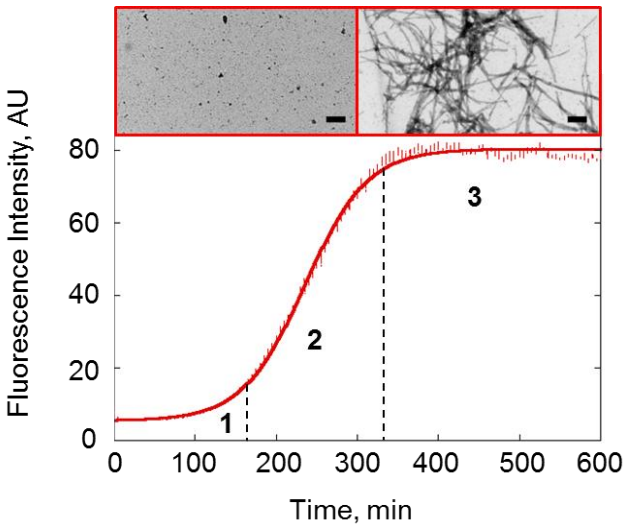

Figure 11. Assembly of α-Syn. Time course of α-Syn (100 μM) assembly at 37 °C monitored by thioT binding. AU, arbitrary units. Lag phase, 1; elongation, 2 and steady state, 3.

Negative stained electron micrographs of α-Syn (100 μM) at 0 min (left) and 1,000 min (right) after the onset of the assembly reaction. Bar, 0.2 μm.

But what triggers the abnormal aggregation of α-Syn in neurodegenerative disease brains? As it was recently shown that endogenous α-Syn exists as a helically folded tetramer which undergoes little or no amyloid-like aggregation (Bartels, Choi et al., 2011), the first step in disease pathogenesis is likely to be the destabilization of this tetramer, to yield aggregation-prone monomers, probably similar to the recombinant form. Some studies associate oxidative stress with the onset of α-Syn aggregation (Giasson, Duda et al., 2000), however others hypothesize that oxidative stress is a result of aberrant α-Syn aggregation (Farooqui and Farooqui, 2011). Otherwise, environmental factors, e.g. chemicals in pesticides and herbicides amongst others, and heavy metals (Shin, Lee et al., 2000; Lee, Lee et al., 2001; Uversky and Eliezer, 2009) could be responsible for triggering α-Syn assembly. These studies documented the effect of said factors on the assembly rate of α-Syn *in vitro*, and in all cases found an increase in the rate of assembly into fibrils. In addition, mutant α-Syn assembles faster than the wildtype protein (Li, Uversky et al., 2001). Considering that the genetically linked mutants A30P, E46K and A53T, which assemble more rapidly, give rise to early onset PD, this strengthens the hypothesis that α-Syn assembly is one of the first steps in the pathogenesis of the disease. Fig. 12 summarizes the potential factors and events associated with the pathogenesis of PD.

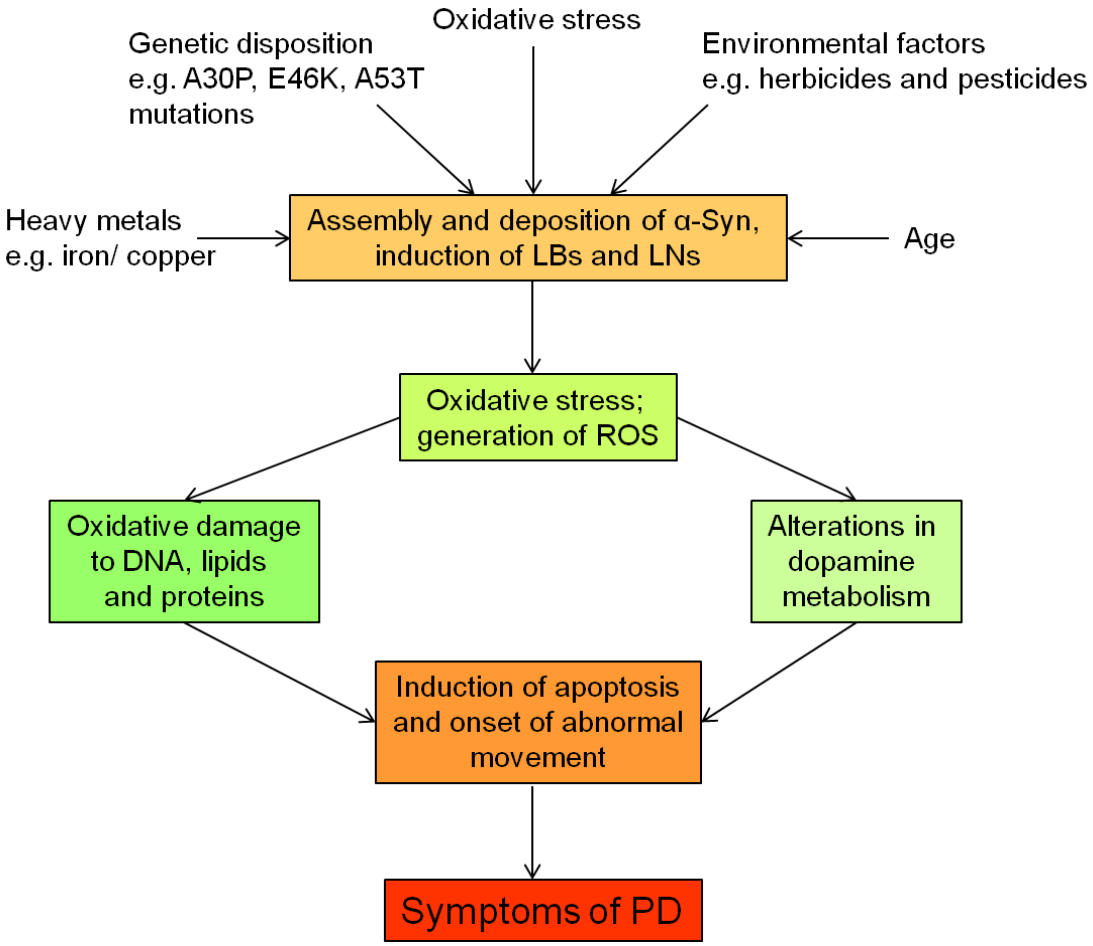

Figure 12. Potential factors and events associated with the pathogenesis of PD. Figure adapted from (Farooqui and Farooqui, 2011).

What we have learnt from neuronal grafting

Considering that the symptoms of PD arise when more than 70 % of dopaminergic terminals and/or neurons have been lost, for over two decades, foetal nigral transplants have been considered as a therapeutic option for PD. This procedure attempts to directly replace the lost dopaminergic cells and replace dopaminergic innervation and synaptic connectivity to the striatum, thus improving locomotive dysfunction. A number of clinical studies reported meaningful benefits for a couple of years to a decade after transplantation, with improved scores on the Unified Parkinson Disease Rating Scale, and requiring lower doses of antiparkinsonian medications (Lindvall, Brundin et al., 1990; Lindvall, 1994; Peschanski, Defer et al., 1994; Kordower, Freeman et al., 1995; Wenning, Odin et al., 1997; Piccini,

Brooks et al., 1999; Mendez, Sanchez-Pernaute et al., 2005). These studies were 'open-label', with the patient aware of whether they had been allocated a placebo or the real treatment. Interestingly, no benefits of the treatment were seen when double-blind, 'sham' controlled trials (where every aspect of the procedure is copied aside from injecting the cells into the brain) were carried out, where the participants and investigators have no idea who is being administered the placebo or the neuronal grafts (Lang, Gill et al., 2006; Marks, Bartus et al., 2010; Gross, Watts et al., 2011). There are many who believe that open trials are riddled with bias, and it is especially complicated when investigating PD, as a patient who knows they are receiving treatment is expectant of a positive outcome, and will naturally release dopamine, thus self-improving their symptoms (de la Fuente-Fernandez, Ruth et al., 2001). Excluding the placebo-effect is clearly not an option in PD as it has a proven effect, thus itself becoming part of the treatment.

Alongside the clinical effects of neuronal grafting, this procedure has taught us about the progression of PD. Several post-mortem analyses have been performed on PD patients who had previously received foetal tissue transplantation, to document morphological and neurochemical alterations. Taking one study as an example, six patients who had received transplants 18-19 months, 4 years, and 14 years earlier were examined using histochemical and immunological methods. All grafts survived, successfully innervated, and formed synaptic contacts. The grafts that survived 14 years, i.e. the grafted cells are 14 years post-natal and far younger than typical PD onset, showed signs of PD, with decreased dopamine transporter, decreased tyrosine hydroxylase (the enzyme responsible for catalyzing the conversion of the amino acid L-tyrosine to dihydroxyphenylalanine, the dopamine precursor), and the presence of LB-like inclusions (Chu and Kordower, 2010). The 4 year old grafts showed decreased dopamine transporter, and increased cytoplasmic α-Syn, while the 18-19 month old grafts did not show any signs of PD. This suggests that PD pathology passes from host-to-graft cells, and subsequent studies showed that this is a result of α-Syn moving from host-to-graft cells, seeding the endogenous α-Syn and propagating α-Syn pathology and ultimately PD (Hansen, Angot et al., 2010).

Molecular chaperones

Molecular chaperones are defined as “any protein that interacts, stabilizes, or helps a non-native protein to acquire its native conformation, but is not present in the final functional structure” (Hartl, 1996; Hartl and Hayer-Hartl, 2009). Chaperones are highly ubiquitous, as they aid newly synthesized proteins to fold into their precise three-dimensional (3D) structures, refold stress-denatured proteins, help proteins to cross membranes, and assist in proteolytic degradation, to name but a few roles (Chang, Tang et al., 2007; Tang, Chang et al., 2007).

Protein folding

Protein folding is often represented by the funnel concept, as shown in Fig. 13. Unfolded proteins have a high free energy and can take on many different 3D shapes. As a protein starts to fold, the free energy drops, and the number of available conformational states, denoted by the width of the funnel, decreases. Proteins composed of more than 100 amino acids (~90 % of all proteins in a cell) tend to reach their native state via folding intermediates, in order to decrease the chance of collapse into non-native states (Brockwell and Radford, 2007; Bartlett and Radford, 2009). These intermediates are either a stepping stone towards the native state, or stable, misfolded conformations which often have a high propensity to aggregate due to exposed hydrophobic regions. Aggregation - the association of two or more non-native protein molecules – can lead to either amorphous structures, or the formation of ordered, fibrillar assemblies, with an even more favourable free energy minimum than the native folded state. Molecular chaperones supposedly recognise and bind to hydrophobic regions exposed on non-native proteins, thereby blocking aggregation.

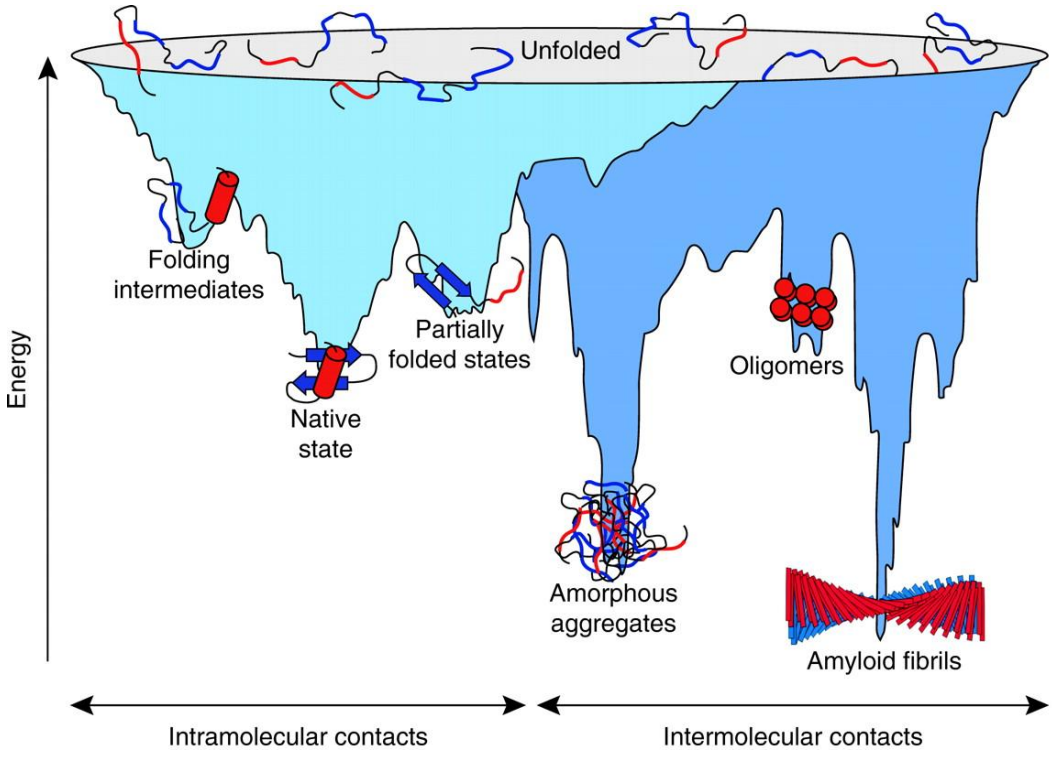

Figure 13. Energy landscape of protein folding and aggregation. The light blue surface shows the multitude of conformations 'funnelling' to the native state via intramolecular contacts and the dark blue area shows the conformations moving toward amorphous aggregates or amyloid fibrils via intermolecular contacts. Both parts of the energy surface overlap. Aggregate formation can occur from intermediates populated during de novo folding or by destabilization of the native state into partially folded states and is normally prevented by molecular chaperones. Cell-toxic oligomers may occur as off-pathway intermediates of amyloid fibril formation. Figure from (Hartl and Hayer-Hartl, 2009).

Heat shock proteins

Many of the components of the elaborate system of molecular chaperones are the so-called heat shock proteins (Hsp). Their major role is to prevent protein misfolding and aggregation, both under normal cellular conditions, and under the influence of stresses which increase the concentration of improperly folded proteins, for example an increase in temperature (heat shock), or ischemia. Under stress, the expression of Hsps is upregulated in order to cope with the increase in misfolded proteins. The chaperones are classified

according to their molecular weight: Hsp40, Hsp60, Hsp70, Hsp90, Hsp100 and the "small" Hsps, less than 35 kDa.

The Hsp70 family

The Hsp70 family of molecular chaperones is one of the most conserved protein families in evolution and it is found in all organisms apart from some hyperthermophilic archaea (Gribaldo, Lumia et al., 1999). The human Hsp70 (or HSPA) family consists of 13 different proteins which became apparent upon completion of the human genome project (Brocchieri, Conway de Macario et al., 2008) (see Table 3).

*Table 3. Nomenclature and characteristics of the human Hsp70 (HspA1A) family. The two Hsp70s used in this thesis are highlighted in **red**. Table adapted from (Hageman, van Waarde et al., 2011).*

Protein name	Alternative name	Molecular mass (kDa)	Sequence identity (%)
HSPA1A	**Hsp70**	**70.0**	**100**
HSPA1B	Hsp70-2	70.0	99
HSPA1L	hum70t	70.4	88
HSPA2	Heat shock 70 kDa protein-2	70.0	83
HSPA5	BIP, GRP78, MIF2	71.0	60
HSPA6	Heat shock 70 kDa protein-6, (Hsp70B')	71.0	81
HSPA7	-	-	-
HSPA8	**Hsc70**	**70.9**	**85**
HSPA9	GRP75, HSPA9B, MOT, MOT2, PBP74, mot-2	73.7	45
HSPA12A	FLJ13874, KIAA0417	141.0	14
HSPA12B	RP23–32L15.1, 2700081N06Rik	75.7	18
HSPA13	Stch	51.9	20
HSPA14	HSP70–4, HSP70L1, MGC131990	54.8	27

Protein localisation prediction methods propose that most of the 13 Hsps are found within the cytosol and nuclear compartment (Daugaard, Rohde et al., 2007; Hageman and Kampinga, 2009). It is therefore unclear why gene expansion produced so many Hsp70s – seemingly not to cope with cellular compartmentalization.

In yeast, the Hsp70s have been divided into two distinct groups: the stress chaperones, and the 'housekeeping' or 'CLIPS' (chaperones linked to protein synthesis). Whereas the stress chaperones are induced in periods of stress, the CLIPS are repressed by

stress, and transcriptionally co-regulated with the translational apparatus (Albanese, Yam et al., 2006). This difference is controlled at the genomic level, as the promoter regions on the genes of each chaperone group differ. The stress chaperones contain promoter regions rich in HSE (heat shock elements) and STRE (stress response elements) whereas the CLIPS chaperones contain binding elements for transcription factors Rap1p and Abf1p, which control the expression of ribosomal genes and other translational components. In humans, although HSPA6 is only expressed after severe cellular stress, and Hsc70 is considered a CLIPS chaperone, the existence of distinct HSP and CLIPS groups in humans is currently unclear. For example, Hsp70 and one of its co-chaperones DNAJB1 show basal expression under normal conditions as well as induction upon cellular stress (Hageman, van Waarde et al., 2011).

Hsp70 and Hsc70

Highlighted in red in Table 3 are two important Hsp70s investigated in this thesis, Hsp70 and its constitutively expressed counterpart, Hs**c**70 (c for constitutive). These chaperones share 85 % primary structure identity, and although historically it was always thought that the two carried out similar cellular roles, it has been shown otherwise. Goldfarb and his colleagues demonstrated in *Xenopus oocytes* that overexpression of Hsc70 or Hsp70 had differential and antagonistic effects on the functional and surface expression of the epithelial sodium channel (Goldfarb, Kashlan et al., 2006; Hageman, van Waarde et al., 2011). Similarly, Hageman *et al* extensively compared all 13 members of the Hsp family, by assessing the effect of overexpression of each chaperone on the refolding of heat-denatured luciferase, and on the inhibition of aggregation of luciferase or a non-foldable, polyglutamine-containing Huntingtin fragment. Hsp70 and Hsc70 both showed activity on luciferase refolding, but Hsc70 to a lesser extent. While neither chaperone could suppress the aggregation of the Huntingtin fragment, Hsp70 was capable of suppressing the aggregation of denatured luciferase, whereas Hsc70 was not (Hageman, van Waarde et al., 2011).

The Hsp70 reaction cycle

Hsp70s have two major functional domains, an ATPase domain (or nucleotide binding domain, NBD) of around 40 kDa at the N-terminal, and a C-terminal peptide binding domain (PBD), of approximately 25 kDa. The PBD is made up of a β-sandwich subdomain (15 kDa) and an α-helical lid fragment (Zhu, Zhao et al., 1996), and can accommodate hydrophobic peptides approximately 7 peptides long (Rudiger, Buchberger et al., 1997). The NBD is structurally similar to actin and hexokinase in that it consists of four smaller domains which form two lobes with a deep cleft, into which MgATP and MgADP bind (Bork, Sander et al., 1992), as indicated in Fig. 14.

The two domains of Hsp70s are reliant upon one another for peptide binding and release to take place. The NBD regulates the conformation of the PBD. Through nucleotide exchange reactions, Hsp70 cycles between an ATP-bound state, where the α-helical lid of the PBD is open, and an ADP-bound state, where the lid is closed. As a result of these conformational changes, on and off rates for client binding are rapid in the ATP-bound state (low client protein affinity), and slow in the ADP-bound state (high client protein affinity).

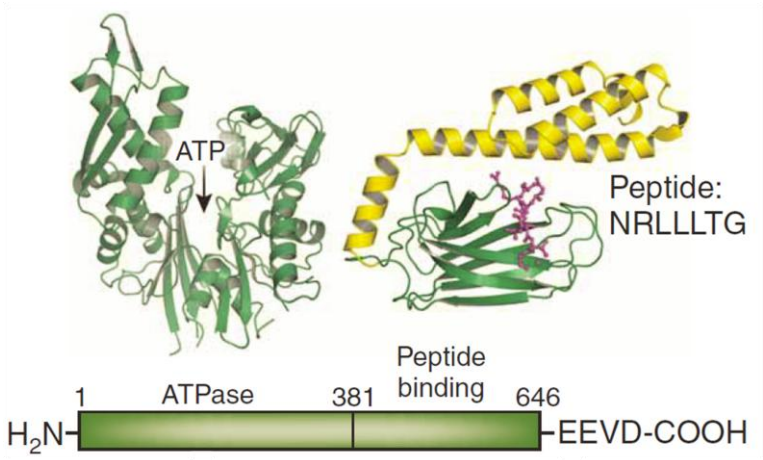

Figure 14. Structures of the ATPase domain (PDB 1DKG, (Hartl and Hayer-Hartl, 2009) and the peptide-binding domain (PDB 1DKZ, (Zhu, Zhao et al., 1996) of Hsp70 shown representatively for E. coli DnaK. The α-helical lid of the peptide binding domain is shown in yellow and the extended peptide substrate as a ball-and-stick model in pink. ATP indicates

the position of the nucleotide-binding site. The amino acid sequence of the peptide is indicated. Residue numbers refer to human Hsp70. Figure adapted from (Hartl and Hayer-Hartl, 2009).

Hsp70 co-chaperones

However, Hsp70s never function alone. They generally collaborate with co-chaperones from the Hsp40 family (also known as the J proteins due to a conserved signature domain which resembles that of the well-studied *E. coli* protein, DnaJ), and nucleotide exchange factors (NEFs) in the ATP regulated binding and release of non-native proteins.

More specifically, the Hsp40s, through interaction of their J-domain with Hsp70, stimulate ATP hydrolysis of the bound Hsp70, converting them to the ADP-bound form with concomitant lid closure, resulting in stable binding of the client protein. The ADP-bound state is stabilized by the co-chaperone Hip (Hsp70-interacting protein), which serves to increase the half-life of substrate complexes (Hohfeld, Minami et al., 1995). To complete the reaction cycle, once ATP hydrolysis has occurred, NEFs bind to the Hsp70 NBD and catalyse ADP-ATP exchange, which results in lid opening and the client protein being released. Upon release, either the client protein has obtained its native fold thus burying hydrophobic residues, or the protein will rebind to the Hsp70, or be transferred to downstream chaperones, as summarized in Fig. 15.

Hsp40s also interact directly with unfolded proteins and can recruit Hsp70 to unfolded client proteins. Although many co-chaperones are soluble cytosolic proteins, some are localised (Young, Barral et al., 2003). The best example of a localised co-chaperone is the J domain co-chaperone auxilin, which plays a vital role in the Hsc70-mediated uncoating of clathrin-coated vesicles which have budded off from the plasma membrane. Auxilin, which has a clathrin-binding domain as well as a J domain, is thought to bind first to clathrin cages, before stimulating free Hsc70 to hydrolyse ATP. The ADP-bound Hsc70 tightly binds to the

clathrin, resulting in disassembly of the cage (Ungewickell, Ungewickell et al., 1995; Holstein, Ungewickell et al., 1996).

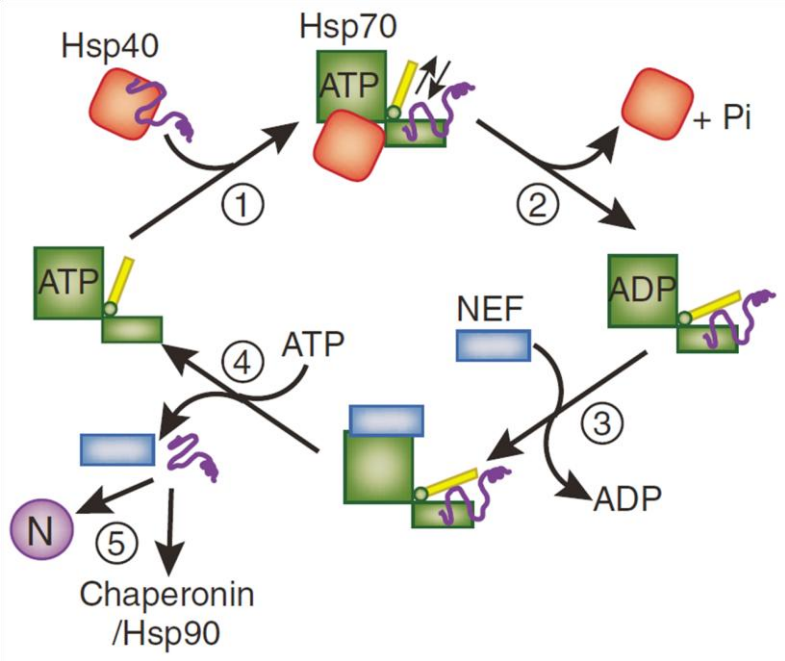

Figure 15. Hsp70 reaction cycle. 1) Hsp40 delivers client protein to ATP-bound Hsp70. 2) Hydrolysis of ATP to ADP is accelerated by Hsp40: lid closes and the client protein is tightly bound by Hsp70. Hsp40 dissociates from Hsp70. 3) Dissociation of ADP is catalyzed by NEF. 4) Induced by ATP binding, the lid opens and the client protein is released. 5) Either the client protein is correctly refolded, or it rebinds Hsp70 or is transferred to other downstream chaperones. Figure adapted from (Hartl and Hayer-Hartl, 2009).

Hsp40s are believed to allow for the functional diversity of Hsp70s. There are over 49 different Hsp40/ DNAJ encoding genes in the human genome (Kampinga, Hageman et al., 2009), which are divided into three distinct groups (DNAJA, DNAJB and DNAJC) based on the presence of certain structural motifs (Cheetham and Caplan, 1998). Considering that there are over 49 J proteins in humans, but only 13 Hsp70s, multiple J proteins interact and function with a single Hsp70, allowing the Hsp70 to act as required (Kabani and Martineau, 2008; Kampinga and Craig, 2010).

The yeast molecular chaperone system

As previously mentioned, the yeast (*Saccromyces cerevisiae)* equivalent of human Hsps is the Ssa family, which consists of four highly conserved proteins, Ssa1, Ssa2, Ssa3 and Ssa4. Ssa1 and Ssa2 are constitutively expressed and share 98 % identity, while Ssa3 and Ssa4 are stress-induced, are 88 % identical, and share 80 % identity with Ssa1 and Ssa2. Abundant expression of at least one Ssa is essential for cell viability (Werner-Washburne, Stone et al., 1987). The Ssa family share the same range of functions as the Hsp family, being involved in protein folding, translocation across the endoplasmic reticulum, facilitating degradation, and translation initiation (Nikolaidis and Nei, 2004). Ssa1p, the most extensively studied cytosolic Hsp, is known to interact with at least five different J proteins (Fig. 16) to allow functional diversity. Ydj1p, Djp1p and Hlj1p are partially membrane bound, and are therefore examples of localised J proteins, with their J domains exposed to the cytosol to stimulate the ATPase activity of Ssa1p (Craig, Huang et al., 2006).

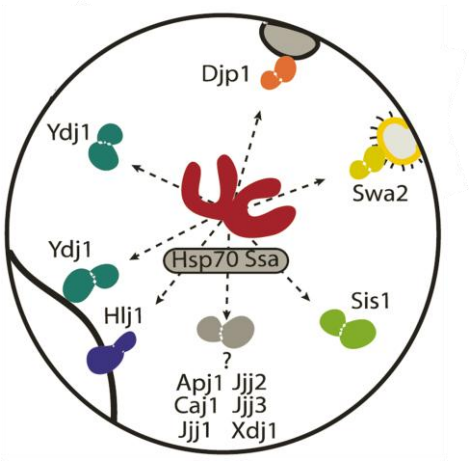

Figure 16. Multiple J proteins interact with yeast Ssa1p to allow functional diversity. Figure adapted from (Craig, Huang et al., 2006).

Returning to the suggestion that Hsp70 and Hsc70, with 85 % identity in primary structure, do not carry out similar cells roles, the same can be seen for the Ssa family in yeast. To investigate whether or not the Ssa proteins were functionally redundant, a yeast model system was used, with strains lacking all four chromosomal *SSA* genes made to

express individual Ssa proteins from plasmids under the control of the SSA2 promoter. In optimal conditions, the strains expressing inducible Ssa proteins (Ssa3 and Ssa4) grew more slowly than their constitutive counterparts (Ssa1 and Ssa2), indicating that the inducible chaperones are partly or totally incapable of performing housekeeping functions as compared to their constitutive counterparts. Similarly, the propagation of yeast prion [*PSI*$^{+}$] in the presence of each of the different chaperones was examined. The strength of [*PSI*$^{+}$] was normal in cells expressing Ssa1p, slightly weaker with Ssa2p, stronger than normal in the presence of Ssa3p, and weakest where Ssa4p was present (Sharma, Martineau et al., 2009). These differences could reflect specific differences in Ssa activities or in client-protein binding. For instance, Ssa4p may bind more tightly to aggregating Sup35p, the protein responsible for the [*PSI*$^{+}$] trait, than the other Ssa chaperones, thus preventing its aggregation.

α-Syn and heat shock proteins

The progression of PD is strongly associated with a change in α-Syn solubility which results in fibrillar α-Syn sequestered within LBs and LNs. As this is widely believed to be the consequence of a conformational change, and, as previously mentioned, heat shock proteins are also found within LBs and LNs, there has been **significant** focus on the possible therapeutic role of molecular chaperones for almost a decade.

Known effects of molecular chaperones on α-Syn

1. Hsp70

The idea of using Hsp70 against aggregating α-Syn almost certainly stemmed from the earlier observation that the neuronal toxicity of abnormal polyQ proteins, incriminated in Huntington's disease amongst others (Table 1), is suppressed by Hsp70 (Warrick, Chan et al., 1999).

In 2002, Auluck and his colleagues were the first to show that Hsp70 co-localises with α-Syn in LBs and LNs, and that Hsp70 is beneficial against aggregating α-Syn. In their

drosophila model of PD, direct expression of α-Syn (WT, A30P or A53T) resulted in 50 % dopaminergic neuronal cell loss, with the concomitant observation of LBs and LNs. Co-expression of Hsp70 prevented this cell loss in flies of the same age; however there was no change in the number, morphology or distribution of LBs and LNs (Auluck, Chan et al., 2002).

In the same year, McLean *et al* showed that a wider range of chaperones localised to LBs and LNs in brain sections of DLB patients (Hsp27, Hsp60, Hsp70, Hsp90, Hsp110, and the co-chaperones Hdj1 and HdjJ2) (McLean, Kawamata et al., 2002).

In 2004, it was then demonstrated for the first time in a mammalian system that overexpression of Hsp70 in a mouse model of PD reduced the amount of high molecular weight, detergent insoluble α-Syn species (Klucken, Shin et al., 2004), and that overexpression of Hsp70 proffered protection against the cytotoxicity of PD-inducing pesticide rotenone, and reduced α-Syn aggregation in a cellular model (Zhou, Gu et al., 2004).

In 2005, advances by Dedmon *et al* described that the presence of Hsp70 shifted the distribution of α-Syn from insoluble to soluble species, by interacting specifically with prefibrillar α-Syn, but, controversially, they also indicated that no decrease in α-Syn cell toxicity was seen when Hsp70 was added (Dedmon, Christodoulou et al., 2005). Expanding on the finding that Hsp70 binds to prefibrillar α-Syn, Huang *et al* in 2006 suggested that Hsp70 plays more than one role in inhibiting α-Syn fibril formation. They showed that Hsp70 inhibited the formation of the aforementioned prefibrillar α-Syn species, but if formed, Hsp70 then bound to these species to inhibit nuclei formation, as well as binding with nuclei to retard fibril elongation. Finally, the research group described that, on binding to prefibrillar species, Hsp70 suppressed the α-Syn-mediated permeabilization of vesicular membranes (Huang, Cheng et al., 2006).

A novel technique developed by Opazo *et al* subsequently allowed for real-time imaging of live cells accumulating α-Syn, and more importantly showed that cells dealt with α-Syn aggregate build-up by forming an aggresome, which could then be cleared from the

cell. Co-expressing Hsp70 not only led to a reduction in the prevalence of α-Syn aggregates, but also increased their clearance via aggresomes (Opazo, Krenz et al., 2008). In the paper, the authors mention that aggresomes share many properties with LBs, and suggest that the formation of LBs is most likely a protective response of the cell as it tries to remove the aggregating α-Syn, rather than a cause of cell death.

On a more specific level, Luk *et al* then described using mutant proteins, that Hsp70 inhibits α-Syn assembly through an interaction between the PBD of Hsp70, and the α-Syn core hydrophobic region (Luk, Mills et al., 2008). This interaction halts assembly before the elongation stage, therefore in agreement with Dedmon *et al's* studies showing that Hsp70 interacts with prefibrillar α-Syn species.

Next, Roodveldt *et al* developed our understanding on the fate of Hsp70 in pathogenic conditions, by showing that Hsp70 depletion in PD is a direct result of the aggregation-prone proteins, as Hsp70 has a tendency to aggregate in the presence of α-Syn and ATP. In the presence of Hip, this co-aggregation is prevented, and the Hsp70 remains soluble and present to fight against aggregating α-Syn (Roodveldt, Bertoncini et al., 2009).

In 2010, Shimshek *et al* published conflicting work, showing that co-overexpression of A53T point-mutated α-Syn and human Hsp70 in mice did **not** decrease the amount of toxic α-Syn species, and nor did Hsp70 show any beneficial effect on α-Syn-mediated motor deficits (Shimshek, Mueller et al., 2010). However, the authors were uncertain of the activity of their Hsp70 over-expressed in vivo, as they suggested that there were several experimental challenges in testing so. It is possible that their Hsp70 was non-functional or only partially functional, explaining their inconsistent results. When a protein is over-expressed *in vivo*, there is an obvious unbalance of normal protein levels. As co-chaperones and NEFs are essential for the proper functioning of Hsp70, it is possible that the over-expressed Hsp70 was unable to function due to an insufficient level of co-chaperones, themselves not over-expressed. Otherwise, the over-expressed Hsp70 may not have folded correctly into its 3D structure necessary for action.

Coming from a different angle, in 2010 Hinault *et al* investigated the effect of monomeric or oligomeric α-Syn on the action of the bacterial Hsp70 chaperone system (DnaK, DnaJ and GrpE; the bacterial equivalents of human Hsp70, Hsp40 and NEF, respectively) *in vitro.* They found that α-Syn oligomers can specifically inhibit the function of the chaperone system, thus suggesting that α-Syn-mediated toxicity could also be a result of α-Syn obstructing the cellular chaperone machinery, leading to collapse of protein homeostasis (Hinault, Cuendet et al., 2010). They did not, however, attempt to reproduce their findings using the human chaperone system, which may or may not give the same results.

The most recent laboratory to publish work on α-Syn and Hsp70 exploited a bioluminescent-protein-fragment complementation assay, where only upon α-Syn assembly, and subsequent interaction of two halves of a non-luminescent protein (humanized *Gaussia princeps* luciferase, hGLuc), is luminescence observed. This assay can be used to observe α-Syn aggregation in living cells, and in culture medium (Remy and Michnick, 2006). They observed that α-Syn is released from axonal terminals into the extracellular space where it continues to oligomerize, and can be taken up by neurons and transported in a retrograde manner back to the cell bodies. They saw evidence for caspase-3 and -7 activation once the α-Syn oligomers had entered the neighbouring cells; the initiation of cell death. Hsp70 not only reduced α-Syn oligomer formation in the extracellular space, but also offered protection against α-Syn-mediated toxicity, as the authors detected less cell death in neurons incubated with culture medium containing α-Syn and Hsp70, than α-Syn alone (Danzer, Ruf et al., 2010).

2. Hsp90

Hsp90 is an abundant molecular chaperone that prevents protein aggregation and increases Hsp expression (Picard, 2002). McLean and colleagues had already demonstrated the presence of Hsp90 within LBs and LNs (McLean, Kawamata et al., 2002) before Uryu *et al* carried out a more extensive, quantitative study on molecular chaperones within

intracellular α-Syn inclusions. They determined immunohistochemically that Hsp90 was the most abundant chaperone within LBs and LNs, and the predominant chaperone to co-localise with α-Syn (Uryu, Richter-Landsberg et al., 2006). Liu *et al* subsequently showed that Hsp90 regulates the rab11a-mediated recycling of α-Syn (Liu, Zhang et al., 2009). Following this, Falsone *et al* described *in vitro* that Hsp90 affects regions in α-Syn that are responsible for vesicle binding and amyloid fibril assembly, thus perturbing both processes. They showed that Hsp90 binds to α-Syn, and inhibits vesicle binding and that Hsp90 modulates the assembly of α-Syn in an ATP-dependent manner. In the absence of ATP, Hsp90 inhibited α-Syn fibril formation and promoted α-Syn oligomer accumulation, however, in the presence of ATP and Hsp90, fibril formation was favoured, as summarized in Fig. 17 (Falsone, Kungl et al., 2009).

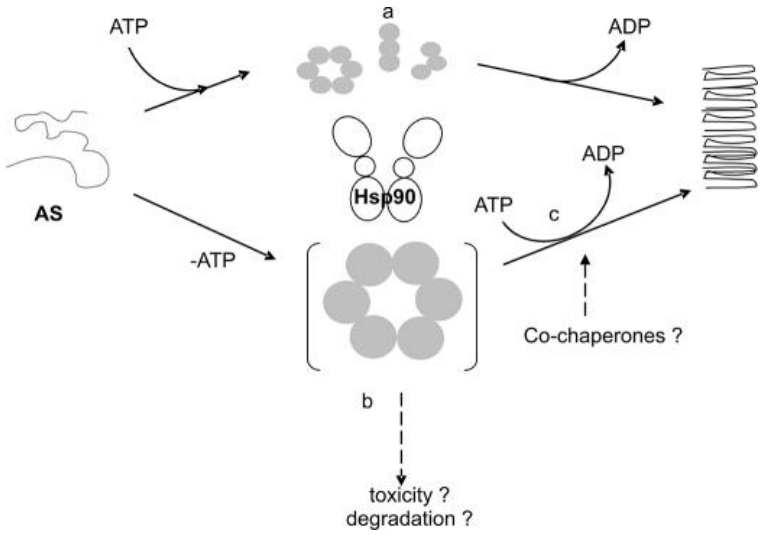

Figure 17. An in vitro model for Hsp90 modulated α-Syn assembly. In the presence of ATP, Hsp90 promotes the rapid conversion of monomeric α-Syn into fibrils. Stable oligomeric intermediates do not accumulate (a). In the absence of ATP, Hsp90 stabilizes intermediate pre-fibrillar oligomers, which consequently accumulate in solution (b). The addition of ATP restores their conversion into insoluble fibrils (c). Figure from (Falsone, Kungl et al., 2009).

According to the literature, Hsp90 seems to have the opposite effect to Hsp70 on α-Syn: Hsp70 inhibits fibrils formation whilst Hsp90 promotes it. As there is on-going scepticism

as to which α-Syn conformer is toxic to cells (oligomers or fibrils), it is difficult to understand whether Hsp90 is beneficial in PD pathogenesis or not. If oligomers are the toxic α-Syn species, then Hsp90 is protective as it speeds up the conversion of oligomers to fibrils. Indeed, there are several who believe that when cellular quality control systems are overwhelmed or functionally impaired (i.e. if α-Syn inhibits the proper functioning of the chaperone system as suggested by Hinault *et al*), cells protect themselves by sequestering aggregation-prone proteins as aggregates, i.e. fibrils found within LBs and LNs (Kopito, 2000; Nollen, Salomons et al., 2001; Kaganovich, Kopito et al., 2008). However, if fibrillar α-Syn is more toxic to cells than oligomers, then Hsp90 promotes disease progression. Lastly, these findings have yet to be tested *in vivo*, which may or may not yield the same conclusions.

A further study used brain-permeable small molecule inhibitors of Hsp90 in an *in vitro* model of α-Syn oligomerization and toxicity, and found that these inhibitors can rescue α-Syn-mediated toxicity and oligomerization in a dose-dependent manner (Putcha, Danzer et al., 2010). Together with the work of Falsone *et al,* this suggests that Hsp90 does in fact promote PD, and is therefore a strong candidate for therapeutic action in PD.

3. Hsp104

Hsp104 is a special case. As described above, Hsp70 is seemingly efficient in preventing α-Syn aggregation, in the many different models tested. However, Hsp70 is incapable of acting upon and resolving protein aggregates once they have formed. Hsp104 in yeast (*Saccromyces cerevisiae)* is an ATP-dependent chaperone which, alongside Hsp70 and Hsp40, is capable of resolving protein aggregates and cross-β amyloid conformers (Glover and Lindquist, 1998). Unfortunately, there is no equivalent of Hsp104 in the animal kingdom and although the chaperone has apparent beneficial roles, it is puzzling why it has been lost from metazoan lineages. However, Hsp104's effect on α-Syn has nonetheless been investigated. In a rat model whereby α-Syn and Hsp104 are administered intracerebrally using a lentiviral vector, Hsp104 reduces α-Syn-induced toxicity and the

formation of inclusions. As it was difficult to determine whether Hsp104 was preventing aggregation, or disassembling α-Syn after it had aggregated, the effect of Hsp104 was also tested *in vitro*. Here, it was successfully found to rapidly disassemble fibrillar α-Syn to yield the soluble form, an action which is further enhanced by Hsc70 and Hdj2 (Lo Bianco, Shorter et al., 2008). It remains to be tested whether Hsp104 has the same effect *in vivo*, and whether, in the long run there are detrimental effects of expressing a yeast protein in a mammalian system.

4. Small heat shock proteins: Hsp27 and αB-crystallin

Along with Hsp70, Hsp27 is one of the main inducible heat shock proteins in the nervous system, and proffers protection against a variety of stresses, including heat or oxidative stress. Interestingly, in 2004 Zourlidou *et al* suggested that Hsp27, to a **greater** extent than Hsp70, was protective against α-Syn-mediated cell death. Hsp27 was shown to reduce α-Syn-induced cell death in neuronal cell lines and cultures of midbrain dopaminergic cells (Zourlidou, Payne Smith et al., 2004), and to reduce aggregation in cell culture (Outeiro, Klucken et al., 2006).

αB-crystallin (also known as HspB5) is found primarily in the lens of the eye, and has high homology with the small heat shock proteins (Ingolia and Craig, 1982). αB-crystallin carries out chaperone-like roles in under stress conditions (Augusteyn, 2004), which is thought to be important in maintaining the transparency of the lens and preventing cataracts (Maulucci, Papi et al., 2011). Against α-Syn, αB-crystallin was shown to be a potent inhibitor of α-Syn fibril assembly *in vitro*, through its interaction with partially folded α-Syn monomers (Rekas, Adda et al., 2004; Outeiro, Klucken et al., 2006; Rekas, Jankova et al., 2007).

Thesis work

MY THESIS

The aim of my thesis was to expand the catalogue of known effects of molecular chaperones on α-Syn, by documenting the effect of two previously unstudied molecular chaperones on the assembly of α-Syn into fibrils: Hsc70, the human constitutive heat shock protein, and Ssa1p, the yeast equivalent of Hsc70. Even though Hsc70 is one of the first chaperones to encounter α-Syn in the early stages of PD on account of it being constitutively expressed, the interaction of α-Syn with Hsc70 had not been previously documented. The research that I carried out in Ronald Melki's group, "Protein folding in vivo and conformational disease" is divided into three parts, two of which focus on the PD-incriminated protein α-Syn, with a third project based on the interaction of the yeast prion protein Ure2p, with Ssa1p.

Before my arrival, α-Syn had not been studied to a great extent in the laboratory, aside from Ronald Melki's involvement with rat α-Syn, while elucidating the effect of PA700 - the regulatory complex of the 26S proteasome - on α-Syn assembly. However, preceding members of the laboratory had published comprehensive work detailing the interaction of molecular chaperones with the aggregation prone protein in two yeast prion models: Ure2p (Savistchenko, Krzewska et al., 2008) and Sup35p (Krzewska and Melki, 2006).

Branching away from yeast to study a human aggregating protein associated with Parkinson's disease, we not only documented the effect of Hsc70, Ssa1p and their respective co-chaperones on α-Syn assembly, but characterized these interactions on a molecular scale.

Finally, I had a small role in a project investigating the interaction of Ssa1p with the yeast prion Ure2p, which is described in the annex due to the change in topic. This work allowed me to become familiar with the tools that I am currently using to determine the site of interaction between α-Syn and Ssa1p, to design a minichaperone.

Part one

PART ONE

Article 1: Hsc70 Protein Interaction with Soluble and Fibrillar α-Synuclein.

Samantha Pemberton, Karine Madiona, Laura Pieri, Mehdi Kabani, Luc Bousset, Ronald Melki (2011). J Biol Chem 286 (40): 34690-34699.

Article 2: The interaction of Hsc70 protein with fibrillar α-Synuclein and its therapeutic potential in Parkinson's disease.

Samantha Pemberton, Ronald Melki (2012). Communicative and Integrative Biology, in press.

OBJECTIVE

Although the subject of molecular chapeone action on α-Syn assembly has been extensively studied, no one had yet to investigate the effect of the constitutively expressed human Hsp, Hsc70.

Based on the facts that Hsp70 and Hsc70 do not have the same cellular function, and have been shown to have different effects on aggregated luciferase and polyQ protein, as earlier described, and that the constitutive chaperone encounters α-Syn before its inducible counterpart Hsp70, we thought it beneficial to characterize the effect of Hsc70 on α-Syn.

We wanted to find out what effect Hsc70 has on α-Syn. Does it play a similar, protective role against α-Syn assembly akin to that of Hsp70; an opposite, fibril-promoting effect comparable with Hsp90, or even a potent role in the dissassembly of α-Syn aggregates, similar to that of the yeast chaperone Hsp104? Studying the interaction of α-Syn with molecular chaperones allows us to identify which are effective in inhibiting α-Syn, provides more information about the molecular mechanisms responsible for PD, and helps target future therapeutic strategies.

As first author of the following paper published in *The Journal of Biological Chemistry*, I had the major role in this research, with help from colleagues with specific techniques for

example analytical ultracentrifugation and electron microscopy. I wrote the article with help and guidance from my thesis director and the team leader, Ronald Melki.

Following publication of this article, we were contacted by the Editor of *Communicative and Integrative Biology*, and invited to write an addendum - essentially an auto-commentary piece to include views and opinions - which was then accepted for publication, and follows the J Biol Chem article in its in press format.

THE JOURNAL OF BIOLOGICAL CHEMISTRY VOL. 286, NO. 40, pp. 34690–34699, October 7, 2011

Hsc70 Protein Interaction with Soluble and Fibrillar α-Synuclein*[S]

Received for publication, May 18, 2011, and in revised form, August 9, 2011 Published, JBC Papers in Press, August 10, 2011, DOI 10.1074/jbc.M111.261321

Samantha Pemberton, Karine Madiona, Laura Pieri, Mehdi Kabani, Luc Bousset, and Ronald Melki[1]

From the Laboratoire d'Enzymologie et Biochimie Structurales, CNRS, 91198 Gif-sur-Yvette, France

The aggregation of α-synuclein (α-Syn), the primary component of Lewy bodies, into high molecular weight assemblies is strongly associated with Parkinson disease. This event is believed to result from a conformational change within native α-Syn. Molecular chaperones exert critical housekeeping functions *in vivo* including refolding, maintaining in a soluble state, and/or pacifying protein aggregates. The influence of the stress-induced heat shock protein 70 (Hsp70) on α-Syn aggregation has been notably investigated. The constitutively expressed chaperone Hsc70 acts as an antiaggregation barrier before cells are overwhelmed with α-Syn aggregates and Hsp70 expression induced. Here, we investigate the interaction between Hsc70 and α-Syn, the consequences of this interaction, and the role of nucleotides and co-chaperones Hdj1 and Hdj2 as modulators. We show that Hsc70 sequesters soluble α-Syn in an assembly incompetent complex in the absence of ATP. The affinity of Hsc70 for soluble α-Syn diminishes upon addition of ATP alone or together with its co-chaperones Hdj1 or Hdj2 allowing faster binding and release of client proteins thus abolishing α-Syn assembly inhibition by Hsc70. We show that Hsc70 binds α-Syn fibrils with a 5-fold tighter affinity compared with soluble α-Syn. This suggests that Hsc70 preferentially interacts with high molecular weight α-Syn assemblies *in vivo*. Hsc70 binding certainly has an impact on the physicochemical properties of α-Syn assemblies. We show a reduced cellular toxicity of α-Syn fibrils coated with Hsc70 compared with "naked" fibrils. Hsc70 may therefore significantly affect the cellular propagation of α-Syn aggregates and their spread throughout the central nervous system in Parkinson disease.

Fibrillar α-synuclein (α-Syn)[2] is one of the principal components of intracellular Lewy bodies, whose presence in the central nervous system is a defining feature of Parkinson disease (PD) and other synucleinopathies (1). Symptoms of PD are apparent after more than 70% of dopaminergic terminals and/or neurons have been lost, with some of the remaining neurons containing filamentous α-Syn. The precise cellular function of soluble α-Syn is unknown. There is, however, evidence that it plays an important role at presynaptic termini (2–4) and it has recently been suggested that the protein is a cellular ferrireductase (5). Various factors, including genetic susceptibility and environmental influences, can induce the aggregation of the naturally unfolded, soluble α-Syn (6, 7), leading to PD pathogenesis.

Molecular chaperones assist newly synthesized proteins to reach their native-fold and are in charge of refolding misfolded or unfolded proteins (8). As the progression of PD is strongly associated with a change in α-Syn solubility, which is widely believed to be the consequence of a conformational change, there has been significant focus on the possible therapeutic role of molecular chaperones in the past 5 years (9). Previous investigations have focused on heat shock protein 70 (Hsp70) (10–13), a molecular chaperone whose expression is induced when a cellular environment is under stress such as heat shock, ischemia, or other stresses (14). The reports are, however, conflicting as, whereas Hsp70 has been shown to inhibit α-Syn fibril formation (11, 15), protect against α-Syn toxicity *in vitro* (13, 16, 17), and to reduce the amount of α-Syn aggregates *in vivo* (13), Hsp70 overexpression has also been shown neither to influence the formation of α-Syn oligomeric species nor to counteract the unbeneficial motor deficits associated to α-synucleinopathy in a mouse model (18).

The constitutively expressed heat shock protein Hsc70 is a major member of the 70-kDa HSP family (19). Human Hsc70 and Hsp70 share 85% primary structure identity, and whereas it has always been thought that the two chaperones play similar cellular roles, there is evidence to prove otherwise (20, 21). Hsc70 and its co-chaperones from the HSP40 family confront high molecular weight α-Syn assemblies prior to Hsp70, as the expression of the latter protein is stress dependent. Thus, Hsc70 action, if any, is critical in the early stages of α-Syn aggregation. It is only when this constitutive molecular chaperone and its co-chaperones are overwhelmed that Hsp70 expression is induced and comes into play.

Here we document the effect of Hsc70 on α-Syn assembly. We show that Hsc70 inhibits α-Syn assembly by sequestering it in an assembly incompetent state, and describe the nucleotide dependence of this interaction. An interaction between Hsc70 and preformed α-Syn fibrils is also described and we show that the fibrils can be saturated with Hsc70. The affinities of Hsc70 for soluble and fibrillar α-Syn were determined and the apparent dissociation constants measured show that Hsc70 binds to fibrillar α-Syn with a higher affinity. The effect of Hsc70 co-

* This work was supported by the French Ministry of Education, Research and Technology, the Centre National de la Recherche Scientifique (CNRS), the Era-Net Neuron, Agence Nationale pour la Recherche Grant ANR-08-NEUR-001-01, and the Human Frontier Science Program.

This work is dedicated to Dr. Tamas Erdos.

[S] The on-line version of this article (available at http://www.jbc.org) contains supplemental Figs. S1–S5.

[1] To whom correspondence should be addressed. Tel.: +33-6982-3503; E-mail: melki@lebs.cnrs-gif.fr.

[2] The abbreviations used are: α-Syn, alpha-synuclein; Hsc, constitutive heat shock protein; PD, Parkinson disease; SDD-AGE, semi-denaturing detergent-agarose gel electrophoresis; ThioT, thioflavin T; Tricine, *N*-[2-hydroxy-1,1-bis(hydroxymethyl)ethyl]glycine.

chaperones Hdj1 and Hdj2 on α-Syn assembly is also documented. Finally, our results reveal a major conformational change within Hsc70 upon binding to oligomeric α-Syn, and a reduced toxicity of α-Syn fibrils coated with Hsc70 compared with "naked" α-Syn fibrils.

EXPERIMENTAL PROCEDURES

Expression and Purification of α-Syn, Hsc70, and Its Co-chaperones Hdj1 and -2—Recombinant wild-type α-Syn was expressed in *Escherichia coli* strain BL21(DE3) (Stratagene) and purified as described (22). α-Syn concentration was determined spectrophotometrically using an extinction coefficient of 5960 M^{-1} cm^{-1} at 280 nm. Pure α-Syn (0.5–1 mM) in 50 mM Tris-HCl, pH 7.5, 50 mM KCl was filtered through sterile 0.22-μm filters and stored at −80 °C.

The vectors allowing the bacterial expression of His_6, N-terminal-tagged Hsc70, Hdj1, and Hdj2 were obtained by subcloning the BamHI-NotI fragments from pcDNA5/FRT/TO-HSPA8 (Hsc70), pcDNA5/FRT/TO-DNAJB1 (Hdj1), and pcDNA5/FRT/TO-DNAJA1 (Hdj2) plasmids (23) into pPRO-EX-HTb (Invitrogen) at the same cloning sites. BL21(DE3) *E. coli* were transformed with the resulting expression vectors. The cells were then grown to an absorbance at 600 nm of 2 in a 16-liter fermentor at 37 °C. Protein expression was induced with 0.5 mM isopropyl 1-thio-β-D-galactopyranoside for 3 h at 20 °C. The cells were harvested and the pellets were resuspended in 25 mM HEPES, pH 7.5, 300 mM NaCl, 5% glycerol, and 5 mM β-mercaptoethanol, and lysed by freezing in liquid nitrogen followed by thawing, addition of 0.1 mg/ml of lysozyme, 10 mM imidazole, and sonication at 4 °C. After centrifugation at 5000 × *g* and 4 °C, the supernatant was loaded onto a nickel-charged chelating Sepharose column (GE Healthcare) equilibrated in 25 mM HEPES, pH 7.5, 300 mM NaCl, 40 mM imidazole, pH 8.0, and 5% glycerol, and eluted by a gradient of 40–500 mM imidazole. The fractions containing Hsc70, Hdj1, and Hdj2 were assembled and dialyzed against 50 mM Tris-HCl, pH 7.5, 150 mM KCl, filtered through a sterile 0.22-μm filter and stored at −80 °C. The activity of the purified Hsc70 alone or in the presence of its co-chaperones Hdj1 and Hdj2 was assessed using a luciferase refolding assay. Briefly, firefly luciferase (Sigma) at 1 mg/ml was denatured in 7 M guanidine hydrochloride for 2 h at room temperature. 1 μl of denatured luciferase was added to 139 μl of refolding buffer (25 mM HEPES, pH 7.5, 50 mM KCl, 5 mM $MgCl_2$, 2 mM DTT) in the absence or presence of Hsc70 (2 μM) alone or Hsc70 and Hdj1 or Hdj2 (2 μM). The mixtures were incubated at 30 °C and the time course of refolding activity was measured, in the absence or presence of 2 mM ATP or ADP, by withdrawing 5-μl aliquots and mixing with 95 μl of luciferase assay reagent (Promega) at different time intervals. Luminescence was only observed in the presence of ATP, suggesting that Hsc70 is only fully functional (binding, refolding, and releasing client proteins) where ATP is present. Luminescence measurements were performed in a Cary Eclipse fluorescence spectrophotometer (Varian Inc., Palo Alto, CA) in bioluminescence mode at 550 nm. Native luciferase activity was taken as 100%. The ATPase activity of Hsc70 alone or in the presence of its co-chaperones and unfolded luciferase was also monitored as described (24).

Assembly of α-Syn into Fibrils—Soluble wild-type α-Syn was assembled in 50 mM Tris-HCl, pH 7.5, 150 mM KCl, 15 μM thioflavin T (ThioT), in the absence or presence of Hsc70, with or without ADP-$MgCl_2$ or ATP-$MgCl_2$ and co-chaperones Hdj1 or Hdj2 in 1-ml cuvettes (path length 1 cm). Assembly was induced by incubating the cuvette at 37 °C with magnetic stirring in the Cary Eclipse spectrofluorimeter with excitation and emission wavelengths set at 440 and 480 nm, respectively, and an averaging time of 10 s. The nature of the oligomeric species was assessed using a Jeol 1400 transmission electron microscope (Jeol Ltd.) following adsorption of the samples onto carbon-coated 200-mesh grids and negative staining with 1% uranyl acetate. The images were recorded with a Gatan Orius CCD camera (Gatan). The assembly of α-Syn into fibrils was also assessed using a sedimentation assay. Aliquots (90 μl) were withdrawn at different time intervals from the assembly reaction and spun at 40,000 × *g* at 20 °C in a TL100 tabletop ultracentrifuge (Beckman). The proteins within the supernatant and pellet fractions were analyzed by SDS-PAGE and quantified following staining/destaining using the ImageJ software.

Analytical Ultracentrifugation—Sedimentation velocity measurements were carried out using a Beckman Optima XL-A ultracentrifuge equipped with an AN60-Ti four-hole rotor and cells with two-channel 12-mm path length centerpieces. 400 μl of protein were spun at 90,000 × *g* at 15 °C. Sample displacement profiles were obtained by recording the absorbance at 280 nm every 5 min. Data were analyzed with the programs Sedfit (25) and Svedberg. The partial specific volume (0.7305 ml/g), buffer viscosity (1.1534 cP), and density (1.00765 g/ml) were calculated with the software Sednterp.

Circular Dichroism—For CD measurements, 5, 10, or 25 μM Hsc70 was incubated for 1 h at 37 °C in 50 mM Tris-HCl, pH 7.5, 50 mM KCl, 0.5 mM ATP, and 0.05 mM $MgCl_2$ with 50 μM soluble α-Syn. Far-UV CD spectra were recorded at 20 °C using a JASCO J-810 dichrograph equipped with a thermostated cell holder using a 0.1-cm path length quartz cuvette. Each spectrum was the average of 10 acquisitions recorded in the 260–195 nm range with 0.5-nm steps, a bandwidth of 2 nm, and at a speed of 100 nm min^{-1}. All spectra were buffer corrected.

Filter Trap Assay, SDS-PAGE, Semidenaturing Detergent-Agarose Gel Electrophoresis (SDD-AGE), and Western Blotting—Binding of Hsc70 to fibrillar α-Syn was followed by a filter retardation assay where fibrils and associated proteins are retained on a membrane. α-Syn fibrils (0.5, 1, or 2 μM) were incubated for 1 h at 37 °C with increasing concentrations of Hsc70 (0.1 to 1 μM), in 650 μl of assembly buffer or 0.5% SDS. 200 μl of each sample were filtered in triplicate through cellulose acetate membranes (0.2 μm pore size, Millipore Corp., Bedford, MA) using a 48-slot slot-blot filtration apparatus (GE Healthcare). After filtration of the sample, 500 μl of buffer or 0.5% SDS were filtered twice in each slot. The cellulose acetate membranes were incubated with 3% skim milk, probed with an antibody against Hsc70 (Assay Designs, MI), and developed with the enzyme-coupled luminescence technique (ECL, Thermo Scientific) according to the recommendation of the manufacturer. SDS-PAGE was performed in 7.5–13% Tricine-SDS-polyacrylamide gels (26).

SDD-AGE was carried out as previously described (27). Briefly, samples of α-Syn (100 μM) in the absence or presence of Hsc70 (1–10 μM), at the beginning (0 min) or at the steady state of the assembly reaction (1000 min) were mixed with 4× sample buffer (2× Tris acetate-EDTA (TAE), 20% glycerol, 8% SDS, 0.05% bromphenol blue). After 10 min of incubation at room temperature, samples were loaded onto a 1.6% agarose gel in 1× TAE buffer containing 0.1% SDS. Following electrophoresis, proteins were blotted onto nitrocellulose membranes by capillary transfer in Tris-buffered saline buffer. The membrane was analyzed by Western blotting using an anti-α-Syn antibody (BD Biosciences) and chemiluminescence reagents (Pierce) before stripping the antibody by heating for 1 h at 50 °C in 62.5 mM Tris-HCl, pH 6.8, 2% SDS, 100 mM β-mercaptoethanol, and reanalyzing with an anti-Hsc70 antibody (Assay Designs) and chemiluminescence reagents.

Cell Viability Assays—Murine endothelioma H-END cells were kindly provided by Prof. F. Bussolino (University of Turin, Italy) and cultured in Dulbecco's modified Eagle's medium containing 10% fetal bovine serum (FBS), 2.0 mM glutamine, 100 units/ml of penicillin, and 100 μg/ml of streptomycin in a 5% CO_2 humidified atmosphere at 37 °C. All materials used for cell culture were from PAA Laboratoires GmbH (Pasching, Austria). The toxicity of soluble and fibrillar α-Syn was assessed by the 3-(4,5-dimethylthiazol-2-yl)-2,5-diphenyltetrazolium bromide reduction inhibition assay, as previously described (28). Formazan absorbance was measured at 570 nm in a FlexStation3 microplate reader (Molecular Devices).

RESULTS

Effect of Hsc70 on α-Syn Assembly—The effect of Hsc70 on α-Syn assembly was monitored using ThioT binding, a widely used dye that fluoresces upon binding to fibrillar species (29), and electron microscopy (EM). In the absence of Hsc70, α-Syn readily assembles into fibrils *in vitro*, with a lag phase of ~160 min at 100 μM. The lack of fibrils at the onset of the assembly reaction, and their presence after 1000 min was confirmed by EM after negative staining (Fig. 1*A*). The length of the lag phase preceding α-Syn assembly increased upon addition of increasing concentrations of Hsc70, indicating that the chaperone slows down α-Syn assembly. EM images of sample aliquots removed at the steady state show that as the concentration of Hsc70 increases, there are less and less fibrils present with a concomitant increase in the amount of oligomeric species (Fig. 1*B*). Where 10 μM Hsc70 is present (molar ratio 1:10, Hsc70:α-Syn), no fibrils are observed in the electron microscope, even though a high ThioT signal was measured. This shows that ThioT not only binds to fibrillar α-Syn but also to the high molecular weight α-Syn-Hsc70 assemblies. The affinity of Hsc70 for soluble α-Syn (Fig. 1*C*) was derived from measurements of the elongation rates of a constant α-Syn concentration in the presence of increasing concentrations of Hsc70. The observed dissociation constant (K_d) was 0.5 μM^{-1}.

The Interaction between Soluble α-Syn and Hsc70—To assess the consequences of Hsc70 addition to assembly competent α-Syn, and better characterize the oligomeric species that form in the presence of Hsc70, we adapted a SDD-AGE assay, first designed to assess the aggregation of yeast prions (30). Comparison of the SDD-AGE profiles of α-Syn in the absence and presence of increasing amounts of Hsc70 at the onset of assembly and at steady state reveal the formation, with time, of α-Syn-Hsc70 assembly incompetent complexes. Although a smear characteristic of fibrillar material was observed upon incubation of α-Syn in the absence of Hsc70, it is no longer apparent in the presence of increasing concentrations of Hsc70. Instead, a slower migrating band was observed, the intensity of which increases with increasing concentrations of Hsc70. This α-Syn band co-localizes with Hsc70 on the gels. This strongly suggests the formation of an α-Syn·Hsc70 assembly incompetent complex.

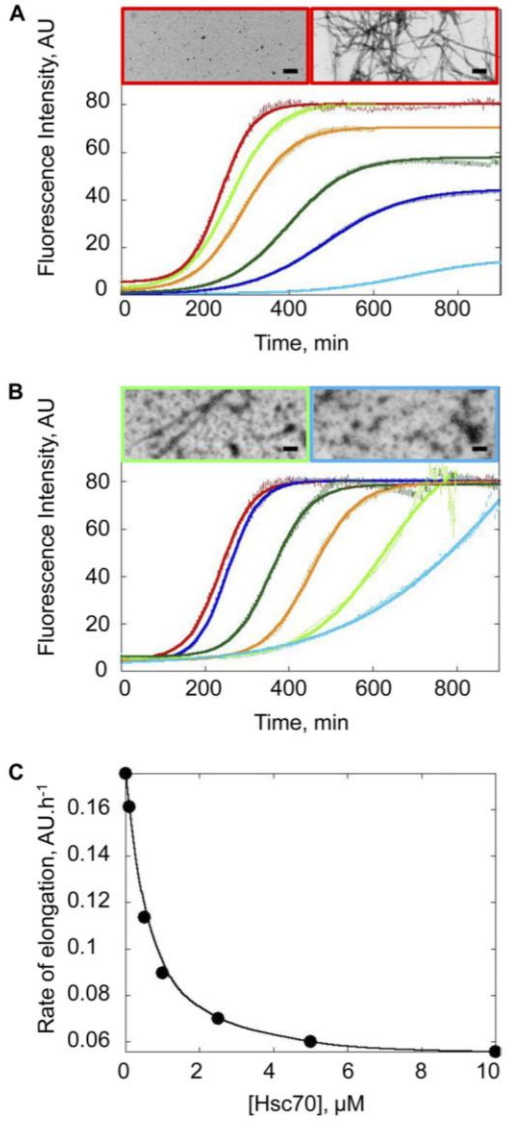

FIGURE 1. **Assembly of α-Syn in the presence of Hsc70.** *A*, time courses of α-Syn assembly at 37 °C and increasing concentrations (10 μM, *light blue*; 20 μM, *dark blue*; 30 μM, *dark green*; 60 μM, *orange*; 80 μM, *light green*; and 100 μM, *red*) in 50 mM Tris-HCl, pH 7.5, 150 mM KCl. The assembly reactions were monitored by ThioT binding. *AU*, arbitrary units. Negative stained electron micrographs of α-Syn (100 μM) at 0 min (*left*) and 1000 min (*right*) after the onset of the assembly reaction. *Bar*, 0.2 μm. *B*, time courses of α-Syn (100 μM) assembly in the absence (*red*) and presence of increasing amounts of Hsc70 (0.1 μM, *dark blue*; 0.5 μM, *dark green*; 1 μM, *orange*; 5 μM, *light green*; 10 μM, *light blue*). Negative stained electron micrographs of α-Syn (100 μM) assemblies obtained in the presence of 5 (*left*) or 10 μM Hsc70 (*right*) at 1000 min. *Bar*, 0.2 μm. *C*, rate of α-Syn fibril elongation at a constant α-Syn concentration (100 μM) and increasing Hsc70 concentrations (0.1–10 μM).

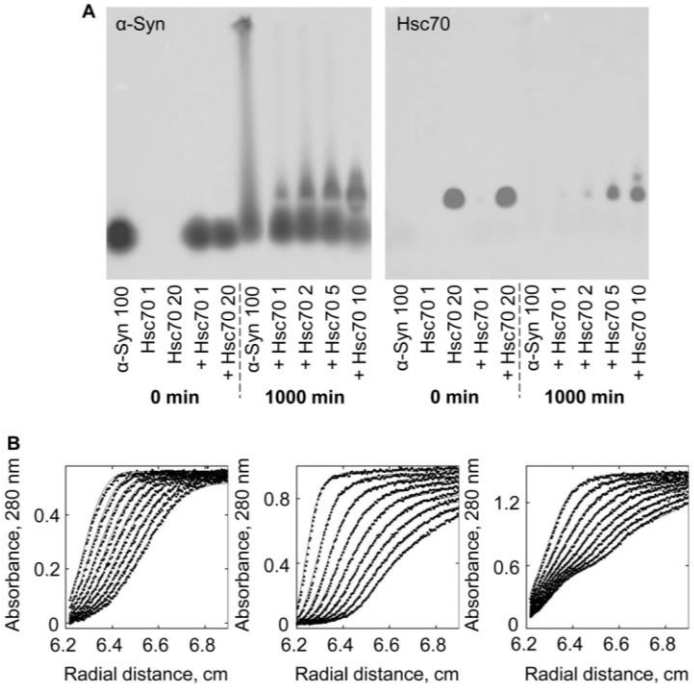

FIGURE 2. **Soluble α-Syn-Hsc70 interaction.** *A*, anti-α-Syn (*left*) and anti-Hsc70 (*right*) antibody staining after SDD-AGE analysis and Southern blotting onto nitrocellulose membranes of sample aliquots at the onset of assembly (0 min) and at the steady state (1000 min). The concentration of α-Syn (100 μM) is held constant, although Hsc70 varies from 1 to 10 μM as indicated. *B*, sedimentation velocity of α-Syn (80 μM, *left*), Hsc70 (20 μM, *middle*), and α-Syn/Hsc70 mixture (80 and 20 μM, respectively, *right*) in 50 mM Tris-HCl, pH 7.5, 150 mM KCl. The positions of the moving boundaries shown were recorded at 5-min intervals by spectrophotometric scanning at 280 nm. The *continuous lines* are best fits of the experimental data (●). The rotor speed was 180,000 × *g* and the temperature 15 °C.

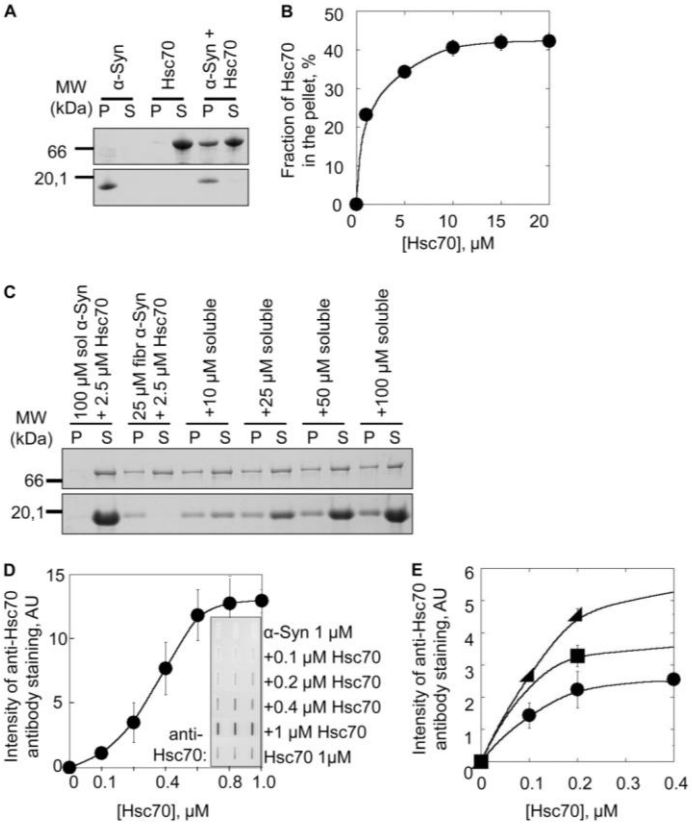

FIGURE 3. **Fibrillar α-Syn-Hsc70 interaction.** *A*, SDS-PAGE analysis of the pellet (*P*) and supernatant (*S*) fractions of fibrillar α-Syn (80 μM), Hsc70 (8 μM), and fibrillar α-Syn (80 μM) incubated with Hsc70 (8 μM) for 1 h at 37 °C. *B*, fraction of Hsc70 in the pellet after incubation at 37 °C for 1 h at a constant amount of fibrillar α-Syn (80 μM) with increasing concentrations of Hsc70 (0–20 μM), followed by ultracentrifugation at 90,000 × *g* for 20 min. *C*, competition between soluble and fibrillar α-Syn for the binding of Hsc70. The binding of Hsc70 to fibrillar α-Syn was assessed by SDS-PAGE analysis of the pellet and supernatant fractions after incubating fibrillar α-Syn (25 μM) with Hsc70 (2.5 μM) and increasing concentrations of soluble α-Syn (0–100 μM), for 1 h at room temperature. *D*, quantification of the amount of Hsc70 bound to a constant concentration of fibrillar α-Syn (1 μM) using a filter trap assay followed by anti-Hsc70 antibody staining (*inset*) at increasing Hsc70 concentrations (0–1 μM). *E*, quantification of the amount of Hsc70 trapped on nitrocellulose filters in the presence of fibrillar α-Syn (*circle*, 0.5 μM; *square*, 1 μM; *triangle*, 2 μM) at increasing concentrations of Hsc70 (0–0.4 μM). The molecular mass markers (in kilodaltons) are shown to the *left* in *A* and *C*. *AU*, arbitrary units.

Analytical ultracentrifugation is a versatile tool used to characterize protein-protein interactions in solution, under equilibrium conditions. We therefore used analytical ultracentrifugation to further characterize the interaction between soluble α-Syn and Hsc70. Fig. 2*B* shows the sedimentation boundaries of α-Syn (80 μM, *left panel*), Hsc70 (20 μM, *middle panel*), and the α-Syn/Hsc70 mixture (80 and 20 μM, respectively, *right panel*) at regular intervals. Raw data (*symbols*) were modeled to a 1-, 3-, or 4-component system and the best fits (continuous lines) yielded a single species with sedimentation coefficient ($s_{20,w}$) of 1 S for α-Syn; three species with sedimentation coefficients 3.8, 5.7, and 8.2 S for Hsc70, and four species with sedimentation coefficients 1, 3.5, 4.8, and 5.9 S for the α-Syn/Hsc70 mixture. No rapidly sedimenting material was detected while the rotor was accelerating to reach the operating speed (180,000 × *g*), ruling out the presence of large aggregates. The sedimentation coefficient measured for α-Syn (1 S) is compatible with the molecular mass of a natively unfolded 14-kDa polypeptide. The species we observe for Hsc70 have been previously described and correspond to monomeric, dimeric, and oligomeric Hsc70 (31). Determination of sedimentation coefficients gives valuable information on the hydrodynamic shape of protein complexes and conformational changes within these complexes. Instead of an increase in the sedimentation coefficient of Hsc70 in complex with α-Syn, we observed a marked decrease of the sedimentation coefficient of the complex. This is indicative of a major conformational change that takes place within the complex or Hsc70 upon its interaction with α-Syn. This change is further assessed.

The Interaction between Fibrillar α-Syn and Hsc70—To determine whether Hsc70 interacts with not only soluble but also fibrillar α-Syn, preformed α-Syn fibrils were incubated with Hsc70 for 1 h at 37 °C. The fibrils were pelleted, and the pellet and supernatant fractions were analyzed by SDS-PAGE. As shown in Fig. 3*A*, controls show that α-Syn is found solely within the pellet, whereas Hsc70 is in the supernatant. After coincubation, Hsc70 was found in the pellet. This indicates that Hsc70 does indeed bind to fibrillar α-Syn. To further characterize the interaction between fibrillar α-Syn and Hsc70, α-Syn fibrils (60 μM) preincubated for 1 h in the presence of increasing concentrations of Hsc70 (0–20 μM) were spun and the amount of Hsc70 in the supernatants and pellets was determined. This yielded a saturation curve (Fig. 3*B*) showing saturation at a molar ratio of 1:4 for Hsc70:α-Syn. This assay also shows that the binding of Hsc70 to fibrillar α-Syn does not lead to fibrils

disassembly, as seen by the sustained absence of soluble α-Syn in the supernatant fractions following incubation with Hsc70.

Having established that Hsc70 binds to both soluble and fibrillar α-Syn, we designed an assay to determine which form Hsc70 binds preferentially. The assay consisted of challenging Hsc70 bound to α-Syn fibrils with increasing amounts of soluble α-Syn. After the challenge (1 h), the fibrils were sedimented and the amount of Hsc70 in the supernatant and pellet fractions was assessed by SDS-PAGE. The data presented in Fig. 3*C* show clearly that Hsc70 remains bound to fibrillar α-Syn even when 4-fold soluble α-Syn is added to the reaction mixture. This strongly suggests that Hsc70 binds to fibrillar α-Syn with a higher affinity.

To determine the affinity of Hsc70 for fibrillar α-Syn, a filter assay where fibrils are retained on an acetate membrane, along with anything that binds to them was used. After washing to remove unbound protein, the membranes were stained with an anti-Hsc70 antibody. There is minimal Hsc70 retained on the membrane in the absence of α-Syn fibrils. In contrast, Hsc70 is quantitatively retained where fibrils are present (Fig. 3*D*). Using this assay and increasing the concentration of fibrillar α-Syn and Hsc70 we determined the affinity of Hsc70 for α-Syn fibrils. The dissociation constant we measured between α-Syn fibrils and Hsc70 is 0.1 μM^{-1} (Fig. 3*E*), consistent with a tighter binding of the chaperone to fibrillar α-Syn.

Nucleotide Dependence of Hsc70-α-Syn Interaction and Consequences on Assembly—The affinity of Hsc70 for its client polypeptides is modulated by nucleotides (ATP or ADP) (32, 33). We therefore documented the effect of ATP and ADP on the inhibition of α-Syn assembly by Hsc70, knowing that the assembly of α-Syn is unaffected by the presence of ATP or ADP (supplemental Fig. S1). In the absence of added nucleotides, the client protein binding site of Hsc70 is in an open conformation. Hsc70 binds α-Syn and an assembly inhibitory effect is observed (Fig. 4*A*). In the presence of ADP, the Hsc70 client protein binding site is in a closed conformation. Hsc70 does not bind α-Syn and no effect on assembly is observed (Fig. 4*A*). In the presence of ATP, and upon subsequent ATP hydrolysis, the Hsc70 client binding site cycles between an open and a closed conformation with simultaneous binding and release of client proteins within the medium (33, 34). Consistent with this, the assembly of α-Syn into protein fibrils in the presence of Hsc70 and ATP is slightly inhibited but to a lesser extent than observed for nucleotide-free Hsc70 (Fig. 4*A*). In all cases fibrillar α-Syn is observed at steady state (800 min, electron micrographs Fig. 4*B*) under the experimental conditions we used. Limited proteolysis of Hsc70-ATP and Hsc70-ADP shows the ADP state to be more resistant to digestion by proteinase K than the ATP state (supplemental Fig. S2). This is coherent with Hsc70 being in a closed conformation with ADP, as the ATPase domain is less susceptible to protease cleavage, and in an open conformation with ATP. The ability of Hsc70 to correctly refold and release chemically denatured luciferase solely in the presence of ATP (supplemental Fig. S3) and its ATPase activity (supplemental Fig. S4) also demonstrates it is fully functional as its activity is modulated by the nature of added nucleotides. We conclude from our observations that the nucleotide-dependent

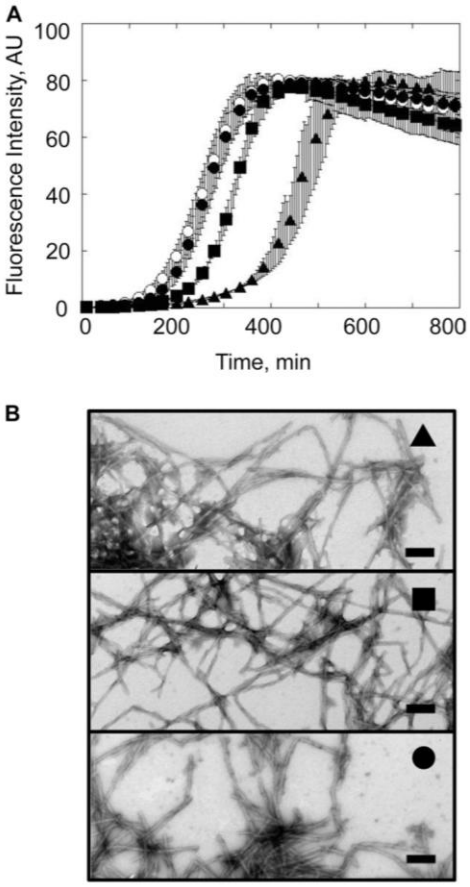

FIGURE 4. **Effect of nucleotides on the assembly of α-Syn in the presence of Hsc70.** *A*, time courses of α-Syn (100 μM) assembly (○) in the presence of Hsc70 (1 μM) in the absence of nucleotide (▲) and the presence of ATP (0.5 mM, ■) or ADP (0.5 mM, ●) in 50 mM Tris-HCl, pH 7.5, 150 mM KCl, 0.05 mM $MgCl_2$. *B*, negative stained electron micrographs of α-Syn assemblies at 1000 min, labeled with *symbols* corresponding to those used for the assembly reactions shown in *A*. *Bar*, 0.2 μm. *AU*, arbitrary units.

effect of Hsc70 on α-Syn assembly is due to changes in the proportion of open and closed forms of Hsc70.

Hsc70 Sequesters α-Syn in an Assembly Incompetent State—Preformed α-Syn fibrils elongate by efficient incorporation of the soluble form of the protein, which can be followed using the ThioT binding assay. The aggregation of α-Syn into nonfibrillar oligomeric species in the presence of Hsc70 is also accompanied by an increase in ThioT fluorescence (Fig. 1*B*). We therefore followed the time course of elongation by assessing the decrease of soluble α-Syn in the supernatant and concomitant increase of fibrillar α-Syn in the pellet fractions, after incubation of soluble α-Syn with preformed fibrils and ultracentrifugation using SDS-PAGE. This experiment was performed at room temperature without agitation so that the soluble α-Syn would not assemble. Fig. 5 shows that the vast majority of the soluble α-Syn has been incorporated into the fibrils within 3 h. In contrast, soluble α-Syn remained in the supernatant fraction upon incubation with fibrillar α-Syn when it was preincubated for 30 min with Hsc70 (Fig. 5). This indicates that soluble α-Syn in complex with Hsc70 is not incorporated into preformed fibrils, in other words that Hsc70 sequesters α-Syn in an assembly incompetent state. Interestingly, and in agreement with the higher affinity of Hsc70 for fibrillar

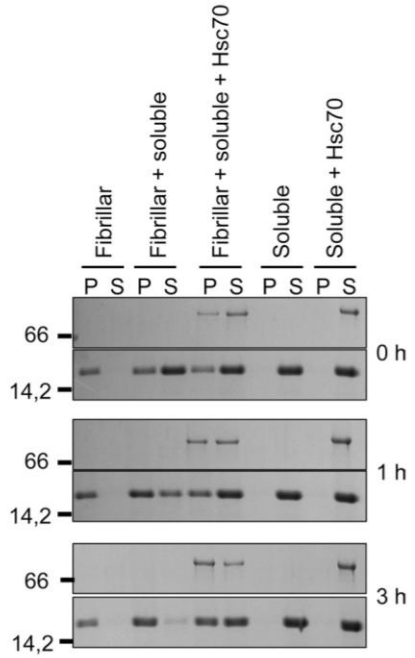

FIGURE 5. **Inhibition of soluble α-Syn incorporation within preformed α-Syn fibrils by Hsc70.** Time course of fibrillar α-Syn elongation assessed by SDS-PAGE analysis of the pellet (*P*) and supernatant (*S*) fractions after incubating fibrillar α-Syn (25 μM) with soluble α-Syn (25 μM) in the absence or presence of Hsc70 (2.5 μM), as indicated. The molecular mass markers (in kilodaltons) are shown to the *left* of the panel.

α-Syn we measured, a progressive binding of Hsc70 to the fibrils was observed (Fig. 5).

Hsc70 Undergoes a Major Conformational Change upon Binding α-Syn—Hsc70 undergoes a remarkable conformational change upon interacting with α-Syn as revealed by the analytical ultracentrifugation measurements we performed (Fig. 2). We further assessed the conformational change accompanying α-Syn binding to Hsc70 using tryptophan fluorescence measurements. Upon titration of different concentrations of Hsc70 (5, 10, or 25 μM) by increasing concentrations of α-Syn (0–100 μM) (Fig. 6*A*), there is an overall decrease in tryptophan fluorescence (excitation and emission wavelengths 285 and 305 nm, respectively) (Fig. 6*B*). It is important to note that the changes in fluorescence seen are not the result of Hsc70 aggregation or α-Syn assembly, which we have controlled by measuring the light scattering of the samples (Fig. 6*A, inset*). We then used circular dichroism to further confirm a conformational change. Fig. 6*C* shows the CD spectrum of α-Syn, Hsc70, and α-Syn incubated with Hsc70 for 1 h. The theoretical spectrum of the α-Syn·Hsc70 complex is also shown. A significant difference at 222 nm was observed upon subtracting the experimental spectrum from the theoretical spectrum (Fig. 6*D*). This change corresponds to a decrease in Hsc70 α-helical content. This change varies from 6 to 9% depending on the Hsc70:α-Syn ratio. Finally, whereas a linear increase in tryptophan fluorescence is recorded for increasing concentrations of Hsc70 alone, no such increase was observed in the presence of a constant, saturating concentration of α-Syn (Fig. 6*E*). When the contribution of increasing concentrations of Hsc70 was subtracted from the overall fluorescence signal, a very significant decrease in tryptophan fluorescence was observed (Fig. 6*F*). We used this change to assess whether Hsc70 co-chaperones Hdj1 or Hdj2 further affect this conformational change. Neither Hdj1 nor Hdj2 affected the Hsc70 conformational change mediated by its interaction with soluble α-Syn.

Hsc70 Co-chaperones Hdj1 and Hdj2 and the Assembly of α-Syn into Fibrils—We first assessed the effect of Hdj1 and Hdj2 on α-Syn assembly into fibrils in the absence or presence of Hsc70. As the ThioT signal we recorded upon assembling α-Syn in the presence of Hsc70 and Hdj1 or Hdj2 were noisy, the reactions were monitored by removing aliquots at different time intervals from the assembling samples, spinning the aliquot at 40,000 × *g*, and quantifying the disappearance of α-Syn from the supernatant and appearance of fibrillar α-Syn by SDS-PAGE. The assembly kinetics of α-Syn (100 μM) in the presence Hsc70 or Hdj1 alone (1 μM) and Hsc70 and Hdj1 (1 μM each) are presented in Fig. *7A*. Hdj1 on its own slows down the assembly of α-Syn into fibrils. The Hsc70 concentration we used throughout these experiments (1 μM) significantly delays α-Syn assembly (Fig. 1*B*). Thus, α-Syn assembly should be further slowed down if the effects of Hsc70 and Hdj1 were additive when both proteins are present within the assembly reaction. Surprisingly, the assembly kinetics of α-Syn in the presence of Hsc70 and Hdj1 and α-Syn in the absence of added chaperones and co-chaperones overlay perfectly well, suggesting that Hdj1 abolishes the assembly inhibitory effect of Hsc70. Similar observations were made with Hdj2 (Fig. 7*B*). Unlike Hdj1, however, Hdj2 alone has no effect on the assembly of α-Syn. This is consistent with previous work describing the independent effects of DNAJB (Hdj1) and DNAJA (Hdj2) co-chaperone subfamilies on the aggregation of polyglutamine-containing proteins (35). Hsc70 sequesters α-Syn in an assembly incompetent state (Fig. 1*B*). Hsc70 affinity for α-Syn decreases in the presence of ATP and its assembly inhibitory effects diminishes (Fig. 4*A*). In the presence of ATP, Hdj1 or Hdj2 speed up the binding and release of client proteins from Hsc70. Thus, the amount of assembly competent α-Syn is higher in the presence of Hsc70 and Hdj1 or Hdj2 than in the presence of Hsc70 or its co-chaperones alone. In addition, the amounts of free Hsc70 and Hdj1 or Hdj2 decrease when the chaperone and co-chaperones are present together because of their interaction. Our observations suggest therefore that Hsc70 co-chaperones most probably counteract the Hsc70 inhibitory activity by increasing the amounts of free assembly competent α-Syn.

We then examined the effect of Hdj1 and Hdj2 on Hsc70 interaction with fibrillar α-Syn. Control reactions where α-Syn fibrils (60 μM) were incubated in the presence of Hdj1 or Hdj2 alone revealed that both co-chaperones bind to α-Syn fibrils with a high affinity as witnessed by their co-sedimentation with fibrillar α-Syn (Fig. 7*C*). In the presence of Hdj1, increased amounts of Hsc70 bind to and sediment with α-Syn fibrils. A similar increased Hsc70 binding to the fibrils, although to a lesser extent, was observed in the presence of Hdj2. The yeast orthologs of Hdj1 and Hdj2, Sis1p and Ydj1p, are widely believed to bind client proteins and facilitate their interaction with Ssa1p, the Hsc70 yeast ortholog (36). Our observations are consistent with this view and suggest that Hdj1 and Hdj2 mediate the binding of Hsc70 to α-Syn fibrils. Alternatively, the increased binding of Hsc70 to α-Syn fibrils could simply be due to the binding of Hsc70 to fibril-bound Hdj1 or Hdj2.

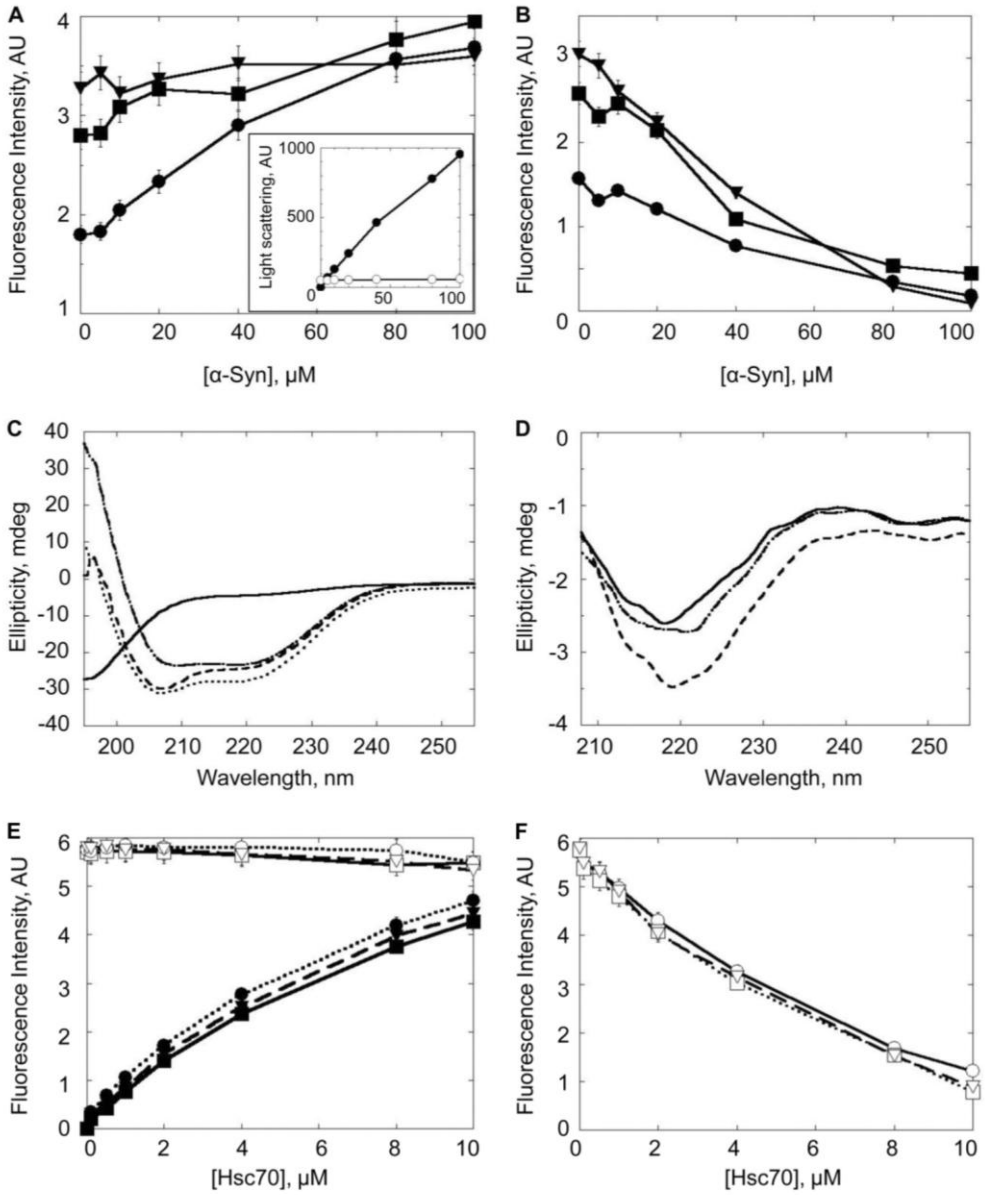

FIGURE 6. **Conformational changes within Hsc70 upon interaction with soluble α-Syn.** *Top panels*, changes in tryptophan fluorescence (excitation 285 nm, emission 305 nm) of Hsc70 incubated for 1 h at 37 °C, in 50 mM Tris-HCl, pH 7.5, 150 mM KCl, 0.5 mM ATP, and 0.05 mM $MgCl_2$ with increasing concentrations of soluble α-Syn. *A*, fluorescence intensity recorded for 5 μM Hsc70 (●), 10 μM Hsc70 (■), or 25 μM Hsc70 (▼) with increasing concentrations of α-Syn. *Inset*, light scattering (at 350 nm) of Hsc70 (25 μM) with increasing concentrations of α-Syn (0.1 to 100 μM) (○) and fibrillar α-Syn as a control (0 to 100 μM, ●). *B*, change in fluorescence intensity after subtracting the contribution of α-Syn from the overall signal in α-Syn/Hsc70 mixtures. *Middle panel*, far-UV circular dichroism. *C*, spectra of Hsc70 (25 μM, *dot-dashed line*), α-Syn (50 μM, *solid line*), and α-Syn·Hsc70 complex (*dashed line*). The latter spectrum clearly differs from the theoretical one (*dotted line*) obtained by summing the spectra of Hsc70 and α-Syn. *D*, difference spectra obtained upon subtracting experimental spectra for 5 (*solid line*), 10 (*dot-dashed line*), or 25 μM (*dotted line*) Hsc70 with 50 μM α-Syn from the calculated theoretical respective spectra. The spectra were obtained at 20 °C using a JASCO J-810 dichrograph equipped with a thermostated cell holder using a 0.1-cm path length quartz cuvette. Each spectrum was the average of 10 acquisitions recorded in the 260–195 nm range with 0.5-nm steps, a bandwidth of 2 nm, and at a speed of 100 nm min^{-1}. *Lower panel,* changes in tryptophan fluorescence (excitation 285 nm, emission 305 nm) of α-Syn (100 μM) incubated for 1 h at 37 °C, in 50 mM Tris-HCl, pH 7.5, 150 mM KCl, 0.5 mM ATP, and 0.05 mM $MgCl_2$ with increasing concentrations of Hsc70 (0.1 to 10 μM, *solid line*), Hsc70 and Hdj1 (*dotted line*), or Hsc70 and Hdj2 (*dashed line*). *A*, fluorescence intensity recorded for increasing concentrations of Hsc70, Hsc70 and Hdj1, or Hsc70 and Hdj2 alone (*filled symbols*) or in the presence of α-Syn (*open symbols*). *B*, change in fluorescence intensity after subtracting the contribution of Hsc70, Hsc70 and Hdj1, or Hsc70 and Hdj2 from the overall signal in α-Syn-Hsc70, Hsc70 and Hdj1, or Hsc70 and Hdj2 mixtures.

Physiological Consequences of Hsc70 and Its Co-chaperones Interacting with Fibrillar α-Syn—We then assessed the physiological consequences of the interaction of Hsc70 with α-Syn fibrils in the absence or presence of ATP and co-chaperones. α-Syn fibril toxicity was assessed using murine endothelioma H-END cells, previously shown to be highly affected by different protein assemblies (28, 37) using the 3-(4,5-dimethylthiazol-2-yl)-2,5-diphenyltetrazolium bromide assay. Fig. 8*A* shows that neither soluble α-Syn nor Hsc70 and its co-chaperones affect cell viability. In contrast, α-Syn fibrils are highly toxic to the cells as witnessed by the 52 ± 1% reduction in cell viability observed upon treatment of the cells for 24 h with 1 μM α-Syn fibrils (Fig. 8*B*). We then determined whether α-Syn fibril toxicity is affected upon their incubation with Hsc70 and/or its co-chaperones. Preformed α-Syn fibrils were therefore incubated for 1 h at 37 °C in the presence of Hsc70, Hdj1,

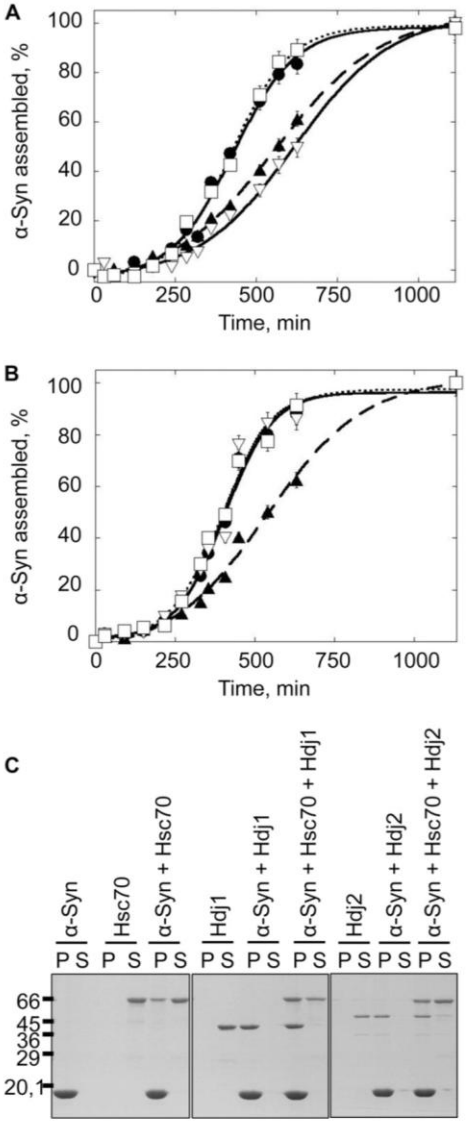

FIGURE 7. **Hdj1 and Hdj2 modulate the interaction between soluble or fibrillar α-Syn and Hsc70.** *A*, time courses of α-Syn (100 μM) assembly in the absence (●) or presence of Hsc70 (1 μM) alone (▲), Hdj1 (1 μM) alone (▽), and Hsc70 and Hdj1 (1 μM each, □) in 50 mM Tris-HCl, pH 7.5, 150 mM KCl, 0.5 mM ATP, and 0.05 mM $MgCl_2$. *B*, time courses of α-Syn (100 μM) assembly in the absence (●) or presence of Hsc70 (1 μM) alone (▲), Hdj2 (1 μM) alone (▽), and Hsc70 and Hdj2 (1 μM each, □) in 50 mM Tris-HCl, pH 7.5, 150 mM KCl, 0.5 mM ATP, and 0.05 mM $MgCl_2$. The assembly reactions in *A* and *B* were monitored by quantifying α-Syn within the supernatant and pellet fractions by SDS-PAGE, as described under "Experimental Procedures." *C*, SDS-PAGE analysis of the pellet (*P*) and supernatant (*S*) fractions of preformed α-Syn fibrils (60 μM) in the absence and presence of Hsc70 (6 μM), Hdj1 (6 μM), Hdj2 (6 μM), or Hsc70 and its co-chaperone (6 μM each), as indicated. Samples were incubated for 1 h at 37 °C prior to 20 min centrifugation at 90,000 × *g*, 20 °C. The molecular mass markers (in kilodaltons) are shown to the *left* of *B*.

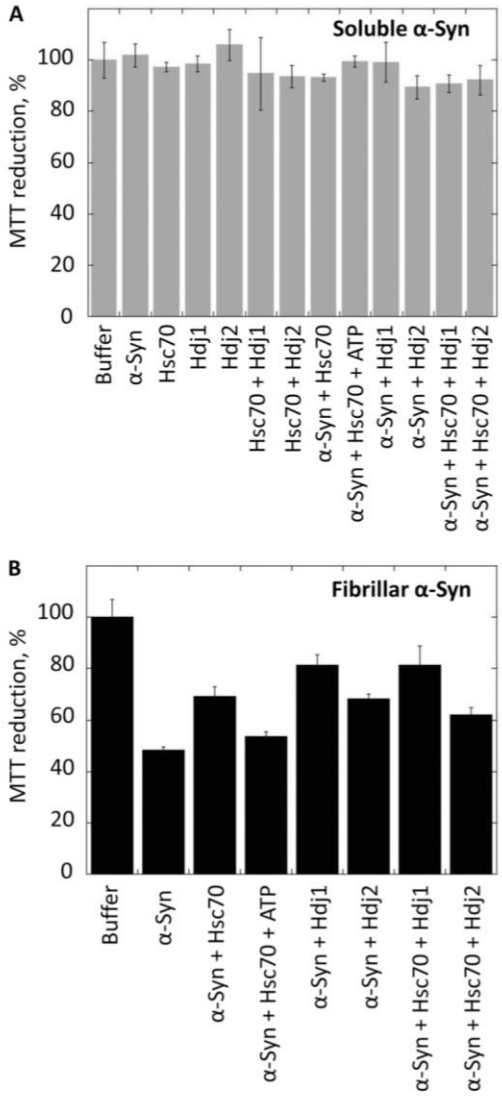

FIGURE 8. **Viability of H-END cells upon exposure to soluble (*A, gray*) or fibrillar (*B, black*) α-Syn in the absence or presence of Hsc70 and/or Hdj1 or Hdj2, as indicated.** Before exposure to cells, soluble or fibrillar α-Syn (100 μM) was incubated for 1 h at 37 °C with Hsc70 (25 μM), Hdj1 (25 μM), Hdj2 (25 μM), Hsc70 and Hdj1 (25 μM each protein), or Hsc70 and Hdj2 (25 μM each protein). Fibrillar α-Syn was centrifuged for 20 min at 16,100 × *g* and the pellet was resuspended in the culture medium to remove unbound Hsc70, Hdj1, or Hdj2. The final protein concentration within the culture medium was 1 μM. The cells were incubated with the different proteins for 24 h. Cell viability is expressed as the percentage of 3-(4,5-dimethylthiazol-2-yl)-2,5-diphenyltetrazolium bromide (*MTT*) reduction using cells treated with the same volume of buffer as a reference (100% 3-(4,5-dimethylthiazol-2-yl)-2,5-diphenyltetrazolium bromide reduction). The values are averages ± S.D. obtained from three independent experiments.

Hdj2 or Hsc70, and Hdj1 or Hdj2. As unbound Hsc70, Hdj1, or Hdj2 could potentially counteract the toxicity of α-Syn fibrils, the fibrils were spun 20 min at 16,100 × *g*. The pelleted fibrils, free of unbound Hsc70, Hdj1, and Hdj2 were resuspended and diluted in the cell culture medium. The proportion of viable cells increases from 48 ± 1% upon addition of α-Syn fibril to 69 ± 3% in the presence of fibrillar α-Syn incubated with Hsc70. The addition of ATP (0.5 mM) to the latter fibrils prior to their dilution in the cell culture medium restores toxicity as the proportion of viable cells decreases to 54 ± 2%. The proportion of viable cells exposed to fibrillar α-Syn incubated with Hdj1 alone is 81 ± 4%, whereas that of fibrillar α-Syn incubated with Hdj2 alone is 68 ± 2%, consistent with the tighter binding of Hdj1 to fibrillar α-Syn (Fig. 7*C*). Similar survival rates (81 ± 7 and 66 ± 3%) were measured for cells exposed to fibrillar α-Syn incubated with Hdj1 and Hsc70 or Hdj2 and Hsc70 suggesting that Hdj1 or Hdj2 and Hsc70 do not counteract toxicity in an additive manner. We conclude from these observations that Hsc70 and its co-chaperones binding to fibrillar α-Syn has physiological consequences in that it reduces the toxicity of α-Syn fibrils. We further conclude, upon comparison of the data presented in Figs. 7*C* and 8*B*, that the toxicity reduction we observe is proportional to the amount of Hsc70 bound to the fibrils as the

latter is significantly higher in the presence of Hdj1 than in the presence of Hdj2 and α-Syn fibrils incubated with Hdj1 and Hsc70 are less toxic than those incubated with Hdj2 and Hsc70.

DISCUSSION

The pathogenesis of PD is strongly associated with the aggregation of α-Syn into high molecular weight assemblies. This is widely believed to result from a conformational change within soluble α-Syn. Molecular chaperones exert critical housekeeping functions *in vivo* including refolding, maintaining proteins in a soluble state, and/or pacifying protein aggregates (8). Hsp90, for example, modulates α-Syn assembly (38). The inducible molecular chaperone, Hsp70, has been previously shown to inhibit α-Syn assembly into fibrils (11, 15). This is also the case in our hands, as shown in supplemental Fig. S5. Hsp70 has also been previously shown to reduce the size of α-Syn aggregates *in vivo*, and protect against α-Syn toxicity (13, 16, 17). However, and in contradiction with the latter, Hsp70 induction has also been shown to be unbeneficial in a mouse model of α-synucleinopathy (18). The constitutive molecular chaperone Hsc70 is among the very first anti-aggregation barriers any aggregation-prone protein must overcome. It is only when Hsc70 activity is overwhelmed that the cellular stress response is induced and the isoform Hsp70 is expressed. Thus, Hsp70 appears late in the cellular response to protein aggregation. Considering that Hsc70 encounters soluble and aggregating α-Syn before its inducible counterpart, it is of importance to investigate the interaction of Hsc70 with soluble and/or fibrillar α-Syn to determine what role, if any, Hsc70 may have in the onset of PD.

We therefore designed experiments to document the interaction between Hsc70 and α-Syn, the consequences of α-Syn-Hsc70 interaction, and the role of modulators of α-Syn-Hsc70 interaction, *e.g.* nucleotides and Hsc70 co-chaperones. We show here that Hsc70, *in vitro* and in the absence of ATP, inhibits α-Syn fibril formation (Fig. 1). Hsc70 binds soluble α-Syn with a high affinity (0.5 μM^{-1}). We show using a technique (SDD-AGE) adapted for α-Syn assembly into fibrils, by electron microscopy analysis and fibril elongation assays that α-Syn is maintained within the α-Syn·Hsc70 complex in an assembly incompetent state (Figs. 1, 2, and 5). The interaction between Hsc70 and α-Syn is, as expected, dependent on the nature of the nucleotide bound to Hsc70 and Hsc70 co-chaperones Hdj1 and Hdj2 (Figs. 4 and 7). We demonstrate that the affinity of Hsc70 for α-Syn decreases in the presence of ATP (Fig. 4) and that the sequestering activity of Hsc70 is abolished in the presence of ATP and Hdj1 or Hdj2 (Fig. 7). Analytical ultracentrifugation, intrinsic fluorescence measurements, and circular dichroism reveal a major conformational change occurring within Hsc70 upon its interaction with α-Syn (Figs. 2 and 6). Finally, we also show that Hsc70 binds fibrillar α-Syn (Fig. 3), the consequence of which is a significant reduction in fibril-associated toxicity (Fig. 8).

The major conformational change within Hsc70 we report unequivocally demonstrates that Hsc70 binds, holds, and releases α-Syn in a nucleotide-dependent manner. By facilitating nucleotide exchange, Hsc70 co-chaperones accelerate the binding, holding, and release cycle. In its Hsc70-bound form, α-Syn is assembly incompetent. Consistent with this is the observation that Hsp70 in the absence of added nucleotides and co-chaperones inhibits α-Syn assembly (see Refs. 11 and 15 and supplemental Fig. S5). In the absence of ATP, the chaperone binds client proteins, but as no nucleotide cycling takes place, the client proteins are not released (33, 34). The inhibition effect seen is therefore simply the consequence of α-Syn sequestration. The functional cycle of Hsp70 comprises ATP binding and hydrolysis, an exchange mediated by co-chaperones. As ATP and co-chaperones Hdj1 or Hdj2 are added to the Hsc70, the system closer resembles that of a cellular environment. The proportion of α-Syn bound at any time to Hsc70 decreases and consequently, the pool of free, assembly competent α-Syn increases leading to a reduction in the molecular chaperone assembly inhibitory effect. Therefore, our study reconciles conflicting results. Indeed, we show that ATP and Hsc70 co-chaperones, which are in abundance *in vivo*, counteract the Hsp70-mediated α-Syn assembly inhibition reported in the absence of added nucleotide. This accounts for why no beneficial effect of Hsp70 overexpression was seen in a mouse model of α-synucleinopathy (18).

The finding that Hsc70 binds to preformed α-Syn fibrils with a higher affinity than soluble α-Syn (Fig. 3) suggests that the main role of Hsc70 within the cell is preferentially binding the high molecular weight α-Syn assemblies as opposed to a minor role in inhibiting α-Syn assembly. We show that besides interacting individually with soluble α-Syn and affecting assembly, Hsc70 co-chaperones Hdj1 and Hdj2 further increase Hsc70 binding to α-Syn assemblies (Fig. 7). Hsc70, Hdj1, and/or Hdj2 binding to high molecular weight α-Syn assemblies undoubtedly affects their physicochemical properties. The first possible consequence is a reduction of α-Syn aggregate size as observed upon overexpression of Hsp70 *in vivo* (18) that could be due to the binding of Hsc70 and its co-chaperones to preformed fibrils, leading to changes in their bundling propensity. The second possible consequence could be a change in the physiological properties of the fibrils. We therefore compared cell viability in the presence of soluble and fibrillar α-Syn in the absence or presence of Hsc70, Hdj1, Hdj2, and Hsc70 and Hdj1 or Hdj2 (Fig. 8). No toxicity was associated to soluble α-Syn in contrast to what is observed for α-Syn fibrils. The binding of Hsc70 and its co-chaperones to fibrillar α-Syn has an important physiological consequence in that it reduces fibril toxicity.

We and others previously contributed evidence for intercellular propagation of α-Syn aggregates *in vivo* (39, 40). α-Syn assemblies were in particular shown to be taken up by cells through endocytosis, interact with intracellular α-Syn and seed the assembly of endogenous α-Syn. The cell-to-cell propagation of α-Syn aggregates was also proposed to contribute to the progressive spreading of α-synucleinopathies throughout the nervous system (41, 42). The changes in the physicochemical properties of the high molecular weight α-Syn assemblies upon binding of Hsc70, Hdj1 and/or Hdj2 could certainly affect their capacity to bind the cell membrane and/or be taken up. Thus, intercellular propagation of α-Syn assemblies that are, for example, actively exported or passively released upon neuronal death in the brain may strongly depend on their Hsc70, Hdj1 and/or Hdj2 surface saturation levels. In other words, the

changes proffered by tightly bound chaperones may be sufficient to interfere with and/or halt cell to cell transmission, and consequently delay the systematic spread of misfolded α-Syn assemblies strongly associated to Parkinson disease. Further characterization of the potential pacifying role of molecular chaperones and co-chaperones will lead to a better understanding of their role in modulating the propagation of misfolded protein assemblies in Parkinson diseases. Such studies together with a thorough description of the changes affecting the cellular proteostasis machinery upon the aggregation of α-Syn will provide additional insights into the molecular events underlying PD pathogenesis and the cellular defenses selected through evolution to suppress the formation of α-Syn assemblies and/or their intercellular propagation.

Acknowledgment—We thank Dr. Harm Kampinga for molecular chaperone plasmids.

REFERENCES

1. Spillantini, M. G., Schmidt, M. L., Lee, V. M., Trojanowski, J. Q., Jakes, R., and Goedert, M. (1997) *Nature* **388,** 839–840
2. Norris, E. H., Giasson, B. I., and Lee, V. M. (2004) *Curr. Top. Dev. Biol.* **60,** 17–54
3. Jakes, R., Spillantini, M. G., and Goedert, M. (1994) *FEBS Lett.* **345,** 27–32
4. Burré, J., Sharma, M., Tsetsenis, T., Buchman, V., Etherton, M. R., and Südhof, T. C. (2010) *Science* **329,** 1663–1667
5. Davies, P., Moualla, D., and Brown, D. R.(2011) *PLoS One* **6,** e15814
6. Uversky, V. N., Li, J., Bower, K., and Fink, A. L. (2002) *Neurotoxicology* **23,** 527–536
7. Ross, C. A., and Smith, W. W. (2007) *Parkinsonism Relat. Disord.* **13,** Suppl. 3, S309–315
8. Vabulas, R. M., Raychaudhuri, S., Hayer-Hartl, M., and Hartl, F. U. (2010) *Cold Spring Harbor Perspect. Biol.* **2,** a004390
9. Witt, S. N. (2010) *Biopolymers* **93,** 218–228
10. Danzer, K. M., Ruf, W. P., Putcha, P., Joyner, D., Hashimoto, T., Glabe, C., Hyman, B. T., and McLean, P. J. (2011) *FASEB J.* **25,** 326–336
11. Dedmon, M. M., Christodoulou, J., Wilson, M. R., and Dobson, C. M. (2005) *J. Biol. Chem.* **280,** 14733–14740
12. Huang, C., Cheng, H., Hao, S., Zhou, H., Zhang, X., Gao, J., Sun, Q. H., Hu, H., and Wang, C. C. (2006) *J. Mol. Biol.* **364,** 323–336
13. Klucken, J., Shin, Y., Masliah, E., Hyman, B. T., and McLean, P. J. (2004) *J. Biol. Chem.* **279,** 25497–25502
14. Richter, K., Haslbeck, M., and Buchner, J. (2010) *Mol. Cell* **40,** 253–266
15. Luk, K. C., Mills, I. P., Trojanowski, J. Q., and Lee, V. M. (2008) *Biochemistry* **47,** 12614–12625
16. Opazo, F., Krenz, A., Heermann, S., Schulz, J. B., and Falkenburger, B. H. (2008) *J. Neurochem.* **106,** 529–540
17. Outeiro, T. F., Klucken, J., Strathearn, K. E., Liu, F., Nguyen, P., Rochet, J. C., Hyman, B. T., and McLean, P. J. (2006) *Biochem. Biophys. Res. Commun.* **351,** 631–638
18. Shimshek, D. R., Mueller, M., Wiessner, C., Schweizer, T., and van der Putten, P. H. (2010) *PLoS One* **5,** e10014
19. Ohtsuka, K., and Suzuki, T. (2000) *Brain Res. Bull.* **53,** 141–146
20. Goldfarb, S. B., Kashlan, O. B., Watkins, J. N., Suaud, L., Yan, W., Kleyman, T. R., and Rubenstein, R. C. (2006) *Proc. Natl. Acad. Sci. U.S.A.* **103,** 5817–5822
21. Hageman, J., van Waarde, M. A., Zylicz, A., Walerych, D., and Kampinga, H. H. (2011) *Biochem. J.* **435,** 127–142
22. Ghee, M., Melki, R., Michot, N., and Mallet, J. (2005) *FEBS J.* **272,** 4023–4033
23. Hageman, J., and Kampinga, H. H. (2009) *Cell Stress Chaperones* **14,** 1–21
24. Melki, R., Carlier, M. F., and Pantaloni, D. (1990) *Biochemistry* **29,** 8921–8932
25. Schuck, P. (2000) *Biophys. J.* **78,** 1606–1619
26. Laemmli, U. K. (1970) *Nature* **227,** 680–685
27. Halfmann, R., and Lindquist, S. (2008) *J. Vis. Exp.* **17**
28. Pieri, L., Bucciantini, M., Guasti, P., Savistchenko, J., Melki, R., and Stefani, M. (2009) *Biophys. J.* **96,** 3319–3330
29. Wolfe, L. S., Calabrese, M. F., Nath, A., Blaho, D. V., Miranker, A. D., and Xiong, Y. (2010) *Proc. Natl. Acad. Sci. U.S.A.* **107,** 16863–16868
30. Kryndushkin, D. S., Alexandrov, I. M., Ter-Avanesyan, M. D., and Kushnirov, V. V. (2003) *J. Biol. Chem.* **278,** 49636–49643
31. Benaroudj, N., Batelier, G., Triniolles, F., and Ladjimi, M. M. (1995) *Biochemistry* **34,** 15282–15290
32. Chirico, W. J., Markey, M. L., and Fink, A. L. (1998) *Biochemistry* **37,** 13862–13870
33. Borges, J. C., and Ramos, C. H. (2006) *Arch. Biochem. Biophys.* **452,** 46–54
34. Freeman, B. C., Myers, M. P., Schumacher, R., and Morimoto, R. I. (1995) *EMBO J.* **14,** 2281–2292
35. Hageman, J., Rujano, M. A., van Waarde, M. A., Kakkar, V., Dirks, R. P., Govorukhina, N., Oosterveld-Hut, H. M., Lubsen, N. H., and Kampinga, H. H. (2010) *Mol. Cell* **37,** 355–369
36. Kampinga, H. H., and Craig, E. A. (2010) *Nat. Rev. Mol. Cell Biol.* **11,** 579–592
37. Pieri, L., Bucciantini, M., Nosi, D., Formigli, L., Savistchenko, J., Melki, R., and Stefani, M. (2006) *J. Biol. Chem.* **281,** 15337–15344
38. Falsone, S. F., Kungl, A. J., Rek, A., Cappai, R., and Zangger, K. (2009) *J. Biol. Chem.* **284,** 31190–31199
39. Hansen, C., Angot, E., Bergström, A. L., Steiner, J. A., Pieri, L., Paul, G., Outeiro, T. F., Melki, R., Kallunki, P., Fog, K., Li, J. Y., and Brundin, P. (2011) *J. Clin. Invest.* **121,** 715–725
40. Desplats, P., Lee, H. J., Bae, E. J., Patrick, C., Rockenstein, E., Crews, L., Spencer, B., Masliah, E., and Lee, S. J. (2009) *Proc. Natl. Acad. Sci. U.S.A.* **106,** 13010–13015
41. Braak, H., Del Tredici, K., Rüb, U., de Vos, R. A., Jansen Steur, E. N., and Braak, E. (2003) *Neurobiol. Aging* **24,** 197–211
42. Brundin, P., Melki, R., and Kopito, R. (2010) *Nat. Rev. Mol. Cell Biol.* **11,** 301–307

SUPPLEMENTARY FIGURES

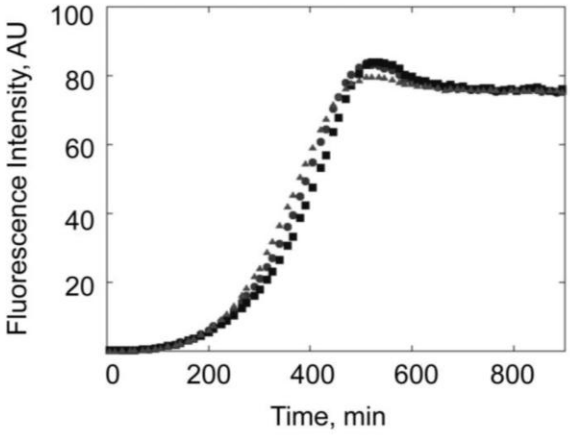

SUPPLEMENTARY FIGURE S1. Effect of nucleotides on the assembly of α-Syn. Time courses of α-Syn (100 μM) assembly in the absence of nucleotides (●), in the presence of 0.5 mM ATP (■) or 0.5 mM ADP(▲) in 50 mM Tris-HCl pH 7.5, 150 mM KCl, 0.05 mM $MgCl_2$.

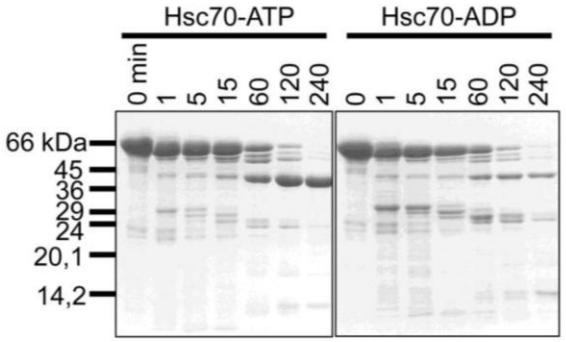

SUPPLEMENTARY FIGURE S2. Conformational analysis of Hsc70-ATP and Hsc70-ADP by limited proteolysis. Hsc70 was incubated for 1h at 37 °C in 50 mM Tris-HCl pH 7.5, 150 mM KCl, 0.05 mM $MgCl_2$ with addition of either 0.5 mM ATP or 0.5 mM ADP. The proteins were digested with proteinase K at a protein: protease ratio of 1000: 1 for the times indicated, and the digestion terminated by addition of 10mM PMSF prior to denaturation and SDS-PAGE.

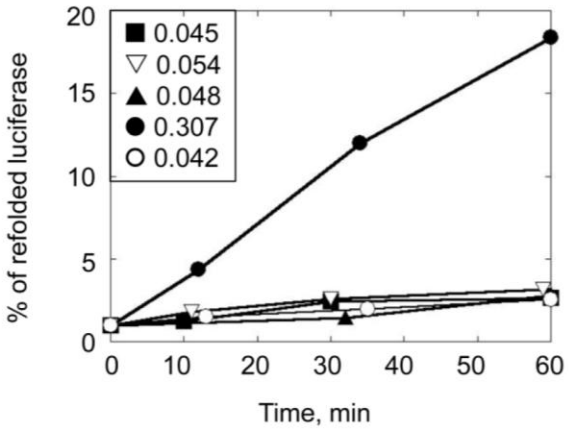

SUPPLEMENTARY FIGURE S3. Refolding of chemically denatured luciferase (0.1 µM) in the absence of chaperones (■), in the presence of Hsc70 (2 µM, ▽), Hdj1 (2 µM, ▲) or Hsc70 and Hdj1 (2 µM each), in the absence (○) or presence of 2 mM ATP (●), in 25 mM Hepes-OH, 50 mM KCl, 5 mM $MgCl_2$, 2 mM DTT. *Inset*, rate of luciferase refolding, *%. min*$^{-1}$.

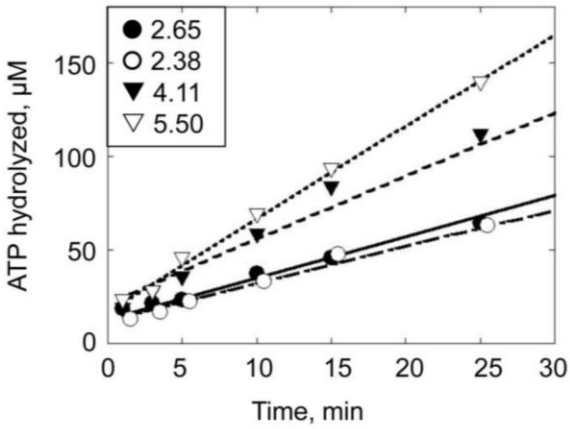

SUPPLEMENTARY FIGURE S4. ATPase activity of Hsc70 (1 µM,●), in the presence of luciferase (0.1 µM, ○), in the presence of Hdj1 (1 µM, ▼) or in the presence of Hdj1 and luciferase (1 µM and 0.1 µM respectively, ▽). *Inset*, rate of ATP hydrolysis, *µM. min*$^{-1}$. We measured ATP hydrolysis at 37 °C in assembly buffer (50 mM Tris-HCl pH 7.5, 150 mM KCl) by extraction of the [32P] phosphomolybdate complex formed in 1 N HCl.

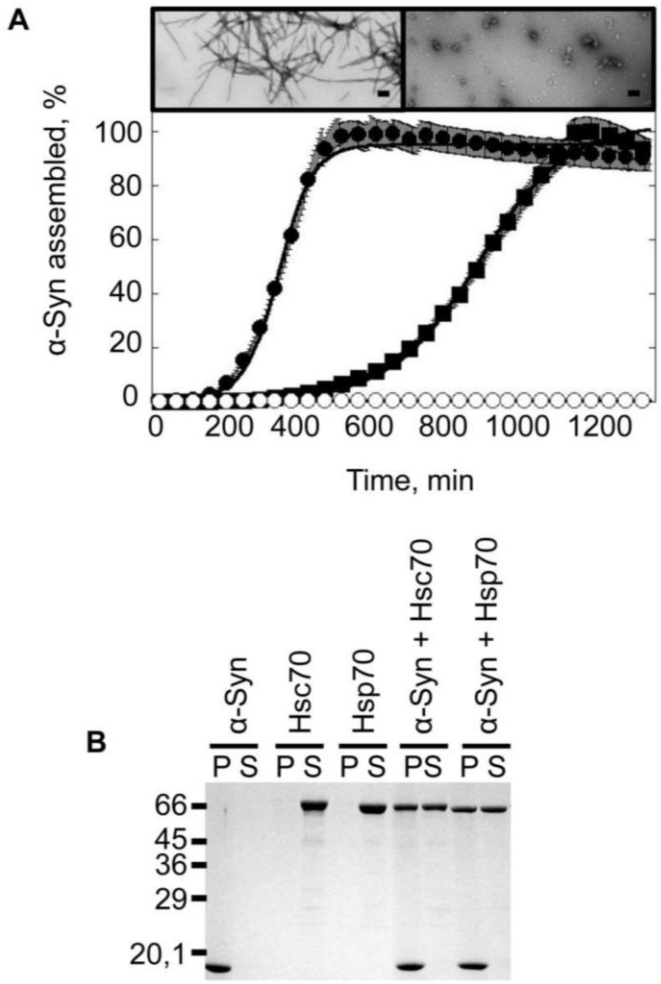

SUPPLEMENTARY FIGURE S5. α-Syn – Hsp70 interaction. *A*, Time courses of α-Syn (100 μM) assembly in the absence (●) and the presence of Hsp70 (5 μM, ■) and Hsp70 alone (5 μM, ○). The assembly reactions were monitored by thioT binding and are presented as the proportion of assembled α-Syn. Negative stained electron micrographs of α-Syn (100 μM) assemblies obtained in the absence (left) or presence (right) of 5 μM Hsp70 at time 1400 min. *Bar*, 0.2 μm. *B*, SDS-PAGE analysis of the pellet (*P*) and supernatant (*S*) fractions of preformed α-Syn fibrils (60 μM) in the absence and presence of Hsc70 (6 μM) or Hsp70 (6 μM). Samples were incubated for 1 h at 37 °C prior to 20 min centrifugation at 90,000 x *g*, 20 °C. The molecular mass markers (in kilodaltons) are shown to the left of *B*.

The interaction of Hsc70 protein with fibrillar α-Synuclein and its therapeutic potential in Parkinson's disease

Samantha Pemberton, Ronald Melki[1]

Laboratoire d'Enzymologie et Biochimie Structurales, CNRS, 91198 Gif-sur-Yvette, France

Communicative and Integrative Biology. Accepted 20th October 2011.

Key words: alpha synuclein, chaperones, heat shock protein, Hsc70, Parkinson's disease

Abbreviations: α-Syn, alpha synuclein; Hsc, constitutive heat shock protein; LB, Lewy body; LN, Lewy neurite; PD, Parkinson's disease

We recently described the effect of the constitutively expressed chaperone, Hsc70 protein, on α-Synuclein aggregation, a phenomenon associated with Parkinson's disease. *In vitro*, Hsc70 binds to soluble α-Syn and slows down its assembly into fibrils. Hsc70 also binds fibrillar α-Syn, fivefold tighter than soluble α-Syn. This interaction reduces the cytotoxicity associated with naked α-Syn fibrils. Herein, we discuss the feasibility of engineering a "minichaperone" which could be used against α-Syn assembly propagation in Parkinson's disease: taking what is necessary and sufficient within Hsc70 to protect against the damaging repercussions of high molecular weight α-Syn species' passage from one neuron to another in the brain.

[1] Correspondence to: Ronald Melki; Email: melki@lebs.cnrs-gif.fr

Addendum to: Pemberton S, Madiona K, Pieri L, Kabani M, Bousset L, Melki R. Hsc70 Protein Interaction with Soluble and Fibrillar α-Synuclein. J Biol Chem 2011; 286: 34690-9.

Intracellular Lewy bodies (LBs) and Lewy neurites (LNs) which contain a fibrillar form of the synaptic terminal protein α-Synuclein (α-Syn) as their principal component are neuropathological markers of Parkinson's disease (PD).[1] Although extensive research has previously shown various members of the human molecular chaperone family to hinder or promote the progression of soluble α-Syn into fibrils (Hsp70, Hsp27, αB-crystallin or Hsp90 respectively; for a review see refs. [2-3]), no one had yet to investigate the effect of the constitutively expressed human heat shock protein, Hsc70. This was surprising as not only have Hsp70 and Hsc70 been shown to have different cellular roles and different effects on aggregated luciferase and polyQ protein but being constitutively expressed, Hsc70 is the first molecular chaperone to encounter assembling α-Syn in a cellular context. [4, 5]

We showed that Hsc70 inhibits the assembly of α-Syn into fibrils, by binding with high affinity to the soluble form of α-Syn. We also showed that Hsc70 binds fibrillar α-Syn, with a dissociation constant fivefold lower than that we measured for soluble α-Syn. Hsc70 binding to fibrils has a cytoprotective effect, as it renders α-Syn fibrils less toxic to mammalian cultured cells. [6]

The point mutations within α-Syn at the origin of familial early onset PD suggest that the stochastic aggregation of α-Syn within cells is an important factor which contributes to the onset of PD. [7, 8] A second recently discovered and documented factor, namely the propagation of aggregates from one cell to another accounts for the neurodegenerative patterns described, which play a critical role in PD. [9, 10] Indeed, exogenous α-Syn fibrils enter cells and recruit soluble endogenous α-Syn, which results in synaptic dysfunction and neuronal cell death. [11, 12] As our work demonstrated that Hsc70 reduces the toxicity of fibrils most likely because binding alters their physicochemical properties, there is a possibility

that Hsc70 could be effective as a therapeutic agent in PD, by abolishing the cell to cell transfer of α-Syn fibrils, as schematised in Figure 1.

Furthermore, we demonstrated that Hsc70 is capable of binding fibrillar α-Syn in a nucleotide independent manner and in the absence of co-chaperones. [6] This suggests that Hsc70's α-Syn binding site, or a subset of this site may be used as a therapeutic tool to modify fibrillar α-Syn properties and as a consequence their binding to and uptake by neurons. Thus further characterisation of Hsc70 residues that interact specifically with fibrillar α-Syn using a cross-linking and mass spectrometry approach will lead, as in the case of the GroEL apical domain, [13-15] to the design of an Hsc70 derived minichaperone.

However, there is a chance that basing a therapeutic agent on Hsc70, an endogenous protein, may evoke an autoimmune response when introduced to the body. An exogenous engineered polypeptide which has a similar if not the same effect on α-Syn toxicity and crosses the blood-brain barrier to reach its target may be more successful as an eventual therapeutic agent – does the answer to PD lie in a bacterial or yeast homolog of Hsc70?

References

1. Spillantini MG, Schmidt ML, Lee VM, Trojanowski JQ, Jakes R, Goedert M. Alpha-synuclein in Lewy bodies. Nature 1997; 388:839-40.
2. Bandopadhyay R, de Belleroche J. Pathogenesis of Parkinson's disease: emerging role of molecular chaperones. Trends Mol Med 2010; 16:27-36.
3. Arawaka S, Machiya Y, Kato T. Heat shock proteins as suppressors of accumulation of toxic prefibrillar intermediates and misfolded proteins in neurodegenerative diseases. Curr Pharm Biotechnol 2010; 11:158-66.
4. Goldfarb SB, Kashlan OB, Watkins JN, Suaud L, Yan W, Kleyman TR, et al. Differential effects of Hsc70 and Hsp70 on the intracellular trafficking and functional expression of epithelial sodium channels. Proc Natl Acad Sci U S A 2006; 103:5817-22.
5. Hageman J, van Waarde MA, Zylicz A, Walerych D, Kampinga HH. The diverse members of the mammalian HSP70 machine show distinct chaperone-like activities. Biochem J 2011; 435:127-42.
6. Pemberton S, Madiona K, Pieri L, Kabani M, Bousset L, Melki R. Hsc70 Protein Interaction with Soluble and Fibrillar {alpha}-Synuclein. J Biol Chem 2011; 286:34690-9.
7. Fredenburg RA, Rospigliosi C, Meray RK, Kessler JC, Lashuel HA, Eliezer D, et al. The impact of the E46K mutation on the properties of alpha-synuclein in its monomeric and oligomeric states. Biochemistry 2007; 46:7107-18.
8. Li J, Uversky VN, Fink AL. Effect of familial Parkinson's disease point mutations A30P and A53T on the structural properties, aggregation, and fibrillation of human alpha-synuclein. Biochemistry 2001; 40:11604-13.
9. Braak H, Ghebremedhin E, Rub U, Bratzke H, Del Tredici K. Stages in the development of Parkinson's disease-related pathology. Cell Tissue Res 2004; 318:121-34.
10. Brundin P, Melki R, Kopito R. Prion-like transmission of protein aggregates in neurodegenerative diseases. Nat Rev Mol Cell Biol 2010; 11:301-7.
11. Volpicelli-Daley LA, Luk KC, Patel TP, Tanik SA, Riddle DM, Stieber A, et al. Exogenous alpha-Synuclein Fibrils Induce Lewy Body Pathology Leading to Synaptic Dysfunction and Neuron Death. Neuron 2011; 72:57-71.
12. Hansen C, Angot E, Bergstrom AL, Steiner JA, Pieri L, Paul G, et al. alpha-Synuclein propagates from mouse brain to grafted dopaminergic neurons and seeds aggregation in cultured human cells. J Clin Invest 2010; 121:715-25.
13. Chatellier J, Hill F, Lund PA, Fersht AR. In vivo activities of GroEL minichaperones. Proc Natl Acad Sci U S A 1998; 95:9861-6.
14. Golbik R, Zahn R, Harding SE, Fersht AR. Thermodynamic stability and folding of GroEL minichaperones. J Mol Biol 1998; 276:505-15.
15. Zahn R, Buckle AM, Perrett S, Johnson CM, Corrales FJ, Golbik R, et al. Chaperone activity and structure of monomeric polypeptide binding domains of GroEL. Proc Natl Acad Sci U S A 1996; 93:15024-9.

<u>Figure 1:</u> Possible protective mechanism of Hsc70 as a therapeutic agent. A minichaperone based on Hsc70 could be used to reduce the toxicity of α-Syn fibrils by binding to extracellular fibrils, altering their physicochemical properties, and preventing cell-to-cell propagation.

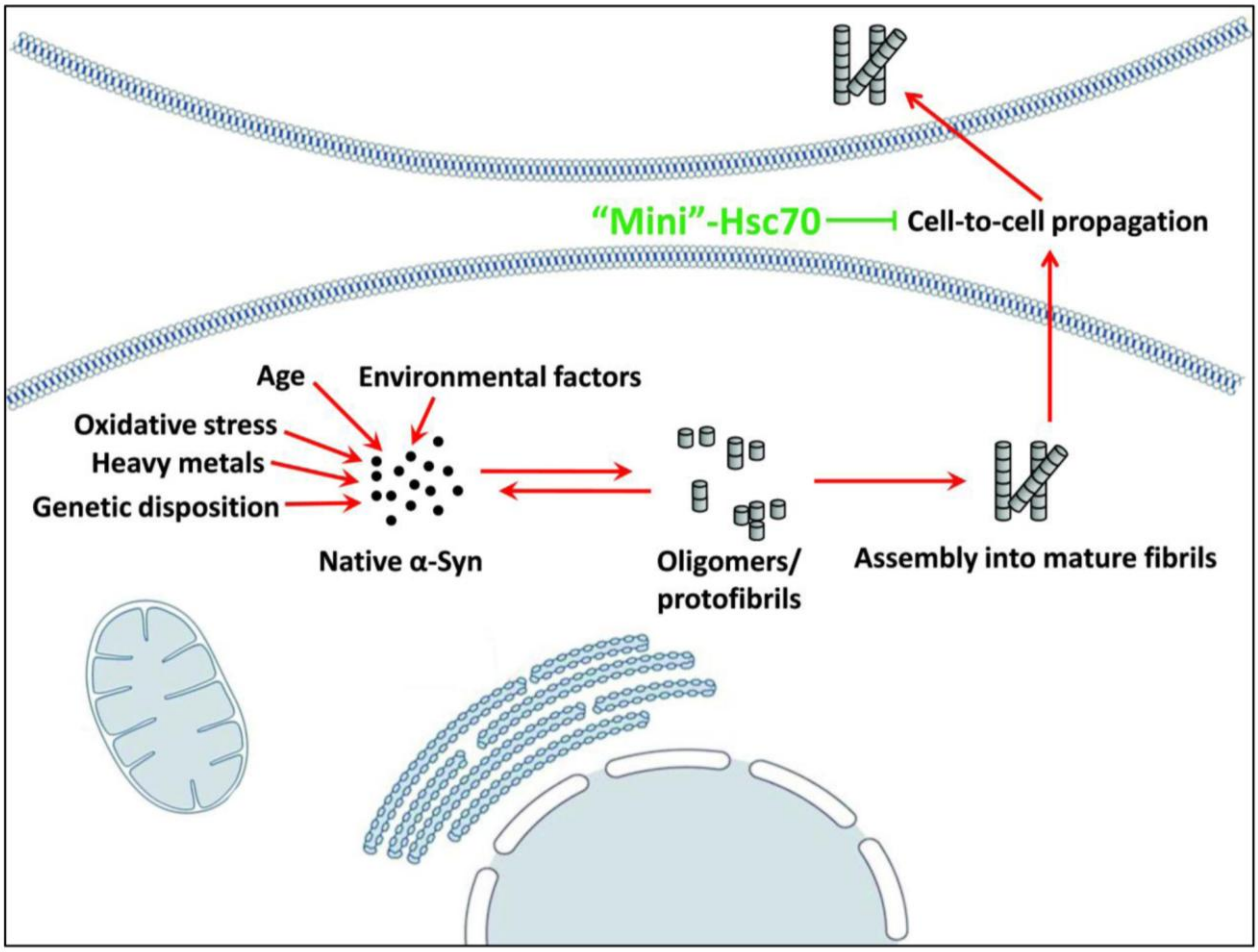

Part two

PART TWO

Article 3: The Yeast Hsp70, Ssa1p, also interacts with Soluble and Fibrillar α-Synuclein.

Samantha Pemberton, Virginie Redeker, Ronald Melki.

BACKGROUND AND OBJECTIVE

Ssa1p, the major cytosolic heat shock protein of *Saccharomyces cerevisiae* is an effective inhibitor of Ure2p, the yeast prion responsible for the [*URE3*] trait. A study carried out by Savistchenko *et al* in our laboratory systematically tested the effect of molecular chaperones from the yeast Hsp40, Hsp70, Hsp90, Hsp100 families and the chaperonin CCT/ Tric, on the assembly of Ure2p into high molecular weight assemblies (Savistchenko, Krzewska et al., 2008). They determined that Ssa1p is the most effective inhibitor of Ure2p aggregation of the chaperones tested. Ssa1p sequesters Ure2p as assembly-incompetent spherical oligomers, and completely inhibits Ure2p aggregation at a molar ratio of Ssa1p:Ure2p of 1:4.

Likewise, research also carried out in our laboratory demonstrated that Ssa1p plays a role in the assembly of another well characterized yeast prion protein, Sup35p, responsible for the prion trait [*PSI*$^{+}$]. Alone, Ssa1p does not inhibit Sup35p assembly but in the presence of either co-chaperone Sis1p or Ydj1p, it is an effective inhibitor (Krzewska and Melki, 2006).

Taking these two points into consideration, we aimed to characterize the effect of Ssa1p and its co-chaperones Sis1p and Ydj1p on α-Syn. In the long run, identifying client protein binding sites and the binding characteristics of different Hsc/p70 family members is critical to design inhibitors of α-Syn assembly or α-Syn-mediated toxicity for therapeutic purposes. Such inhibitors would correspond to minichaperones which possess all that is necessary and sufficient to inhibit α-Syn assembly. Performing such a study using a protein exogenous to the human body (Ssa1p) is advantageous, as the body could potentially mount an autoimunne attack against an endogenous chaperone introduced as a therapeutic agent. Indeed, autoimmune disease can be a serious side effect of some drugs, for instance when

the dopamine precursor levodopa, administered to improve PD symptoms was first introduced, it triggered the autoimmune disease haemolytic anaemia (Cotzias and Papavasiliou, 1969; Territo, Peters et al., 1973; Wanamaker, Wanamaker et al., 1976; Linstrom, Lieden et al., 1977). Since the 1970's, levodopa has been vastly improved and/ or used in combination with other drugs to decrease the side effects, and remains one of the most effective drugs on the market today to alleviate PD symptoms.

The yeast Hsp70, Ssa1p, also interacts with soluble and fibrillar α-Synuclein

Samantha Pemberton, Virginie Redeker, Ronald Melki[1]

Laboratoire d'Enzymologie et Biochimie Structurales, CNRS, 91198 Gif-sur-Yvette, France

ABSTRACT

Fibrillar α-Synuclein (α-Syn) is the principal component of Lewy bodies which are evident in individuals affected by Parkinson's disease. Various members of the molecular chaperone family have previously been shown to hinder or promote the progression of soluble α-Syn into fibrils. To further enhance this catalogue, we have investigated the effect of the yeast chaperone, Ssa1p, on α-Syn. We describe an inhibitory effect of Ssa1p on the assembly of soluble α-Syn into fibrils, and show that Ssa1p also binds to fibrils, but without effect on their cellular toxicity. The Ssa1p peptide which binds to fibrillar α-Syn could be engineered as a "minichaperone" with potential as a therapeutic agent in Parkinson's disease.

Keywords: α-Synuclein; Chaperones; Heat shock protein; Parkinson's disease; Protein assembly, Ssa1p.

List of abbreviations[2]**:** α-Syn, Hsc, PD, Tricine

[1]Corresponding author. E-mail address: melki@lebs.cnrs-gif.fr; Tel. +33169823503; Fax. +33169823129

[2] α-Syn, α-Synuclein; Hsc, constitutive heat shock protein; PD, Parkinson's disease; Tricine, *N*-[2-hydroxy-1,1-bis(hydroxymethyl)ethyl]glycine.

1. Introduction

Various factors, including genetic susceptibility and environmental influences, can trigger the assembly of α-Syn from its soluble state into amyloid-like fibrils with high β-sheet content [1,2]. Molecular chaperones bind to exposed hydrophobic regions on non-native proteins and subsequently block their aggregation [3]. Notably from the Hsp70 family, molecular chaperones are found sequestered within Lewy bodies and Lewy neurites, alongside the principal component fibrillar α-Syn in the brains of Parkinson disease (PD) patients [4]. Consequently, there has been much focus on the potential therapeutic role of molecular chaperones in neurodegenerative diseases, with emphasis on PD (for review see [5]).

In recent years, there has been significant growth in evidence, and subsequent discussion as to whether proteinopathies (i.e. PD) are prion disorders [6-8]. The assembly of yeast prion protein Ure2p into high molecular weight assemblies *in vitro* is totally inhibited in the presence of Ssa1p (a constitutively expressed, 70 kDa molecular chaperone of *S. cerevisiae)*, at an Ssa1p:Ure2p ratio of 1:4 [9]. As well as its action on Ure2p, Ssa1p has an effect on the assembly of Sup35p, the yeast protein responsible for the [PSI^{+}] prion trait. Indeed, Ssa1p plus either one of its co-chaperones, blocks the assembly of Sup35p, and can counter-effect the fibril promoting action of Hsp104p on Sup35p. However, Ssa1p or Sis1p (one of Ssa1p's Hsp40 co-chaperones) alone, do not affect Sup35p assembly. In contrast, Ydj1p (Ssa1p's other Hsp40 co-chaperone) has an inhibitory effect, independent of Ssa1p [10]. In contrast to its fibril-promoting action on Sup35p, the yeast chaperone Hsp104p has an advantageous disassembling action upon α-Syn aggregates *in vitro*, and reduces α-Syn assembly and associated toxicity *in vivo* [11]. Compiling a catalogue of the effect of various molecular chaperones on α-Syn allows us to identify which are effective in inhibiting α-Syn

assembly, and concomitantly provides information on the molecular mechanisms behind PD.

The aim of this paper is to investigate the effect of Ssa1p on α-Syn assembly. We report that Ssa1p, like human Hsp70 and Hsc70, slows down the assembly of soluble α-Syn, by binding with a similar affinity to that of Hsc70. We determine that Ssa1p binds to α-Syn fibrils with even higher affinity than for the soluble α-Syn, and show the physiological consequences of this interaction. Ssa1p's co-chaperones Sis1p and Ydj1p, whilst binding with a higher affinity than Ssa1p to fibrillar α-Syn, do not promote Ssa1p binding. We have stabilised the α-Syn – Ssa1p complex using chemical cross-linkers and the next step is to use mass spectrometry to map the site of interaction between Ssa1p and α-Syn. This is invaluable if a part of Ssa1p that comprises all that is necessary and sufficient to bind α-Syn fibrils and reduce their toxicity is to be used as a therapeutic agent in PD in the future, with its advantage of being a protein exogenous to the human body thus less likely to trigger autoimmune disease. In effect, autoimmune disease can be a real threat in drug use for example the dopamine precursor levodopa triggered the autoimmune disease haemolytic anaemia when it was first introduced to alleviate PD symptoms [12-15].

2. Materials and Methods

2.1 Expression and Purification of α-Syn, Ssa1p and its co-chaperones Ydj1p and Sis1p

Recombinant wild-type α-Syn was expressed in *E. coli* strain BL21(DE3) (Stratagene) and purified as described [16]. α-Syn concentration was determined spectrophotometrically using an extinction coefficient of 5960 $M^{-1}.cm^{-1}$ at 280nm. Pure α-Syn (0.5-1 mM) in 50 mM Tris-HCl, pH 7.5, 50 mM KCl was stored at -80°C.

Recombinant hexahistidine tagged wildtype Ssa1p (yeast strain AJYM28), was purified as previously described [17]. Ssa1p concentration was determined by Bradford

assay [18]. Pure Ssa1p (10-80 µM) in 50 mM Tris-HCl, pH 7.5, 50 mM KCl, 5 mM β-mercaptoethanol, 5 mM $MgCl_2$, 1 mM EGTA and 10 % glycerol was aliquoted and stored at -80 °C. Purified Ydj1p and Sis1p were kindly provided by J. Krzewska, prepared according to [10].

The ATPase activity of Ssa1p alone or in the presence of α-Syn fibrils was also monitored as described [19], using Hsc70 as a reference.

2.2 Assembly of α-Syn into fibrils

Soluble wild-type α-Syn was assembled in 50 mM TrisHCl pH 7.5, 150 mM KCl, 15 µM thioflavin T (thioT), in the absence or presence of Ssa1p, with or without ADP-$MgCl_2$ or ATP-$MgCl_2$ and the co-chaperones Ydj1p or Sis1p in 1ml cuvettes (path length 1cm). Assembly was induced by incubating the cuvette at 37 °C with magnetic stirring. Aliquots (90 µL) were removed at time intervals, spun at 40,000 x *g*, 20 °C, and 20 min in a TL100 tabletop ultracentrifuge (Beckman, USA). The proteins within the supernatant and pellet fractions were analyzed by SDS-PAGE and quantified following staining/ destaining using the ImageJ software (National Institute of Health, USA and available at rsb.info.nih.gov/ij). The nature of the oligomeric species was assessed using a Jeol 1400 transmission electron microscope (Jeol Ltd.) following adsorption of the samples onto carbon-coated 200-mesh grids and negative staining with 1% uranyl acetate. The images were recorded with a Gatan Orius CCD camera (Gatan).

2.3 Crosslinking, SDS-PAGE and Western Blotting

Crosslinking reactions were carried out with the homo-bifunctional sulfo-NHS ester cross-linker reagents BS2G-d0/d4 [bis(sulfosuccinimidyl) glutarate] with a 7.7 Å spacer arm or BS3-d0/d4 [Bis(sulfosuccinimidyl) suberate] with an 11.4 Å spacer arm (Pierce, Waltham, MA, USA). α-Syn (100 µM), Ssa1p (10 µM) or α-Syn and Ssa1p (100 µM and 10 µM

respectively) were incubated for 2 h at 37 °C under agitation in 50 mM TrisHCl, pH 7.5, 150 mM KCl, before dialyzing for 2.5 h at 4 °C against cross-linking buffer (40 mM Hepes-OH, pH 7.5, 75 mM KCl before adding the cross-linker. BS2G or BS3 (50 mM in dimethylsulfoxide) was added to give molar ratio 10: 1 BS2G: α-Syn and 100: 1 BS2G: Ssa1p. After 30 min at room temperature, the reaction was terminated by addition of ammonium bicarbonate (50 mM). Samples for SDS-PAGE were immediately mixed v/v with denaturing buffer and heated at 95 °C. After transferring the proteins to nitrocellulose membranes, the membranes were incubated with 3% milk, probed with an antibody against α-Syn (BD Biosciences) or Ssa1p (Assay Designs, Michigan, US), and developed with the enzyme-coupled luminescence technique (ECL, GE Healthcare) according to the recommendation of the manufacturer.

Binding of Ssa1p to fibrillar α-Syn was followed using a sedimentation assay. High molecular weight α-Syn fibrils sediment upon centrifugation, whereas Ssa1p remains soluble. α-Syn fibrils (60 µM), Ssa1p (20 µM) or α-Syn and Ssa1p (60 µM and from 1-20 µM respectively) were incubated for 1 h before centrifugation at 90,000 x *g*, 20 °C, and 20 min.

SDS-polyacrylamide gel electrophoresis was performed in 7.5-13% tris-tricine polyacrylamide gels following the standard method described by Laemmli [20].

2.4 Cell viability assays

Were carried out as previously described [21].

3. Results and discussion

3.1 Effect of Ssa1p on α-Syn assembly

The effect of Ssa1p on α-Syn assembly was assessed using a sedimentation assay, and electron microscopy (EM). Over time, α-Syn readily assembles into high molecular weight assemblies *in vitro*, which sediment upon centrifugation. Assembly follows a typical

Sigmoidal pattern, with a lag phase, rapid growth and steady state. In the absence of Ssa1p, the lag phase of α-Syn at 200 μM is approximately 200 min. Upon addition of increasing concentrations of Ssa1p, the length of the lag phase increases, indicating that the yeast chaperone slows down α-Syn assembly (Fig. 1A). EM images of the samples at 1200 min show that there are fibrils present in all three conditions, with 0, 2 or 10 μM Ssa1p. While there is no difference between the material present in the absence of Ssa1p or with 2 μM Ssa1p, the presence of Ssa1p is clearly evident in the third EM image. At 1200 min, the reaction with 10 μM Ssa1p is yet to reach the steady state, and as well as α-Syn fibrils, a high proportion of the sample material is in the form of oligomers (Fig. 1B). The dissociation constant between Ssa1p and soluble α-Syn was obtained from measuring the elongation rates of α-Syn in the presence of increasing concentrations of Ssa1p, and is 1.2 μM^{-1} (Fig. 1C). We previously published that the affinity between soluble α-Syn and Hsc70 is 0.5 μM^{-1} [21]. As well as this, Ssa1p binds to the soluble yeast prion Ure2p with an affinity of 0.5 μM^{-1} [9], showing that the affinities between molecular chaperones and aggregating proteins are of a similar magnitude.

3.2 Ssa1p interaction with soluble α-Syn.

We used a mixture of the non-deuterated (d0) and deuterated (d4) forms of the chemical cross-linkers BS2G and BS3 to put into evidence an interaction and complex formation between Ssa1p and soluble α-Syn. BS2G has a spacer arm of 7.7 Å and BS3 11.4 Å, and both react with the ε-amino group of lysine residues and α-amino group from protein N-termini and, to a lesser extent, with the hydroxyl groups of serine, threonine and tyrosine residues [22]. The proteins must be less than 7.7 Å or 11.4 Å away from each other, i.e. already in complex, for the cross-linker to successfully stabilize the interaction. Fig. 2A shows that there is an abundant complex of the two proteins with a molecular weight

around 100 kDa, corresponding to two α-Syn molecules binding per Ssa1p molecule. A similar stoichiometry was observed for the binding between Ssa1p and Ure2p, where Ure2p:Ssa1p complexes of 1:1 and 2:1 were shown, also using a crosslinking method [23]. Using mass spectrometry to investigate these cross-linked species, with the mixture of non-deuterated and deuterated cross-linkers to facilitate cross-linked peptide detection and identification, we are in the process of mapping the interaction site between Ssa1p and α-Syn, with an aim to determine the sequence of the peptide of Ssa1p bound to α-Syn.

The bacterial molecular chaperone GroEL is a large complex of 14 identical, 57 kDa subunits which form a cylinder with a central cavity, and facilitates protein folding by preventing aggregation and correcting misfolding [24,25]. The apical domain (residues 191-376), responsible for peptide binding, has been shown to have high chaperone activity, *independent* of the central cavity or allosteric behaviour, and is thus termed a 'minichaperone'. Designing a minichaperone based on the fragment of Ssa1p which binds α-Syn could be the basis of a therapeutic agent against α-Syn assemblies, if it proves to have the same effect as the entire chaperone. As the agent would be based on an exogenous protein, and as small as possible whilst still effective, there is less chance of auto-antibodies being produced leading to autoimmune disease, similar to that seen when the drug levodopa was first introduced to alleviate PD symptoms [12-15].

3.3 Ssa1p, Sis1p and Ydj1p interaction with fibrillar α-Syn.

As well as an interaction with soluble α-Syn, Ssa1p binds to fibrillar α-Syn. We exploited the fact that fibrillar α-Syn sediments upon centrifugation, whereas Ssa1p remains soluble. Upon co-incubation of the two proteins followed by centrifugation and SDS-PAGE analysis, Ssa1p is found within the pelleted fraction as it is bound to the fibrils (Fig. 3A, left panel). This interaction is saturated at a ratio of 4 α-Syn to 1 Ssa1p. The dissociation constant

between Ssa1p and fibrillar α-Syn was estimated at 0.5 μM^{-1}, as 0.5 μM is the concentration of Ssa1p needed to reduce binding to fibrils by a half (Fig. 3B).

Ssa1p's co-chaperones, Sis1p and Ydj1p (the yeast homologs of human Hdj1 and Hdj2 respectively) also bind to fibrillar α-Syn, with an apparent higher affinity than Ssa1p binding to fibrils. Upon addition of equal concentrations of Ssa1p, Sis1p and Ydj1p to an equal concentration of α-Syn fibrils, not all of Ssa1p is found within the pellet, however all Sis1p and nearly all Ydj1p are bound to the fibrils (Fig. 3A). The presence of either co-chaperone does not increase binding of Ssa1p to the fibrils, although this is the case for Hsc70 with its co-chaperones Hdj1 and Hdj2, as we have previously shown [21].

We previously showed that Hsc70 and its co-chaperones binding to α-Syn fibrils proffers protection against the cellular toxicity of α-Syn fibrils [21]. This is not the case for Ssa1p binding to α-Syn fibrils. Fibrils coated with Ssa1p are no less toxic than naked fibrils, with survival rates of 52 ± 2 % and 53 ± 1 % respectively (Fig. 3C). The difference in physiological consequence of Hsc70 or Ssa1p binding to α-Syn fibrils must be as a result of the five-fold difference in binding affinity, which is 0.1 μM^{-1} for Hsc70-α-Syn fibrils and 0.5 μM^{-1} for Ssa1p-α-Syn fibrils. The difference in observed binding affinities can be explained by a difference in 22 amino acids in the primary sequence of the peptide binding domains (from residues 384 to 507) of Hsc70 and Ssa1p, but could also be the result of different ATPase activities, allowing Hsc70 to bind to α-Syn fibrils more efficiently. Indeed, Fig. 3D suggests that Ssa1p is not as efficient an ATPase as Hsc70, with respective ATP hydrolysis rates of 0.92 $\mu M.min^{-1}$ and 1.48 $\mu M.min^{-1}$ in the absence of client proteins, and 0.75 $\mu M.min^{-1}$ and 1.31 $\mu M.min^{-1}$ in the presence of α-Syn fibrils, concurrent with the idea that α-Syn oligomers inhibit the activity of molecular chaperones [26].

To conclude, increasing concentrations of the yeast chaperone Ssa1p slows down assembly of α-Syn into fibrils by binding to soluble α-Syn with an observed dissociation constant of 1.2 μM^{-1}, similar to the action of the human homologue Hsc70. Ssa1p also binds to fibrillar α-Syn with an observed dissociation constant of 0.5 μM^{-1}, but this weak interaction does not render the fibrils less toxic to cells. We have stabilized an Ssa1p – α-Syn complex using chemical cross-linkers, which shows an interaction of 1 Ssa1p with 2 molecules of α-Syn. We can use mass spectrometry to investigate these cross-linked species to map the interaction site between Ssa1p and α-Syn, with an aim to determine the sequence of the peptide of Ssa1p bound to α-Syn. Following protein engineering to strengthen the interaction between Ssa1p and α-Syn, the specific peptide may function, as in the case of the GroEL apical domain, as a minichaperone which could have therapeutic significance in PD. Indeed, as we hypothesized for Hsc70 [27], a mini Ssa1p could bind to extracellular α-Syn aggregates, change their physicochemical properties and prevent the aggregates from infecting a neighbouring cell thus slowing down the progression of PD.

4. Acknowledgments

This work was supported by the French Ministry of Education, Research and Technology, the Centre National de la Recherche Scientifique (CNRS), the Era-Net Neuron, the Agence Nationale pour la Recherche (ANR-08-NEUR-001-01) and the Human Frontier Science Program. We thank Laura Pieri for help with cellular toxicity assays, and Luc Bousset for help with electron microscopy.

5. References

[1] Uversky, V.N., Li, J., Bower, K. and Fink, A.L. (2002). Synergistic effects of pesticides and metals on the fibrillation of alpha-synuclein: implications for Parkinson's disease. Neurotoxicology 23, 527-36.

[2] Ross, C.A. and Smith, W.W. (2007). Gene-environment interactions in Parkinson's disease. Parkinsonism Relat Disord 13 Suppl 3, S309-15.

[3] Hartl, F.U. and Hayer-Hartl, M. (2009). Converging concepts of protein folding in vitro and in vivo. Nat Struct Mol Biol 16, 574-81.
[4] Auluck, P.K., Chan, H.Y., Trojanowski, J.Q., Lee, V.M. and Bonini, N.M. (2002). Chaperone suppression of alpha-synuclein toxicity in a Drosophila model for Parkinson's disease. Science 295, 865-8.
[5] Witt, S.N. (2010). Hsp70 molecular chaperones and Parkinson's disease. Biopolymers 93, 218-28.
[6] Angot, E., Steiner, J.A., Hansen, C., Li, J.Y. and Brundin, P. (2010). Are synucleinopathies prion-like disorders? Lancet Neurol 9, 1128-38.
[7] Brundin, P., Melki, R. and Kopito, R. (2010). Prion-like transmission of protein aggregates in neurodegenerative diseases. Nat Rev Mol Cell Biol 11, 301-7.
[8] Olanow, C.W. and Prusiner, S.B. (2009). Is Parkinson's disease a prion disorder? Proc Natl Acad Sci U S A 106, 12571-2.
[9] Savistchenko, J., Krzewska, J., Fay, N. and Melki, R. (2008). Molecular chaperones and the assembly of the prion Ure2p in vitro. J Biol Chem 283, 15732-9.
[10] Krzewska, J. and Melki, R. (2006). Molecular chaperones and the assembly of the prion Sup35p, an in vitro study. EMBO J 25, 822-33.
[11] Lo Bianco, C., Shorter, J., Regulier, E., Lashuel, H., Iwatsubo, T., Lindquist, S. and Aebischer, P. (2008). Hsp104 antagonizes alpha-synuclein aggregation and reduces dopaminergic degeneration in a rat model of Parkinson disease. J Clin Invest 118, 3087-97.
[12] Cotzias, G.C. and Papavasiliou, P.S. (1969). Autoimmunity in patients treated with levodopa. JAMA 207, 1353-4.
[13] Linstrom, F.D., Lieden, G. and Enstrom, M.S. (1977). Dose-related levodopa-induced haemolytic anaemia. Ann Intern Med 86, 298-300.
[14] Territo, M.C., Peters, R.W. and Tanaka, K.R. (1973). Autoimmune hemolytic anemia due to levodopa therapy. JAMA 226, 1347-8.
[15] Wanamaker, W.M., Wanamaker, S.J., Celesia, G.G. and Koeller, A.A. (1976). Thrombocytopenia associated with long-term levodopa therapy. JAMA 235, 2217-9.
[16] Ghee, M., Melki, R., Michot, N. and Mallet, J. (2005). PA700, the regulatory complex of the 26S proteasome, interferes with alpha-synuclein assembly. FEBS J 272, 4023-33.
[17] McClellan, A.J. and Brodsky, J.L. (2000). Mutation of the ATP-binding pocket of SSA1 indicates that a functional interaction between Ssa1p and Ydj1p is required for post-translational translocation into the yeast endoplasmic reticulum. Genetics 156, 501-12.
[18] Bradford, M.M. (1976). A rapid and sensitive method for the quantitation of microgram quantities of protein utilizing the principle of protein-dye binding. Anal Biochem 72, 248-54.
[19] Melki, R., Carlier, M.F. and Pantaloni, D. (1990). Direct evidence for GTP and GDP-Pi intermediates in microtubule assembly. Biochemistry 29, 8921-32.
[20] Laemmli, U.K. (1970). Cleavage of structural proteins during the assembly of the head of bacteriophage T4. Nature 227, 680-5.
[21] Pemberton, S., Madiona, K., Pieri, L., Kabani, M., Bousset, L. and Melki, R. (2011). Hsc70 interaction with soluble and fibrillar {alpha}-Synuclein. J Biol Chem

[22] Madler, S., Bich, C., Touboul, D. and Zenobi, R. (2009). Chemical cross-linking with NHS esters: a systematic study on amino acid reactivities. J Mass Spectrom 44, 694-706.
[23] Redeker, V., Bonnefoy, J., Le Caer, J.P., Pemberton, S., Laprevote, O. and Melki, R. (2010). A region within the C-terminal domain of Ure2p is shown to interact with the molecular chaperone Ssa1p by the use of cross-linkers and mass spectrometry. FEBS J 277, 5112-23.
[24] Fenton, W.A. and Horwich, A.L. (1997). GroEL-mediated protein folding. Protein Sci 6, 743-60.
[25] Zahn, R., Buckle, A.M., Perrett, S., Johnson, C.M., Corrales, F.J., Golbik, R. and Fersht, A.R. (1996). Chaperone activity and structure of monomeric polypeptide binding domains of GroEL. Proc Natl Acad Sci U S A 93, 15024-9.
[26] Hinault, M.P., Cuendet, A.F., Mattoo, R.U., Mensi, M., Dietler, G., Lashuel, H.A. and Goloubinoff, P. (2010). Stable alpha-synuclein oligomers strongly inhibit chaperone activity of the Hsp70 system by weak interactions with J-domain co-chaperones. J Biol Chem 285, 38173-82.
[27] Pemberton, S., Melki R. (2012). The interaction of Hsc70 protein with fibrillar α-Synuclein and its therapeutic potential in Parkinson's disease Communicative and Integrative Biology 5.

6. Figure Legends

Fig. 1. Assembly of α-Syn in the presence of Ssa1p. *A*, Time courses of α-Syn (200 µM) in the absence (*red*) and the presence of increasing concentrations of Ssa1p: 1 µM *blue*; 2 µM *dark green*; 5 µM *orange*; 10 µM *light green*. The assembly reactions were monitored by quantifying α-Syn within the pellet and supernatant fractions by SDS-PAGE, as described in the materials and methods section. *B*, Negative stained electron micrographs of α-Syn (200 µM) assemblies obtained in the absence (*left*) or presence of 2 µM (*middle*) or 10 µM Ssa1p (*right*). *Bar*, 0,2 µm. *C*, rate of α-Syn fibril elongation at a constant α-Syn concentration (200 µM) and increasing Ssa1p concentrations (1-10 µM).

Fig. 2. *A*, SDS-PAGE analysis of cross-linked α-Syn and Ssa1p. The reaction products generated upon treatment of α-Syn, Ssa1p and α-Syn in the presence of Ssa1p with the cross-linking agent BS2G were separated on a 7.5% acrylamide SDS-PAGE and stained with

Coomassie blue (*left*) or western blotted and stained with antibodies directed against Ssa1p (*middle*) or α-Syn (*right*).

Fig. 3. Fibrillar α-Syn – Ssa1p interaction. *A*, SDS-PAGE analysis of fractions of the pellet (P) and supernatant (S) fractions of preformed α-Syn fibrils (60 μM) in the absence and the presence of Ssa1p (6 μM), Sis1p (6 μM), Ydj1p (6 μM), or Ssa1p (60 μM) and its co-chaperone (6 μM each), as indicated, in 50 mM TrisHCl, pH 7.5, 150 mM KCl, 0.5 mM ATP, and 0.05 mM $MgCl_2$. Samples were incubated for 1 h at 37 °C prior to 20 min centrifugation at 90,000 x g, 20 °C. The molecular mass markers (in kilodaltons) are shown to the left. *B*, Fraction of Ssa1p in the pellet after incubation at 37 °C for 1h of a constant amount of fibrillar α-Syn (60 μM) with increasing concentrations of Ssa1p (0-20 μM), followed by ultracentrifugation at 90,000 x *g* for 20 min. *C,* Viability of H-END cells upon exposure to fibrillar α-Syn in the absence or presence of Ssa1p and/ or Sis1p or Ydj1p. Before exposure to cells, fibrillar α-Syn (100 μM) was incubated for 1 h at 37 °C with Ssa1p (25 μM), Sis1p (25 μM), Ydj1p (25 μM), Ssa1p and Sis1p (25 μM each protein) or Ssa1p and Ydj1p (25 μM each protein). Fibrillar α-Syn was centrifuged for 20 min at 16,100 x g and the pellet was resuspended in the culture medium to remove unbound Ssa1p, Sis1p or Ydj1p. The final protein concentration of α-Syn within the culture medium was 1 μM. The cells were incubated with the different proteins for 24 h. Cell viability is expressed as the percentage of 3-(4,5-dimethylthiazol-2-yl)-2,5-diphenyltetrazolium bromide (MTT) reduction using cells treated with the same volume of buffer as a reference (100% 3-(4,5-dimethylthiazol-2-yl)-2,5-diphenyltetrazolium bromide reduction). The values are averages ± S.D. obtained from three independent experiments. *D*, ATPase activity of Ssa1p (10 μM, dashed lines) or Hsc70 (10 μM, solid lines) in the absence (●) or presence (■) of α-Syn fibrils (40 μM). We

measured ATP hydrolysis at 37 °C in assembly buffer (50 mM Tris-HCl pH 7.5, 150 mM KCl) by extraction of the [32P] phosphomolybdate complex formed in 1 N HCl.

7. Figures

Figure 1

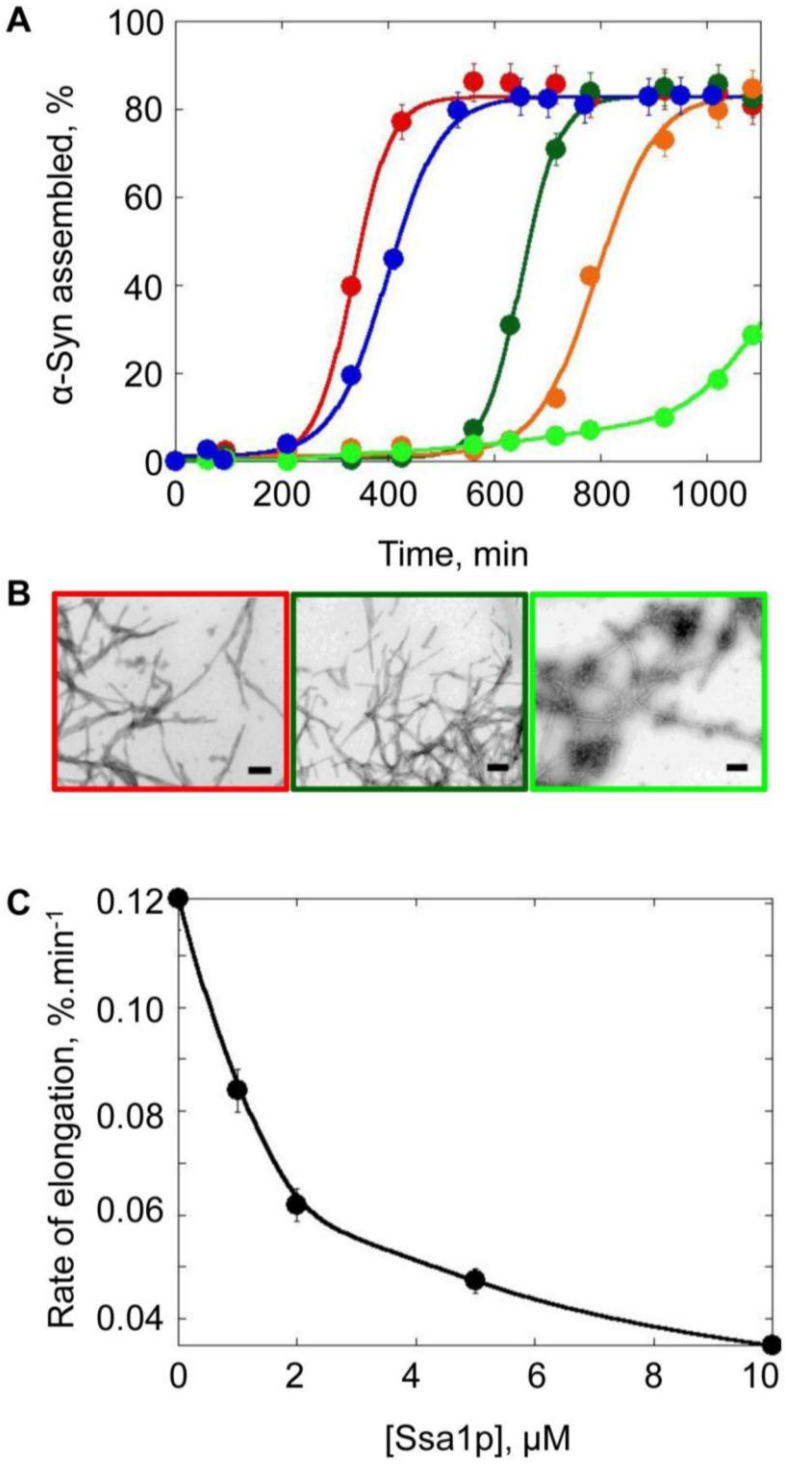

Figure 2

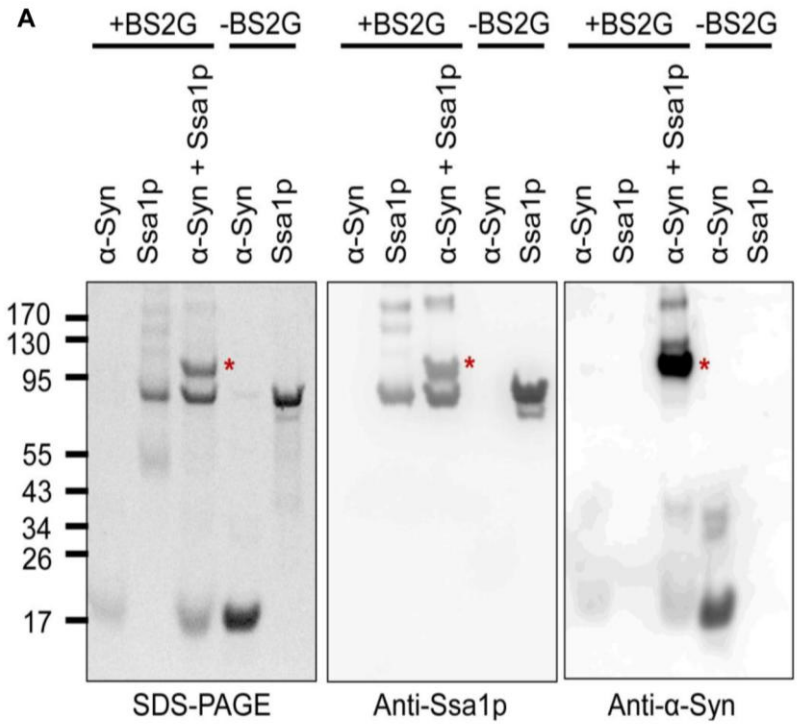
A
+BS2G
-BS2G
+BS2G
-BS2G
+BS2G
-BS2G
α-Syn
Ssa1p
α-Syn + Ssa1p
α-Syn
Ssa1p
α-Syn
Ssa1p
α-Syn + Ssa1p
α-Syn
Ssa1p
α-Syn
Ssa1p
α-Syn + Ssa1p
α-Syn
Ssa1p
170
130
95
55
43
34
26
17
*
*
*
SDS-PAGE
Anti-Ssa1p
Anti-α-Syn

Figure 3

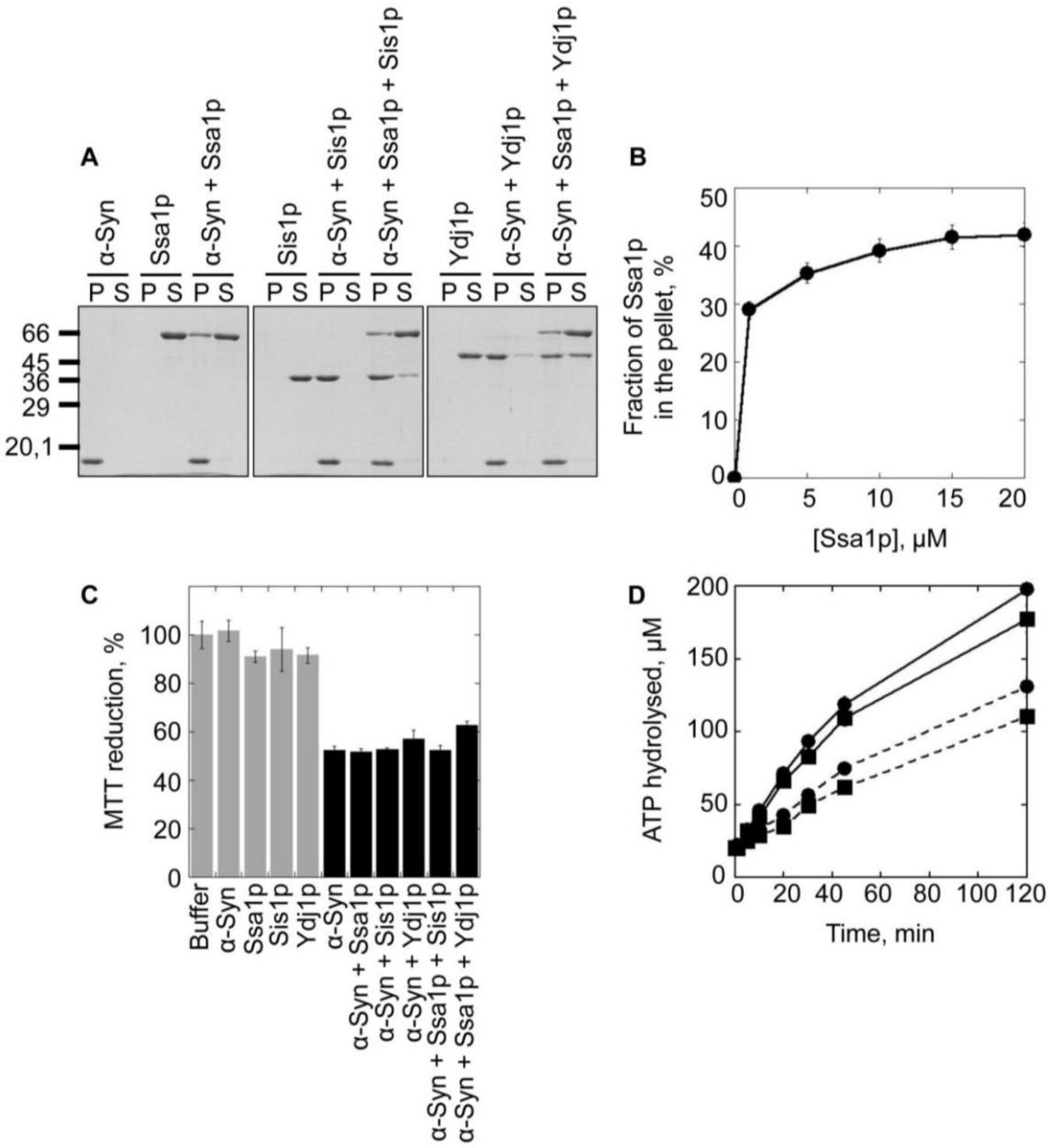
A
α-Syn
Ssa1p
α-Syn + Ssa1p
Sis1p
α-Syn + Sis1p
α-Syn + Ssa1p + Sis1p
Ydj1p
α-Syn + Ydj1p
α-Syn + Ssa1p + Ydj1p
P S
66
45
36
29
20,1
B
Fraction of Ssa1p in the pellet, %
[Ssa1p], μM
C
MTT reduction, %
Buffer
α-Syn
Ssa1p
Sis1p
Ydj1p
α-Syn + Ssa1p
α-Syn + Sis1p
α-Syn + Ydj1p
α-Syn + Ssa1p + Sis1p
α-Syn + Ssa1p + Ydj1p
D
ATP hydrolysed, μM
Time, min

Conclusion and perspectives

CONCLUSIONS

During my PhD, I characterized the effect of Hsc70 and Ssa1p and their respective co-chaperones Hdj1 and Hdj2 or Sis1p and Ydj1p, on the PD incriminated protein α-Syn. Individuals afflicted by PD present intracellular inclusions as pathological hallmarks of disease, of which filamentous α-Syn is the principal component. α-Syn, whose normal cellular role is yet to be definitively defined, undergoes conformational changes as it assembles from soluble, active protein, to fibrillar aggregates. Another major element found sequestered within LBs and LNs are molecular chaperones, notably of the Hsp70 family. Hsps are believed to maintain proteins in a soluble state as part of their various housekeeping roles, under not only normal cell conditions but particularly in periods of stress. For this reason, extensive research had previously determined the effect of Hsp70, Hsp90, yeast Hsp104, and small Hsps on α-Syn, with aim to elucidate the molecular mechanisms at the origin of PD. However, no research had been conducted on the effect of Hsc70, the constitutive counterpart of inducible Hsp70, which encounters assembling α-Syn prior to Hsp70.

Here, we determined that Hsc70 is a molecular chaperone which inhibits α-Syn assembly, similar to the effects of human Hsp70, Hsp27 and αB-crystallin, and yeast chaperone Hsp104, which is also capable of disassembling α-Syn aggregates. Constitutively expressed Hsc70 is the first molecular chaperone to interact with aggregating α-Syn. We have decribed that *in vitro*, Hsc70 binds to soluble α-Syn and slows down its assembly into β-sheet-containing fibrils, by binding to soluble α-Syn with a high affinity. We have shown that Hsc70 binds, holds and releases α-Syn in a nucleotide-dependent manner, during which interaction α-Syn is rendered assembly incompetent. Moreover, Hsc70 also binds to fibrillar a-Syn and even does so preferentially, with 5 times higher affinity; an interaction which is saturated at a molar ratio of 1 Hsc70 to 4 α-Syn. Hsc70 is not capable of disassembling fibrils once they have formed. Physiologically, the α-Syn fibril-Hsc70 interaction has a protective effect as it renders the fibrils less toxic to mammalian cells in culture. As well as this, we

describe that the Hsc70 co-chaperone Hdj1 has an inhibitory effect on α-Syn which is independent of Hsc70, while Hdj2 does not. In terms of action on fibrillar α-Syn, both co-chaperones bind tightly to α-Syn fibrils, and enhance Hsc70 binding, although to different extents.

We speculated that Hsc70 has therapeutic potential in PD. Having shown that Hsc70 binding to fibrils is cytoprotective, it may be feasible to develop a therapeutic agent based on Hsc70 which binds to extracellular α-Syn aggregates, changes their physicochemical properties and inhibits their entry into a neighbouring cell, and thus the spread of PD. It is important to consider the pharmacological repercussions of therapeutic agents, and there is a chance that an exogenous homolog of Hsc70 would be less likely to trigger an autoimmune disease. In the quest to find such a protein, and to further expand the catalogue of known effects of molecular chaperones on α-Syn, we studied the effect of the yeast equivalent of Hsc70, Ssa1p, on α-Syn. Here, we showed that, similar to Hsc70, Ssa1p slows down the assembly of soluble α-Syn into fibrils, by binding with a comparable observed dissociation constant to that of Hsc70-α-Syn. Also akin to Hsc70, Ssa1p binds to fibrils, but this interaction does not proffer protection against the toxicity of α-Syn fibrils. This difference is almost certainly a result of a change in 22 amino acids in the primary sequence of the peptide binding domains of Hsc70 and Ssa1p, but could also be explained by a difference in ATPase activity of the two molecular chaperones. Given that Ssa1p binds to α-Syn fibrils in the absence of ATP and cochaperones (and indeed that ATP hydrolysis favours client protein release), there is a strong possibility that if one were to mutate Ssa1p to leave *only* the region which binds to α-Syn, it would still bind. We instigated the first crucial step towards this “mini-Ssa1p” : mapping the interaction sites between Ssa1p and α-Syn using a chemical cross-linking and mass spectrometry approach.

PERSPECTIVES

1. Hsc70

We believe that there are two militating factors which contribute to PD. Firstly, the stochastic aggregation of α-Syn within cells and secondly the propagation of aggregates from one cell to another. We have demonstrated that Hsc70 is effective against aggregating α-Syn, and that Hsc70 reduces the toxicity of α-Syn fibrils, most likely because Hsc70 binding changes the physicochemical properties of the fibrils. These results open the floodgates to many more questions and entices further exploration, as discussed herein.

Does Hsc70 inhibit α-Syn fibrils binding to membranes?

α-Syn has been seen not only to propagate from cell to cell *in vivo* (Hansen, Angot et al., 2010), but also to transfer from host to graft cells when PD patients received fetal mesencephalic transplants in a quest to replace dopamine producing cells (Chu and Kordower, 2010). We have shown that Hsc70-coated α-Syn fibrils are less toxic than naked fibrils, and speculated that the change in physicochemical properties proffered by bound Hsc70 halts cell-to-cell progression of aggregates, but the mechanism behind this needs to be unravelled. Does bound Hsc70 simply inhibit α-Syn from binding to neighbouring cell membranes? α-Syn is known to bind to plasma membranes and vesicles, and thought to permeabilize membranes via a pore-like mechanism (Volles and Lansbury, 2002), and Van Rooijen *et al* have shown *in vitro* that α-Syn fibrils permeabilize synthetic large unilamellar vesicles (LUVs) composed of phospholipids with negatively charged headgroups (PI, phosphatidylinositol or POPG, 1-palmitoyl, 2-oleoyl phosphatidylglycerol) (van Rooijen, Claessens et al., 2009). It would be interesting to see whether this still occurs when the fibrils are coated with Hsc70. This could be achieved using a calcein efflux assay, where negatively charged LUVs are filled with a self-quenching concentration of the fluorescent dye calcein (50 mM). Upon incubation with α-Syn fibrils or Hsc70 coated fibrils, if the α-Syn binds to and

permeabilizes the vesicles, calcein is leaked, its concentration is diluted and thus fluoresces when excited at 497 nm, which can be measured using a spectrofluorimeter. This is an easy, quantitative method to determine whether or not Hsc70 coated α-Syn fibrils are still capable of binding to and permeabilizing membranes in comparison to "naked" fibrils, thus determining how Hsc70 renders fibrils less toxic.

Does Hsc70 binding to fibrils interfere with α-Syn elongation in vivo?

It has already been shown that fluorescently labelled α-Syn seeds the aggregation of endogenous α-Syn after transferring between cells in culture (Hansen, Angot et al., 2010). *In vitro*, we showed that Hsc70 hinders the elongation of α-Syn fibrils (Fig. 5 of (Pemberton, Madiona et al., 2011)). To confirm whether this phenomenon withstands *in vivo*, one could infect cells which are expressing a reporter α-Syn, fluorescently tagged e.g. with cyan fluorescent protein (CFP), with extracellular, labelled α-Syn fibrils coated with Hsc70. If the endogenous CFP-α-Syn elongates the extracellular, Hsc70-coated fibrils, the fluorescence will colocalize. If no elongation takes place as a result of the bound Hsc70, colocalization of the different fluorescent entities will not be evident.

Characterize the structure of α-Syn fibrils bound by Hsc70

In a quest to further understand the mechanisms behind PD, it would be useful to know how Hsc70 binding to α-Syn fibrils affects α-Syn at a structural level. NMR is an ideal technique for this as unlabelled proteins are essentially 'invisible' to the machine. It is therefore possible to compare the NMR data of nitrogen-15 or carbon-13 isotope-labelled α-Syn fibrils alone, with labelled α-Syn fibrils coated with unlabelled Hsc70 to determine what changes occurs, and how binding takes place. This would also enlighten our understanding of the part(s) of α-Syn essential for fibril assembly. Given that Hsc70 binding decreases α-Syn toxicity, one could imagine that identifying the region of α-Syn bound by Hsc70 could lead to therapeutic applications through the design of peptides with specific structural

properties which allow them to bind specifically to fibrillar α-Syn and to change the physiochemical properties of the fibrils.

Characterize the structure of soluble α-Syn oligomers, and soluble α-Syn bound by Hsc70

Supramolecular mass spectrometry is one of the few techniques capable of characterising heterogeneous species. For this reason, we set up a collaboration during my thesis with Dr. Sanglier-Cianférani and her colleagues at the Bio-Organic Mass Spectrometry Laboratory in Strasbourg. The main aims of this collaboration were to study the oligomerisation state of α-Syn during the first crucial steps of the asssembly process, in which Hsc70 is thought to bind. Although the analyses are far from complete, preliminary results from studying α-Syn in non-covalent, negative and positive ionisation modes show the presence of a pH-dependent, dimeric form of the protein. Ion mobility mass spectrometry confirms the presence of this dimer, as well as a conformational heterogeneity. Information on the oligomeric state of α-Syn will help us to understand the mechanisms of assembly of on- and off-pathway species, and provide insight into how Hsc70 is capable of inhibiting the assembly phenomenon.

Can chaperones retain α-Syn in its supposedly tetrameric, aggregation-resistant conformation?

In light of the recent publication suggesting that physiologically, α-Syn exists as a tetramer *in vivo*, it could be important to assess the role of Hsc70 and/ or other chaperones in the stabilization of α-Syn in its tetrameric form, which is said to be less aggregation prone. This would mean purifying α-Syn from cellular extracts under non-denaturing conditions as per Bartels and colleagues (Bartels, Choi et al., 2011), to preserve it as a tetramer, and assessing its interaction with Hsc70 and other molecular chaperones in comparison to the results obtained with monomeric α-Syn. One could then stress the tetrameric α-Syn in the

absence or presence of the chaperones, for instance by adding heavy metals to reenact events thought to trigger the assembly and deposition of α-Syn in the pathogenesis of PD, and known to induce α-Syn assembly *in vitro* (aluminium, copper(II), iron(III), cobalt(III), or manganese(II) (Uversky, Li et al., 2001)). This would demonstrate whether or not the chaperones are capable of stabilizing the α-Syn.

2. Ssa1p

Map the interaction site between α-Syn and Ssa1p

We are currently in the process of mapping the interaction site between soluble α-Syn and Ssa1p. This involves stablizing the α-Syn-Ssa1p interaction with chemical cross-linkers, separating the complex from unbound protein according to electrophoretic mobility (a function of molecular weight) using denaturing gel electrophoresis, and analysing the cross-linked peptides by mass spectrometry, as we did for the interaction between Ssa1p and Ure2p (Redeker, Bonnefoy et al., 2010).

Engineering an Ssa1p with improved affinity for therapeutic purposes

Once we know the sequence of amino acids on each protein which interact, it would be beneficial to attempt to strengthen the binding within the complex (i.e. enhance the affinity, K_d), via protein engineering methods. The K_d of a protein complex is a function of the rates of association (k_{on}) and dissociation (k_{off}) with the relation $K_d = k_{off}/k_{on}$ for reactions limited by diffusion. k_{off} is influenced by the strength of short range interactions (Van der Waals interactions, hydrogen bonds, hydrophobic interactions and salt bridges), whereas k_{on} is goverened by diffusion and can be increased by optimizing electrostatic forces (Shoup and Szabo, 1982; Berg and von Hippel, 1985; Schreiber and Fersht, 1996). *In silico* algorithms, for example the Binding Affinity Benchmark (Kastritis and Bonvin, 2010) could help determine theoretical possibilities to improve the α-Syn-Ssa1p K_d, before site directed mutagenesis to alter the binding site of Ssa1p accordingly. It would then be necessary to

recharacterise the α-Syn-mutant Ssa1p interaction, to confirm an improvement in the *Kd*, and see what effect this may have on α-Syn.

Furthermore, knowing that Ssa1p is capable of binding to α-Syn fibrils in the absence of co-chaperones or allosteric behaviour from bound nucleotides, it is possible that the chaperone may function as a “minichaperone”. This was successfully achieved for the bacterial GroEL chaperone complex, which normally functions as a large, 14-subunit complex with a central cavity, and requires ATP and co-chaperone GroES for some activities. The apical domain, a 185-residue stretch of a single subunit of GroEL, independently shows high chaperone activity (Zahn, Buckle et al., 1996; Chatellier, Hill et al., 1998; Golbik, Zahn et al., 1998). It would be interesting to mutate Ssa1p to leave the α-Syn-binding region, and test its effect on α-Syn. Therapeutically, the smaller the agent, the more chance it has of not triggering an autoimmune response, aided by the fact that Ssa1p is an exogenous protein.

Overall, as described at the beginning of this thesis, proteinopathies can be a result of a toxic gain of function of the aggregated protein, or a physiological loss of function as the active protein is ‘taken out of action’ when it is sequestered within aggregates. As the debate on the real function of α-Syn is still ongoing, it is difficult to know whether PD is purely the result of the toxicity of α-Syn aggregates. Some of the symptoms of PD could be a result of a lack of α-Syn for its normal function. Ultimately, it is important to know what the cellular function(s) of α-Syn is (are) because introducing a drug or protein compound which renders α-Syn inactive or changes its physiocochemical properties may, in itself have detrimental effects.

Annex

ANNEX: Yeast prion Ure2p and Ssa1p

Article 4: A region within the C-terminal domain of Ure2p is shown to interact with the molecular chaperone Ssa1p by the use of cross-linkers and mass spectrometry.

Virginie Redeker, Jonathan Bonnefoy, Jean-Pierre Le Caer, Samantha Pemberton, Olivier Laprévote and Ronald Melki (2010). FEBS J 277 (24): 5112-23.

BACKGROUND AND OBJECTIVE

In a manner similar to what is observed for the vertebrate prion PrP, a change in the solubility of the *Saccharomyces cerevisiae* protein Ure2 is responsible for the yeast prion state [*URE3*]. Ure2p, which exists principally as a dimer, is comprised of two domains, the N-terminal from residues 1 to 93, and the C-terminal from 94 to 354 (Thual, Komar et al., 1999). Solving the crystal structure of the C-terminal (or "functional") domain by x-ray diffraction revealed a globular structure, which resembles that of the beta class glutathione S-transferases (GST) (Bousset, Belrhali et al., 2001). The N-terminal "prion" domain is unnecessary for function, but it is indispensible for the occurrence, maintenance and transmissibility of the prion phenotype (Masison and Wickner, 1995). *In vitro* at physiological temperature and pH, full-length Ure2p assembles into helical twisted fibrils that are 20 nm wide (Thual, Komar et al., 1999; Ranson, Stromer et al., 2006), but lack typical amyloid structure (Bousset, Thomson et al., 2002; Bousset, Briki et al., 2003; Redeker, Halgand et al., 2007). The isolated prion domain, however, assembles into 5 nm wide amyloid fibrils (Baxa, Wickner et al., 2007; Loquet, Bousset et al., 2009). Further work from our laboratory showed that the minimal region critical for assembly into fibrils is the span of residues from 43-79, as the Ure2p mutant comprising residues 1-42 did not assemble into fibrils, while mutants of residues 1-79 and 1-93 did (Bousset, Bonnefoy et al., 2010). Amyloid fibrils made from these constructs are unable to seed assembly of endogenous Ure2p into fibrils, further suggesting that they do not share structural properties with full-length Ure2p fibrils (Bousset, Bonnefoy et al., 2010).

Despite the importance of protein fibrils in the context of conformational diseases, information on their structure is still sparse, and has only recently begun to be revealed as a result of advances in biophysical approaches, allowing high-resolution insights into molecular organisation. Due to the large and heterogeneous nature of amyloid/ non-amyloid fibrils, X-ray crystallography has only shown success for short peptides (6-7 residues) that form amyloid-like structures (Nelson, Sawaya et al., 2005). Solid state NMR (SSNMR) however has successfully unravelled the structure of full length Ure2p (Loquet, Bousset et al., 2009), and HET-s – a prion protein from the fungus *Podospora anserina* (Wasmer, Schutz et al., 2009). Methods such as cryoelectron microscopy, SSNMR, X-ray crystallography, hydrogen-deuterium exchange and, as used in the following article, mass spectrometry, provide complementary information in the quest to study amyloid and non-amyloid fibril structure.

As previously mentioned, Ssa1p has previously been shown to modulate the assembly of the yeast prion protein Ure2p *in vitro*, by former members of the laboratory (Savistchenko, Krzewska et al., 2008). More specifically, Ssa1p completely inhibits the assembly of Ure2p at a molar ratio of 1 Ssa1p to 4 Ure2p, by binding to soluble Ure2p with an observed dissociation constant of 0.5 μM^{-1}.

For this article, we strived to expand on what is already known about the Ure2p-Ssa1p interaction, by characterising the complexes formed and determining the site(s) of interaction which result in Ure2p being sequestered in an assembly incompetent state. To this aim, we used mass spectrometry to investigate chemically cross-linked Ure2p-Ssa1p peptides.

We show that solvent exposure of a single residue – lysine 339 – is affected upon Ure2p-Ssa1p binding, thus implicating this residue and its flanking amino acids, in the chaperone – prion protein interaction.

I participated to this work by expressing, producing and purifying the molecular chaperone Ssa1p which was used in these studies.

the FEBS Journal

A region within the C-terminal domain of Ure2p is shown to interact with the molecular chaperone Ssa1p by the use of cross-linkers and mass spectrometry

Virginie Redeker[1], Jonathan Bonnefoy[1], Jean-Pierre Le Caer[2], Samantha Pemberton[1], Olivier Laprévote[2] and Ronald Melki[1]

1 Laboratoire d'Enzymologie et Biochimie Structurales, CNRS, Gif-sur-Yvette, France
2 Institut de Chimie des Substances Naturelles, CNRS, Gif-sur-Yvette, France

Keywords
cross-linker; mass spectrometry; molecular chaperone; oligomerization; Ure2p; prion

Correspondence
Virginie Redeker or Ronald Melki, Laboratoire d'Enzymologie et Biochimie Structurales, CNRS, Avenue de la terrasse, 91198 Gif-sur-Yvette, Cedex, France
Fax: +33 1 69 82 31 29
Tel: +33 1 69 82 34 60 or
+33 1 69 82 35 03
E-mail: virginie.redeker@lebs.cnrs-gif.fr, ronald.melki@lebs.cnrs-gif.fr

(Received 28 July 2010, revised 5 October 2010, accepted 12 October 2010)

doi:10.1111/j.1742-4658.2010.07915.x

The propagation of yeast prion phenotypes is highly dependent on molecular chaperones. We previously demonstrated that the molecular chaperone Ssa1p sequesters Ure2p in high molecular weight, assembly incompetent oligomeric species. We also determined the affinity of Ssa1p for Ure2p, and its globular domain. To map the Ure2p–Ssa1p interface, we have used chemical cross-linkers and MS. We demonstrate that Ure2p and Ssa1p form a 1 : 1 complex. An analytical strategy combining in-gel digestion of cross-linked protein complexes, and both MS and MS/MS analysis of proteolytic peptides, allowed us to identify a number of peptides that were modified because they are exposed to the solvent. A difference in the exposure to the solvent of a single lysine residue, lysine 339 of Ure2p, was detected upon Ure2p–Ssa1p complex formation. These observations strongly suggest that lysine 339 and its flanking amino acid stretches are involved in the interaction between Ure2p and Ssa1p. They also reveal that the Ure2p amino-acid stretch spanning residues 327–339 plays a central role in the assembly into fibrils.

Structured digital abstract

- MINT-8044534: *Ure2p* (uniprotkb:Q8NJQ9) and *Ure2p* (uniprotkb:Q8NJQ9) *bind* (MI:0407) by *cross-linking study* (MI:0030)
- MINT-8044522: *Ssa1p* (uniprotkb:C8Z3H3) and *Ssa1p* (uniprotkb:C8Z3H3) *bind* (MI:0407) by *cross-linking study* (MI:0030)
- MINT-8043971, MINT-8043985, MINT-8044494, MINT-8044548: *Ure2p* (uniprotkb:Q8NJQ9) and *Ssa1p* (uniprotkb:C8Z3H3) *bind* (MI:0407) by *cross-linking study* (MI:0030)

Introduction

The aggregation of the prion Ure2p is at the origin of the [*URE3*] trait in the baker's yeast *Saccharomyces cerevisiae* [1,2]. The propagation of the prion element [*URE3*] is highly dependent on the expression of a number of molecular chaperones from the Hsp100, Hsp70 and Hsp40 protein families [3–5]. For example, over-expression of the Hsp70 Ssa1p cures [*URE3*] [4] and a mutation in the peptide-binding domain of Ssa2p abolishes [*URE3*] propagation [5]. We have shown *in vitro* that Ssa1p sequesters Ure2p in an assembly incompetent state [6]. Affinity measurements performed with full-length Ure2p and the compactly folded globular domain of the protein [7,8] revealed that Ssa1p interacts with both full-length Ure2p and the C-termi-

Abbreviations
amu, atomic mass unit; EDC, 1-ethyl-3-(3-dimethylaminopropyl)carbodiimide hydrochloride; HXMS, hydrogen/deuterium exchange measurement by mass spectrometry; LTQ, linear ion trap; NHS, *N*-hydroxysuccinimide; TFA, trifluoroacetic acid.

nal domain of the protein [6]. The slightly higher affinity of Ssa1p for full-length Ure2p was interpreted as being the consequence of a preferential interaction with the flexible N-terminal domain of Ure2p, critical for assembly into fibrils. To further identify the regions involved in Ure2p–Ssa1p interaction, we set up a chemical cross-linking strategy coupled to the identification of the chemically modified polypeptides by MS.

Covalent cross-linking approaches allow: (a) the identification of surface areas involved in protein-protein interactions within protein complexes; (b) the characterization of the distance constraints within a protein complex; and (c) the assessment of regions exposed or not to the solvent within a protein [9–14]. Cross-linking of protein complexes generates three types of products: (a) mono-linked peptides when the cross-linker binds to a reactive residue at one end, whereas the other reactive group is hydrolyzed; (b) loop-linked peptides when both ends of a cross-linker molecule bind to a single polypeptide chain; and (c) cross-linked peptides when the ends of a cross-linker bind two distinct polypeptide chains. Although far from straightforward [15], the proof of protein–protein interactions comes from the identification of cross-linked peptides [16–23]. The interfaces involved in protein–protein interactions can be also identified from the changes in the intensity of mono-linked peptides, before and after complex formation [13,24].

In the present study, we document Ure2p–Ssa1p complex formation using two homo-bifunctional *N*-hydroxysuccinimide (NHS)-ester cross-linkers and the zero length carbodiimide cross-linker 1-ethyl-3-(3-dimethylaminopropyl) carbodiimide hydrochloride (EDC). The stoichiometry of the Ure2p–Ssa1p complexes that we generate is determined. Using MS after chemical cross-linking and proteolysis, we map the solvent accessibility of reactive residues on Ure2p and Ssa1p before and after Ure2p–Ssa1p complex formation and identify a region, located within the C-terminal domain of Ure2p that interacts with Ssa1p. Because the C-terminal domain of Ure2p is tightly involved in the assembly of the prion into fibrils [25–28] and because Ssa1p sequesters Ure2p in an assembly incompetent state, we conclude that this region and its surroundings are involved in the Ure2p fibrillar scaffold.

Results

Analysis of the intact cross-linked protein complexes

The cross-linking conditions were optimized using SDS/PAGE. The optimal Ure2p and Ssa1p concentrations are 20 and 10 μM, respectively, compatible with both a total inhibition of Ure2p assembly by Ssa1p and the formation of high amounts of protein complexes [6]. The two homo-bifunctional NHS-esters, BS2G and BS3, were selected for their ability to cross-link significant amounts of polypeptide chains at a protein to cross-linker ratio of 1 : 20. Mixtures of deuterium labeled (d4) and unlabeled (d0) cross-linkers were used to facilitate cross-linked peptide detection and identification. The zero-length cross-linker EDC was also used (not shown).

We previously demonstrated that Ssa1p–Ure2p interaction is nucleotide dependent [6]. We also showed through assembly kinetic measurements that Ssa1p binds a hexameric form of Ure2p in the presence of ATP, whereas the form that is bound in the presence of ADP is different, and probably dimeric [6]. We therefore performed Ure2p and Ssa1p cross-linking reactions in the presence of ATP or ADP (Fig. 1A). Regardless of the nucleotide present, two specific Ure2p–Ssa1p complexes with apparent molecular masses of 120 and 160 kDa were observed. Western blot analysis confirmed the presence of Ure2p and Ssa1p in all protein complexes (Fig. 1B). The extent of Ure2p–Ssa1p complex formation was significantly higher in the presence of ADP than in the presence of ATP, as seen by SDS/PAGE, This is in agreement with the finding that Ssa1p binds hexameric Ure2p in the presence of ATP, whereas it binds dimeric Ure2p in the presence of ADP [6]. Because Ssa1p efficiently inhibits Ure2p assembly in the presence of ADP and as higher amounts of Ure2p–Ssa1p cross-links are obtained in the presence of ADP, all cross-linking reactions and subsequent analysis were performed in the presence of ADP.

It should be noted that Ure2p cross-links into dimers with distinct conformations, and thus different mobilities (Fig. 1B). Similarly, nucleotide-dependent conformational changes occurring within Ssa1p were observed. Fast migrating monomeric and oligomeric Ssa1p species, most likely corresponding to compact Ssa1p species, were observed in the presence of ATP. No change in the mobility of the Ure2p–Ssa1p complexes was detected in the presence of ATP.

The stoichiometry of Ure2p and Ssa1p within the 120 and 160 kDa cross-linked complexes was assessed using high-mass MALDI-TOF MS (Fig. 2). In agreement with the SDS/PAGE, two Ure2p–Ssa1p complexes were observed in the mass spectrum (Fig. 2C): one where a single Ure2p is cross-linked to a single Ssa1p (110 993 Da), and another where two Ure2p molecules are bound to one Ssa1p (151 346 Da). Because the binding of the cross-linkers leads to an increase in the molecular mass (Table S1), the number of cross-linkers bound

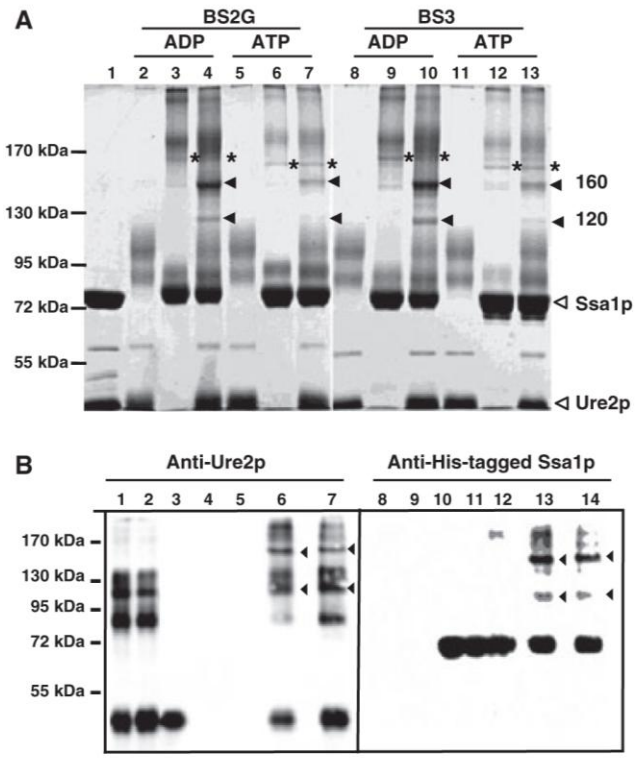

Fig. 1. SDS/PAGE analysis of cross-linked protein products. The reaction products generated upon treatment of Ure2p, Ssa1p and Ure2p in the presence of Ssa1p with the cross-linking agents BS2G and BS3 were separated on a 7.5% acrylamide SDS/PAGE and stained with Coomassie blue (A) or western blotted and stained with antibodies directed against Ure2p or His-Tagged Ssa1p (B). (A) A mixture of untreated Ure2p and Ssa1p (lane 1); Ure2p alone (lanes 2, 5, 8 and 11), Ssa1p alone (lanes 3, 6, 9 and 12), and Ure2p incubated in presence of Ssa1p (lanes 4, 7, 10 and 13) were treated with BS2G (lanes 2–7) or BS3 (lanes 8–13), in the presence of ADP 0.5 mM (lanes 2–4 and 8–10) or 4 mM ATP and 5 mM $MgCl_2$ (lanes 5–7 and 11–13). (B) Western blots of cross-linked products obtained in the presence of 0.5 mM ADP stained with antibodies directed against Ure2p (lanes 1–7) and His-Tagged Ssa1p (lanes 8–14); a mixture of untreated Ure2p and Ssa1p is seen in lanes 3 and 10. Ure2p, Ssa1p and Ure2p incubated with Ssa1p treated with BS2G are seen in lanes 1 and 8, 4 and 11 and 6 and 13, respectively. Similar samples treated with BS3 are seen in lanes 2 and 9, 5 and 12 and 7 and 14, respectively. The arrows show the cross-linked Ure2p–Ssa1p complexes with apparent molecular masses of 120 and 160 kDa. Nucleotide-dependent changes in Ssa1p conformation following BS3 treatment at the origin of electrophoretic modifications are labeled with stars.

to Ure2p and Ssa1p can be estimate as 5 ± 1 and 10 ± 1 for BS2G and BS3, respectively.

Identification of modified and cross-linked polypeptides

The analytical strategy used to characterize the polypeptides involved in Ure2p–Ssa1p interaction is schematized in Fig. S1. Cross-linked Ure2p, Ssa1p and Ure2p–Ssa1p complexes resolved by SDS/PAGE were treated with both trypsin and chymotrypsin to obtain high protein sequence coverage (86% and 84.7% for Ure2p and Ssa1p, respectively; Fig. S2). The modified peptides were detected by MS using the 4.0247 atomic mass unit (amu) mass difference conferred by the binding of the nondeuterated or deuterated cross-linkers (Fig. 3A) [13,29]. Detection of modified peptides was further confirmed using the 42.0469 amu mass difference as a result of the difference in the spacer arm length of BS2G and BS3 (Fig. 3). A list of peptides modified by BS2G or BS3 cross-linkers was derived from MS analyses as described in the Materials and methods and Fig. S1. Given the variety of theoretical cross-links and modifications, exact mass measurements were insufficient to unambiguously identify all the peptides in our list using the available softwares (GPMAW [30], XQUEST [31] and MSX-3D [12]) with a mass tolerance of 5 p.p.m. We therefore used MALDI-TOF-TOF and/or nanoLC-Orbitrap tandem MS to further identify peptides from this list. Twenty-five mono-linked peptides and five loop-linked peptides from Ure2p or Ssa1p (Table 1) were thus identified. Most of the modified or loop-linked amino acid residues that we identified are exposed to the solvent as shown on the 3D structure of Ure2p and Ssa1p (Fig. 4). No intermolecular cross-links were detected. This is probably a result of the low abundance of cross-linked peptides and potential changes in their ionization properties [32]. Because changes in the reactivity of amino-acid residues to the cross-linkers can be efficiently used to map conformational changes or protein–protein interaction interfaces [13,24], we further compared the modified peptides derived from Ure2p and Ssa1p alone and the two Ure2p–Ssa1p complexes.

Changes in the reactivity of Ure2p amino acid residues upon Ure2p–Ssa1p complex formation

Most of the peptides originating from Ure2p were found in both Ure2p–Ssa1p complexes. Their intensities were also similar. A similar observation was made for peptides originating from Ssa1p. Two unique differences were observed: one for Ure2p and one for Ssa1p. The peptide spanning residues 337–343 from Ure2p was found modified on lysine 339 (Fig. 5) in monomeric Ure2p and the Ure2p–Ssa1p complex with an apparent molecular mass of 160 kDa but not that of 120 kDa (Fig. S3). The finding that the Ure2p 337–343 fragment is neither detected unmodified, nor modified, in the 120 kDa Ure2p–Ssa1p complex strongly suggests that it is cross-linked to Ssa1p. Similarly,

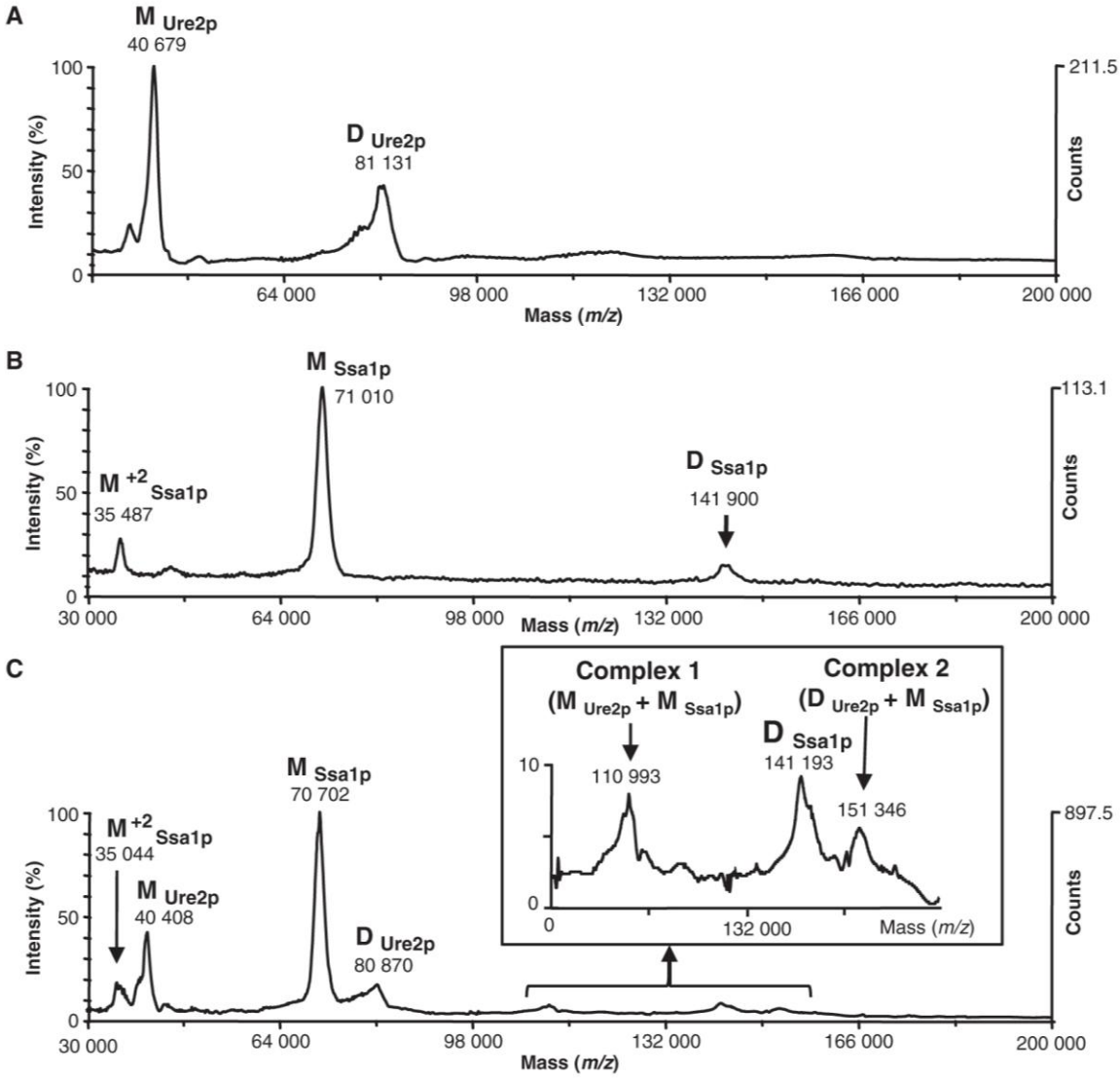

Fig. 2. High-mass MALDI-TOF mass spectra of the products generated upon cross-linking. Ure2p (A), Ssa1p (B) and Ure2p incubated with Ssa1p (C) were cross-linked with BS3 in the presence of 0.5 mM ADP. The mass of each peak and its identity are given (M, monomer; D, dimer). The part of the spectrum containing the Ure2p–Ssa1p complexes is enlarged; inset in (C). The stoichiometry within the Ure2p–Ssa1p complexes is indicated.

lysine 325 was found to be modified in Ssa1p but not in Ure2p–Ssa1p complexes.

These observations strongly suggest that the exposure to the solvent of lysine 339 from Ure2p and lysine 325 from Ssa1p changes upon the formation of a 1 : 1 Ure2p–Ssa1p complex. Indeed, Ure2p is dimeric and lysine 339 from each monomer within the dimer is exposed to the solvent and can interact with Ssa1p. When cross-linking occurs between Ure2p and Ssa1p, a 120 kDa product is generated. When, in addition to the latter covalent bond, the two monomers within Ure2p dimer are cross-linked, a 160 kDa product is observed. Additional complexes with apparent molecular weight higher than 200 kDa that are immuno stained by both antibodies directed against Ure2p and Ssa1p are also seen (Fig. 1B). The latter products correspond to species where covalent bonds between Ure2p monomers and each Ure2p monomer and Ssa1p have been established. Ssa1p lysine 325 is not located within the client binding pocket of the chaperone. Its lack of modification upon complex formation can only be attributed to a conformational rearrangement within Ssa1p that occurs upon Ure2p–Ssa1p complex formation.

Discussion

The propagation of the [*URE3*] trait is highly dependent on the expression of molecular chaperones [3–5]. We recently showed that Ssa1p modulates the assem-

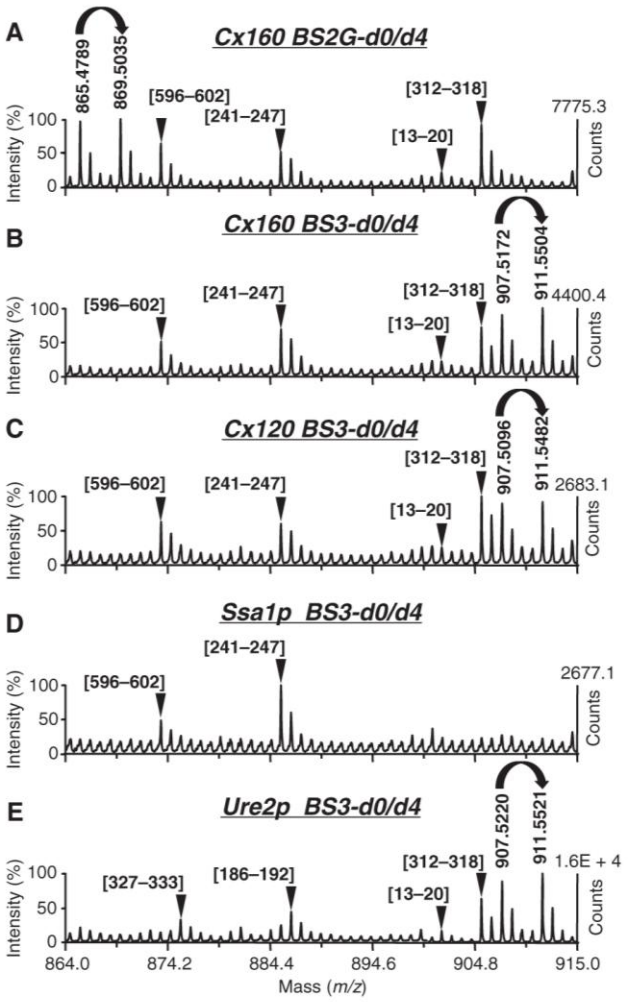

Fig. 3. Detection of chymotryptic peptides modified by nondeuterated and deuterated cross-linkers by MALDI-TOF-TOF mass spectrometry. A selection of mass spectra illustrates how the comparison of chymotryptic peptides from different cross-linked complexes and protein controls allows the detection of modified peptides. (A, B) Mass spectra of the 160 kDa Ure2p–Ssa1p complex cross-linked with BS2G-d_0/d_4 and BS3-d_0/d_4, respectively. The mass spectra of the 120 kDa Ure2p–Ssa1p complex cross-linked with BS3-d_0/d_4 and that of Ssa1p, and Ure2p after treatment with BS3-d_0/d_4 are shown in (C–E). The curved arrows indicate the 4.0247 amu increase conferred by the binding of (light/heavy, d_0/d_4) cross-linkers. A 42.0469 amu mass difference between the doublet peaks recorded upon binding of BS2G-d_0/d_4 (A) and BS3-d_0/d_4 (B) is observed. The peptides indicated by arrowheads were identified by exact mass measurement. The peptide labeled by curved arrows was identified by tandem mass spectrometry as a mono-linked Ure2p [S^{100}RITK*F^{105}] where K* is the mono-linked residue.

bly of Ure2p into protein fibrils *in vitro* and sequesters Ure2p into assembly incompetent oligomeric species [6]. Using fluorescence polarization, full-length Ure2p and an Ure2p fragment spanning residues 94–354, we assessed the affinity of Ssa1p for full-length Ure2p and its compactly folded C-terminal domain (30 and 20 nM, respectively). The finding that Ssa1p binds with slightly higher affinity to full-length Ure2p than its compactly folded C-terminal domain was interpreted as a consequence of the additional interaction between Ssa1p and the flexible N-terminal moiety of Ure2p, which is critical for assembly. An alternative explanation that can account for this observation is that Ssa1p binds with higher affinity a conformational state of Ure2p as a result of the presence of the N-terminal domain of the protein that slightly differs from that adopted by its C-terminal moiety.

The only amino acid residue belonging to Ure2p which exposure to the solvent is affected upon the interaction of Ure2p with Ssa1p is lysine 339. This suggests that lysine 339 and its flanking amino acid residues are involved in Ure2p–Ssa1p complex formation. Because the binding of Ssa1p prevents Ure2p assembly, it is reasonable to consider that the Ure2p region centered on lysine 339 is involved in the assembly of this prion into fibrils. Interestingly, hydrogen/deuterium exchange measurements by mass spectrometry (HXMS) have revealed a decrease in the exposure to the solvent of the amino acid stretch spanning residues 327–335 upon assembly of Ure2p into fibrils [33]. Thus, the binding of Ssa1p in the vicinity of this stretch interferes with Ure2p assembly into fibrils either because of a change in the conformation of this stretch or the crowding of a surface interface involved in intermolecular interactions within the fibrils or both. Alternatively, the inability of Ure2p to form fibrils upon binding of Ssa1p to Ure2p region centered on lysine 339 could be a consequence of its incapacity to acquire an assembly competent conformation. We recently showed that the regions centered on residue 6 and 137 establish intramolecular interactions in assembly competent Ure2p [26]. Interestingly, phenylalanine 137 and lysine 339 are located 27 Å apart within the same area in the 3D structure of Ure2p. Thus, the binding of Ssa1p to the region centered on lysine 339 could abolish the acquisition by Ure2p of an assembly competent state.

The results obtained in the present study provide a rationale for the inhibition of Ure2p assembly by Ssa1p and underline the key role of the C-terminal domain of Ure2p in assembly into fibrils [25–28]. The results, together with those previously obtained by HXMS [33], further narrow the region critical either for modulating Ure2p assembly into fibrils, or for the establishment of intermolecular interactions between Ure2p molecules within the fibrils, to that spanning lysines 327–339.

The finding that lysine 325 from Ssa1p, which is located at the interface between the nucleotide and cli-

Table 1. Mono- and loop-linked peptides list. The tryptic and chymotryptic peptides that were identified are denoted T and CT, respectively. The protonated monoisotopic experimental masses (MH+exp) and the calculated mass difference (p.p.m.) with the theoretical monoisotopic mass of the identified peptide are given. The presence of the modified peptides in the Ure2p, Ssa1p and Ure2p–Ssa1p complexes with apparent molecular masses 160 and 120 kDa tryptic and chymotryptic reaction products is indicated by an X. The amino acid sequences and the modification sites are indicated. Loop-linked peptides are labeled (T1). ND, not determined.

	BS2G		BS3		Peptide detection				Peptide identification in Ssa1p		Peptide identification in Ure2p	
	MH+exp	p.p.m.	MH+exp	p.p.m.	Cx160	Cx120	Ssa1p	Ure2p	Sequence	Site	Sequence	Site
CT	865.4783	0.5	907.5245	0.2	X	X		X			S_{100}RITKF$_{105}$	K104
CT	1125.6722	1.6	1167.722	1.2	X	X	X		K_{243}RKNKKDL$_{250}$	K243, K247 (T1)		
CT	1407.646	2.6	1449.6946	0.9	X	X	X		T_{378}GDESSKTQDLL$_{389}$	K384		
CT	1427.7954	1.1	1469.8446	1.1	X	X	X		K_{243}RKNKKDLSTN$_{253}$	K243, K247 (T1)		
CT	1478.8682	0.7	1520.9146	1.3	X	X	X		V_{334}GGSTRIPKVQKL$_{346}$	K342, K345 (T1)		
CT	1502.7592	0.6	1544.8064	0.3	X	X		X			H_{237}SQKIASAVERY$_{248}$	K240
CT	1616.7878	3.7	ND		X			X			H_{237}SQKIASAVERY$_{248}$	K240, S243
CT	1842.9832	2.5	ND				X		R_{319}DAKLDKSQVDEIVL$_{333}$	K322 or K325		
CT	1973.9536	1.3	2015.9996	0.4	X	X	X		N_{149}DSQRQATKDAGTIAGLN$_{166}$	K157		
T	1002.5442	2.4	1044.5926	1	X	X	X		N_{414}STIPTKK$_{421}$	K420		
T	1075.5522	0.5	1117.5962	2.5	X	X	X		L_{507}SKEDIEK$_{514}$	K509		
T	1103.5114	1.1	1145.5578	1.6	X			X			W_{337}TKHMMR$_{343}$	K339
T	1119.5052	2.2	1161.5534	0.9	X			X			W_{337}TKHMMR$_{343}$ (*1M$_{ox}$*)	K339
T	1131.5986	1.8	1173.6466	0.8	X	X	X		I_{498}TITNDKGR$_{506}$	K504		
T	1135.5033	1	1177.5468	2.5	X			X			W_{337}TKHMoxMoxR$_{343}$ (*2M$_{ox}$*)	K339
T	1136.7232	3.1	1178.7712	2	X			X			R_{344}PAVIKALR$_{352}$	K349
T	1137.7082	2.1	1179.6844	7.3	X			X			R_{344}PAVIKALR$_{352}$	K349
T	1299.664	1.1	1341.7112	0.8	X	X	X		N_{246}KKDLSTNQR$_{255}$	K247, K248 (T1)		
T	1414.696	0.1	1456.742	1.1	X	X		X			A_{153}PEFVSVNPNAR$_{164}$	S158
T	1427.758	2.1	1469.8068	0.3	X	X	X		K_{245}NKKDLSTNQR$_{255}$	K247,K248 (T1)		
T	1544.8222	0.2	ND		X		X		L_{234}VNHFIQEFKR$_{244}$	K243		
T	1649.8272	1	1691.8724	2.7	X	X		X			Y_{235}FHSQKIASAVER$_{247}$	K240
T	1741.9448	0.5	1783.9916	0.4	X	X	X		Q_{154}ATKDAGTIAGLNVLR$_{169}$	K157		
T	1915.0585	3.7	1957.1016	0.2	X		X		L_{234}VNHFIQEFKRKNK$_{247}$	K243 or K245		
T	1990.9105	3.6	ND		X	X		X			M_1MNNNGNQVSNLSNALR$_{17}$	M1
T	2006.9006	1.2	ND		X			X			M_1MNNNGNQVSNLSNALR$_{17}$ (*1Mox*)	M1
T	2022.8986	1.8	2064.9464	2.7	X			X			M_1MNNNGNQVSNLSNALR$_{17}$ (*2Mox*)	M1
T	2043.1486	1.2	ND		X		X		L_{234}VNHFIQEFKRKNKK$_{248}$	K245		
T	2297.0602	0.1	ND		X		X		M_{515}VAEAEKFKEEDEKESQR$_{532}$	K521		
T	2453.1048	1.3	2495.1526	2.1	X	X		X			N_{66}GSQNNDNENNIKNTLEQHR$_{85}$	K78

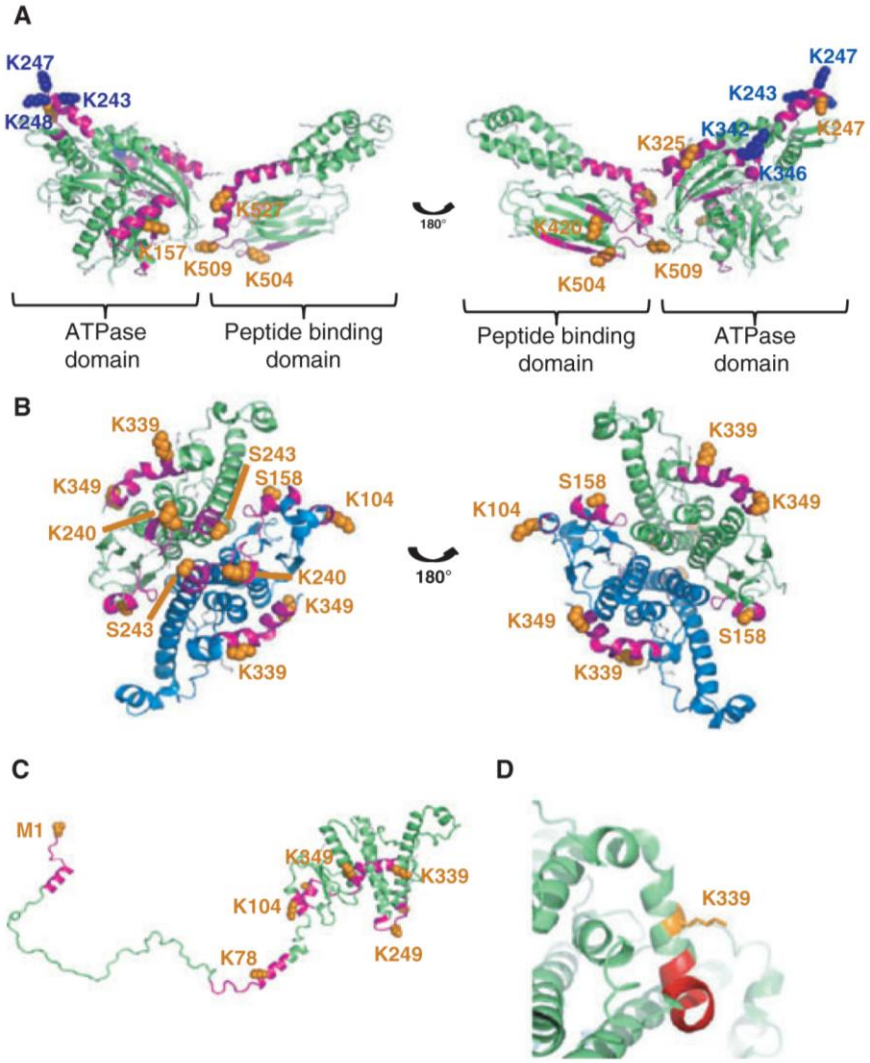

Fig. 4. Location of the mono-linked and loop-linked lysines in Ure2p and Ssa1p. Peptides containing modified and loop-linked lysine are colored magenta in Ssa1p (A) and Ure2p (B–D) structures. Loop-linked residues are colored blue. Mono-linked residues are colored orange. The Ssa1p 3D model in (A) was built using the ATPase domain of bovine Hsc70 (P19120), and the peptide binding domain of *E. coli* DnaK (P0A6Y8), Protein Data Bank accession numbers 3HSC and 1BPR, respectively. The two monomers constituting Ure2p dimer (Protein Data Bank accession number 1G6Y) in (B) are colored green and blue. A model of full-length Ure2p is presented in (C) to map modified peptides. This model was built from the X-ray structure of the C-terminal domain of Ure2p and integrates the finding that the N-terminal domain of Ure2p is flexible. An enlargement of the region of Ure2p involved in the interaction with Ssa1p is shown in (D). Lysine 339 is shown in orange; the region of Ure2p whereby exposure to the solvent was shown to change upon assembly into fibrils by HXMS [33] is colored red. The figure was generated with PYMOL (http://www.pymol.org).

ent protein binding domains of Ssa1p, is modified in Ssa1p but not in Ssa1p–Ure2p complexes exquisitely illustrates the conformational rearrangements that affect Ssa1p domains upon its interaction with Ure2p with the burial of a Ssa1p stretch comprising lysine 325.

The results reported in the present study are consistent with the view that subtle conformational changes modulate the assembly of Ure2p into fibrils and further highlight the involvement of the C-terminal domain of Ure2p in the fibrillar scaffold. Mutagenesis approaches targeting Ure2p stretch 325–340 will provide additional insight into the mechanism of Ure2p assembly into fibrils and the manner with which molecular chaperones modulate this process under physiological conditions.

Materials and methods

Production of proteins

Ure2p was expressed in *Escherichia coli*, purified and stored as described previously [34]. Ssa1p was expressed with an N-terminal His-tag in *S. cerevisiae*, purified and stored as

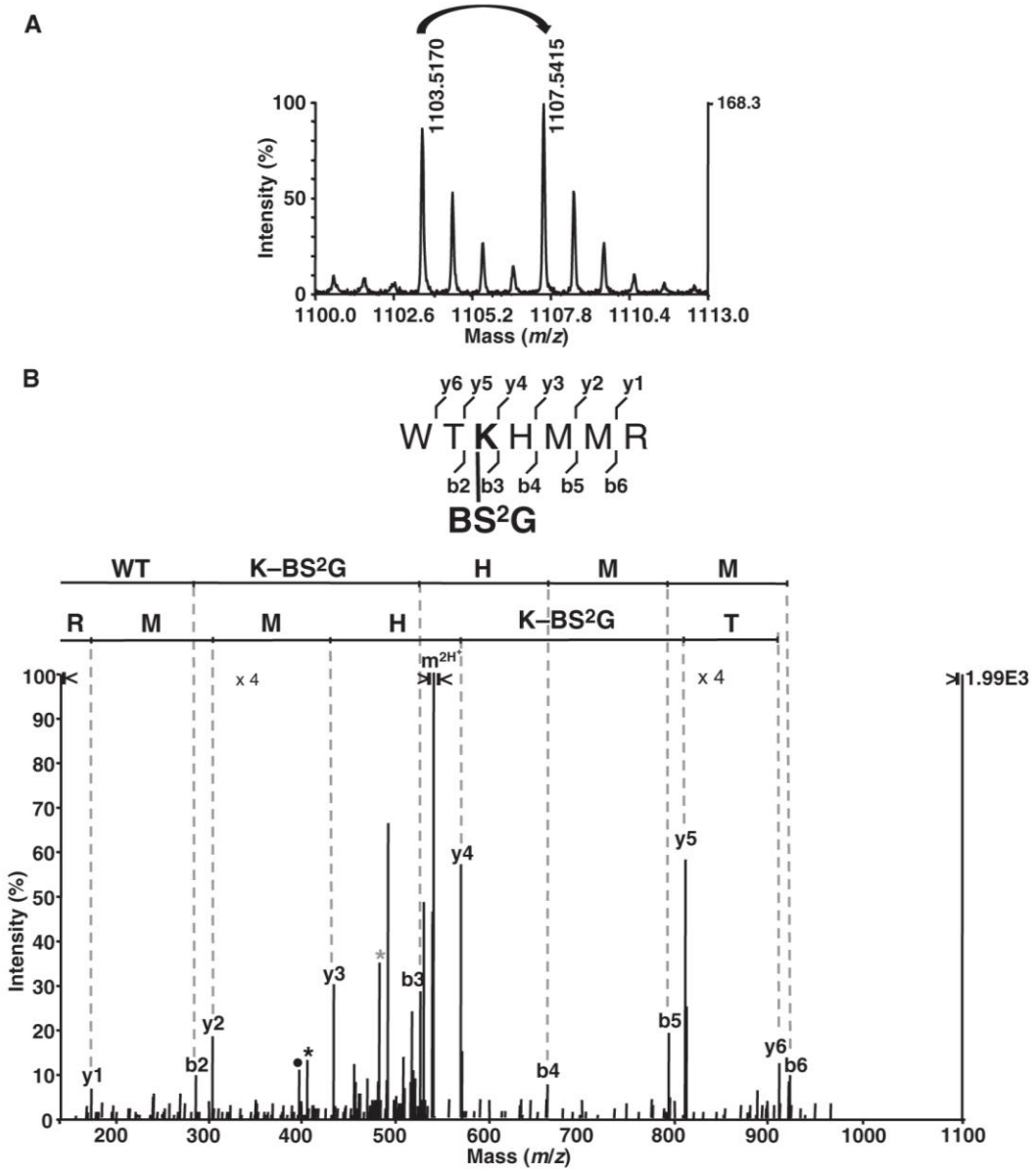

Fig. 5. NanoLC-LTQ-Orbitrap identification of the mono-linked Ure2p peptide [337–343]. Mass spectra of the tryptic peptide [337–343] from Ure2p treated with BS2G-d_0/d_4. (A) MALDI-TOF-TOF mass spectrum of the light (d0) and heavy (d4) precursor ions presenting a mass difference of 4.024 Da (indicated by the curved arrow). (B) Fragmentation mass spectrum of the double-charged d0 precursor ion obtained using nanoLC-LTQ-Orbitrap MS/MS analysis in the LTQ. The sequence of the loop-linked peptide $V_{340}FGGSTRIPK^*VQK^*L_{352}$ is presented with the identified y and b fragment ions. Black and grey stars and black circles correspond to y^{2+}, b^{2+} and internal fragment ions respectively. K* is the mono-linked residue.

described previously [35]. Ure2p and Ssa1p concentrations were determined as reported previously [6] and using the Bradford dye assay, respectively.

Cross-linking reaction

Cross-linking reactions were carried out with mixtures of deuterium labeled (d4) and unlabeled (d0) homo-bifunctional sulfo-NHS esters cross-linker reagent: BS2G-d0/d4 [bis(sulfosuccinimidyl) glutarate] with a 7.7 Å spacer arm and BS3-d0/d4 [bis(sulfosuccinimidyl) suberate] with a 11.4 Å spacer arm (Pierce, Waltham, MA, USA). Both cross-linkers react with the ε-amino group of lysine residues and α-amino group from protein N-termini and, to a lesser extent, with the hydroxyl groups of serine, threonine and tyrosine residues [36]. The zero-length EDC cross-linker cross-links carboxyl groups to primary amines. The proteins were dialyzed for 2 h at 4 °C against cross-linking buffer (40 mM Hepes-KOH, pH 7.5, 75 mM KCl) before cross-linking. The samples were then spun for 10 min at

15 000 ***g*** and 4 °C. To generate the Ure2p–Ssa1p complexes, the Ure2p and Ssa1p concentrations were adjusted to 20 and 10 μM, respectively. The reaction mixture containing 0.5 mM ADP or 4 mM ATP and 5 mM $MgCl_2$ was then incubated for 2 h at 10 °C under mild agitation. Control reactions consisted of incubating Ure2p and Ssa1p individually under the same experimental conditions. The NHS-ester cross-linkers (5 mM) were dissolved in dimethylsulfoxide. A mixture of deuterated and nondeuterated (1 : 1) cross-linkers were added to Ure2p, Ssa1p and Ure2p incubated with Ssa1p, with up to 20-fold molar excess. Cross-linking was performed at room temperature for 30 min and the reaction was terminated by the addition of ammonium bicarbonate (50 mM). EDC cross-linking was performed for 60 min in the presence of 4 mM EDC and 5 mM sulfo-NHS (*N*-hydroxysulfosuccinimide). The reaction was stopped by addition of β-mercaptoethanol and hydroxylamine (20 and 10 mM, respectively). Samples for SDS/PAGE analysis were immediately mixed (1 : 1 volume ratio) with denaturing buffer and heated at 95 °C. For high-mass MALDI-TOF MS, the samples were directly spotted on the MALDI plate.

SDS/PAGE and western blotting

SDS/PAGE analysis was performed on 7.5% polyacrylamide gels (8 × 7 × 0.15 cm) as described by Laemmli [37]. Equal amounts of proteins (10 μg) were loaded in each well. The gels were Coomassie blue stained, destained and imaged using a Sony charge-coupled device camera (Sony Corp., Tokyo, Japan). The proteins within the gels were transferred to nitrocellulose membranes. Ure2p and Ssa1p protein bands were probed with polyclonal antibody directed against full-length Ure2p and monoclonal anti-His-tag serum for His-tagged Ssa1p (Sigma-Aldrich, St Louis, MO, USA) and the membranes were developed with the enzyme-coupled luminescence technique (ECL; GE Healthcare, Milwaukee, WI, USA). All images were analyzed using NIH IMAGE software (available at: http://rsb.info.nih.gov/nih-image/).

Peptide preparation

The protein bands resolved by SDS/PAGE and, corresponding to monomeric Ure2p, monomeric Ssa1p and Ure2p–Ssa1p complexes with apparent molecular masses of 120 and 160 kDa were excised. Each protein band was subjected to in-gel enzymatic cleavage after reduction and alkylation of cysteine residues in the presence of 10 mM dithiothreitol and 55 mM iodocetamide [38]. Trypsin (Promega Gold; Promega, Madison, WI, USA) or Chymotrypsin (Roche, Basel, Switzerland) (12.5 $ng{\cdot}\mu L^{-1}$) treatments were performed overnight at 37 °C under mild agitation in 25 mM ammonium bicarbonate. Peptides were extracted in 100% acetonitrile following the incubation under agitation of the reaction products with 5% formic acid at 37 °C for 15 min. The extracted peptides were vacuum dried, dissolved in 1% formic acid and stored at −20 °C until MS analysis.

High mass MALDI-TOF MS

High-mass MALDI-TOF mass spectra of the intact protein complexes were obtained using a MALDI-TOF mass spectrometer (Voyager DE STR; Applied Biosystems, Foster City, CA, USA) equipped with an HM1 high-mass detection system (CovalX, Zürich, Switzerland) [39]. The instrument was operated in positive and linear mode with a 25 kV acceleration voltage, 85% grid voltage and 2000 ns delayed extraction time. Mass spectra were obtained by averaging 100–1000 shots. The instrument was externally calibrated with enolase (10 μM) using the double-charged monomer, and the single-charged monomer and dimer. Calibration was checked using noncross-linked Ure2p and Ssa1p. The mass accuracy was ~ 100–200 Da at 150 kDa. One volume of cross-linked proteins was diluted with one volume of 1% trifluoroacetic acid (TFA). This acidified sample was mixed 1 : 1 (v/v) with a saturated solution of sinapinic acid (10 $mg{\cdot}mL^{-1}$ in 30% acetonitrile and 0.1% TFA).

MALDI-TOF-TOF MS

The samples were desalted (with 5% acetonitrile, 0.1% TFA) and eluted from a C18 reversed-phase Zip-Tip® (Millipore, Billerica, MA, USA) in 40% acetonitrile, 0.1% TFA. Peptides samples were mixed 1 : 5 to 1 : 20 (v/v) with α-cyano-4-hydroxycinnamic acid (4 $mg{\cdot}mL^{-1}$ in 50% acetonitrile, 10 mM ammonium citrate and 0.1% formic acid) and spotted (0.5 μL) on a stainless steel MALDI target (Opti-TOF; Applied Biosystems). MALDI-TOF-TOF MS and MS/MS spectra were acquired with a MALDI-TOF/-TOF™ 4800 mass spectrometer (Applied Biosystems) in the positive and reflector mode. An external calibration was performed using standard peptide solution Cal Mix1 and Cal Mix2 (Applied Biosystems) and an additional internal calibration was performed during mass spectra analysis using nonmodified peptides of both Ure2p and/or Ssa1p. Acquisition and data analysis were performed using the EXPLORER 3.5.2 and DATA EXPLORER 4.9 software from Applied Biosystems.

NanoLC-linear ion trap (LTQ)-Orbitrap mass spectrometry

Tryptic and chymotryptic peptide digests were analyzed by NanoLC MS/MS using a HPLC system (Ultimate U3000; Dionex, Sunnyvale, CA, USA) coupled online to a LTQ-Orbitrap (ThermoScientific, Waltham, MA, USA) equipped

with a nanoelectrospray ion source after separation on a reversed-phase C18 pepmap 100 column (75 μm inner diameter, 5 μm particules of 100 Å diameter, 15 cm length) from Dionex. The peptides were loaded at a flow rate of 20 $\mu L \cdot min^{-1}$, and eluted at a flow rate of 200 $nL \cdot min^{-1}$ by a three step gradient: (a) 2–60% solvent B for 40 min; (b) 60–100% solvent B for 1 min; and (c) 100% solvent B for 20 min. Solvent A was 0.1% formic acid in water, whereas solvent B was 0.1% formic acid in 100% acetonitrile. NanoLC-MS/MS experiments were conducted in the data-dependent acquisition mode. The mass of the precursors was measured with a high resolution (60 000 FWHM) in the Orbitrap. The four most intense ions, above an intensity corresponding to 400 ions, were selected for fragmentation in the LTQ.

The isotope label of cross-linked peptides results in doublet signals with *m/z* differences of 4.0247, 2.0123 and 1.341 for mono-protonated, double or triple-protonated peptides, respectively. This information was used for LC-MS post-acquisition filtering using the software VIPER (http://omics.pnl.gov/software/VIPER.php). First, nanoLC-MS/MS data were de-isotoped using the DECON2LS software (available at: http://omics.pnl.gov/software/Decon2LS.php). The resulting csv files were further analyzed with VIPER [40]. A list with a delta *m/z* of 4.0247 corresponding to labeled ion pairs with a maximum mass tolerance of 10 p.p.m. was generated. Mass deviation and peptide elution time were used to filter the list of peptide doublets, corresponding to candidate cross-linked peptides. The list of light and heavy precursor masses was further used either to analyze the MS/MS spectra acquired in the data-dependent acquisition analysis or to build an inclusion list with the light and heavy precursor masses for cross-linked candidate peptides analysis. NanoLC-LTQ-Orbitrap data were processed automatically as described as well as manually.

Acknowledgements

We are grateful to Luc Bousset for designing a program for exploiting the MS data and for building the Ssa1p 3D model. We thank Alain Brunelle for helpful discussions about MALDI-TOF-HM1 MS. This work was supported by the French Ministry of Education, Research and Technology through the Centre National de la Recherche Scientifique (CNRS), the Institut National de la Santé et de la Recherche Médicale (INSERM) and the Agence Nationale pour la Recherche (ANR-06-BLAN-0266 and ANR-08-PCVI-0022-02).

References

1 Masison DC, Maddelein ML & Wickner RB (1997) The prion model for [URE3] of yeast: spontaneous generation and requirements for propagation. *Proc Natl Acad Sci USA* **94**, 12503–12508.
2 Masison DC & Wickner RB (1995) Prion-inducing domain of yeast Ure2p and protease resistance of Ure2p in prion-containing cells. *Science* **270**, 93–95.
3 Moriyama H, Edskes HK & Wickner RB (2000) [URE3] prion propagation in *Saccharomyces cerevisiae*: requirement for chaperone Hsp104 and curing by overexpressed chaperone Ydj1p. *Mol Cell Biol* **20**, 8916–8922.
4 Schwimmer C & Masison DC (2002) Antagonistic interactions between yeast [PSI(+)] and [URE3] prions and curing of [URE3] by Hsp70 protein chaperone Ssa1p but not by Ssa2p. *Mol Cell Biol* **22**, 3590–3598.
5 Roberts BT, Moriyama H & Wickner RB (2004) [URE3] prion propagation is abolished by a mutation of the primary cytosolic Hsp70 of budding yeast. *Yeast* **21**, 107–117.
6 Savistchenko J, Krzewska J, Fay N & Melki R (2008) Molecular chaperones and the assembly of the prion Ure2p in vitro. *J Biol Chem* **283**, 15732–15739.
7 Thual C, Bousset L, Komar AA, Walter S, Buchner J, Cullin C & Melki R (2001) Stability, folding, dimerization, and assembly properties of the yeast prion Ure2p. *Biochemistry* **40**, 1764–1773.
8 Bousset L, Belrhali H, Janin J, Melki R & Morera S (2001) Structure of the globular region of the prion protein Ure2 from the yeast *Saccharomyces cerevisiae*. *Structure (Camb.)* **9**, 39–46.
9 Sinz A (2006) Chemical cross-linking and mass spectrometry to map three-dimensional protein structures and protein-protein interactions. *Mass Spectrom Rev* **25**, 663–682.
10 Lutter LC & Kurland CG (1975) Chemical determination of protein neighbourhoods in a cellular organelle. *Mol Cell Biochem* **7**, 105–116.
11 Cohen FE & Sternberg MJ (1980) On the use of chemically derived distance constraints in the prediction of protein structure with myoglobin as an example. *J Mol Biol* **137**, 9–22.
12 Heymann M, Paramelle D, Subra G, Forest E, Martinez J, Geourjon C & Deléage G (2008) MSX-3D: a tool to validate 3D protein models using mass spectrometry. *Bioinformatics* **24**, 2782–2783.
13 Pimenova T, Nazabal A, Roschitzki B, Seebacher J, Rinner O & Zenobi R (2008) Epitope mapping on bovine prion protein using chemical cross-linking and mass spectrometry. *J Mass Spectrom* **43**, 185–195.
14 Pimenova T, Pereira CP, Schaer DJ & Zenobi R (2009) Characterization of high molecular weight multimeric states of human haptoglobin and hemoglobin-based oxygen carriers by high-mass MALDI MS. *J Sep Sci* **32**, 1224–1230.

15 Kalkhof S & Sinz A (2008) Chances and pitfalls of chemical cross-linking with amine-reactive N-hydroxysuccinimide esters. *Anal Bioanal Chem* **392**, 305–312.
16 Seebacher J, Mallick P, Zhang N, Eddes JS, Aebersold R & Gelb MH (2006) Protein cross-linking analysis using mass spectrometry, isotope-coded cross-linkers, and integrated computational data processing. *J Proteome Res* **5**, 2270–2282.
17 Gao QX, Doneanu CE, Shaffer SA, Adman ET, Goodlett DR & Nelson SD (2006) Identification of the interactions between cytochrome P450 2E1 and cytochrome b(5) by mass spectrometry and site-directed mutagenesis. *J Biol Chem* **281**, 20404–20417.
18 Kalkhof S, Ihling C, Mechtler K & Sinz A (2005) Chemical cross-linking and high-performance Fourier transform ion cyclotron resonance mass spectrometry for protein interaction analysis: application to a calmodulin/target peptide complex. *Anal Chem* **77**, 495–503.
19 Tang XT, Munske GR, Siems WF & Bruce JE (2005) Mass spectrometry identifiable cross-linking strategy for studying protein-protein interactions. *Anal Chem* **77**, 311–318.
20 Sinz A, Kalkhof S & Ihling C (2005) Mapping protein interfaces by a trifunctional cross-linker combined with MALDI-TOF and ESI-FTICR mass spectrometry. *J Am Soc Mass Spectrom* **16**, 1921–1931.
21 Schmidt A, Kalkhof S, Ihling C, Cooper DMF & Sinz A (2005) Mapping protein interfaces by chemical cross-linking and Fourier transform ion cyclotron resonance mass spectrometry: application to a calmodulin/adenylyl cyclase 8 peptide complex. *Eur J Mass Spectrom* **11**, 525–534.
22 Dimova K, Kalkhof S, Pottratz I, Ihling C, Rodriguez-Castaneda F, Liepold T, Griesinger C, Brose N, Sinz A & Jahn O (2009) Structural insights into the calmodulin-Munc13 interaction obtained by cross-linking and mass spectrometry. *Biochemistry* **48**, 5908–5921.
23 Manolaridis I, Mumtsidu E, Konarev P, Makhov AM, Fullerton SW, Sinz A, Kalkhof S, McGeehan JE, Cary PD, Griffith JD *et al.* (2009) Structural and biophysical characterization of the proteins interacting with the herpes simplex virus 1 origin of replication. *J Biol Chem* **284**, 16343–16353.
24 Jaya N, Garcia V & Vierling E (2009) Substrate binding site flexibility of the small heat shock protein molecular chaperones. *Proc Natl Acad Sci USA* **106**, 15604–15609.
25 Bousset L, Redeker V, Decottignies P, Dubois S, Le Maréchal P & Melki R (2004) Structural characterization of the fibrillar form of the yeast Saccharomyces cerevisiae prion Ure2p. *Biochemistry* **43**, 5022–5032.
26 Fay N, Redeker V, Savischenko J, Dubois S, Bousset L & Melki R (2005) Structure of the prion Ure2p in protein fibrils assembled in vitro. *J Biol Chem* **280**, 37149–37158.
27 Ranson N, Stromer T, Bousset L, Melki R & Serpell LC (2006) Insights into the architecture of the Ure2p yeast protein assemblies from helical twisted fibrils. *Protein Sci* **15**, 2481–2487.
28 Bousset L, Bonnefoy J, Sourigues Y, Wien F & Melki R (2010) Structure and assembly properties of the N-terminal domain of the prion Ure2p in isolation and in its natural context. *PLoS ONE* **5**, e9760.
29 Maiolica A, Cittaro D, Borsotti D, Sennels L, Ciferri C, Tarricone C, Musacchio A & Rappsilber J (2007) Structural analysis of multiprotein complexes by cross-linking, mass spectrometry, and database searching. *Mol Cell Proteomics* **6**, 2200–2211.
30 Peri S, Steen H & Pandey A (2001) GPMAW – a software tool for analyzing proteins and peptides. *Trends Biochem Sci* **26**, 687–689.
31 Rinner O, Seebacher J, Walzthoeni T, Mueller LN, Beck M, Schmidt A, Mueller M & Aebersold R (2008) Identification of cross-linked peptides from large sequence databases. *Nat Methods* **5**, 315–318.
32 Leitner A, Walzthoeni T, Kahraman A, Herzog F, Rinner O, Beck M & Aebersold R (2010) Probing native protein structures by chemical cross-linking, mass spectrometry and bioinformatics. *Mol Cell Proteomics* **9**, 1634–1649.
33 Redeker V, Halgand F, Le Caer JP, Bousset L, Laprévote O & Melki R (2007) Hydrogen/deuterium exchange mass spectrometric analysis of conformational changes accompanying the assembly of the yeast prion Ure2p into protein fibrils. *J Mol Biol* **369**, 1113–1125.
34 Thual C, Komar AA, Bousset L, Fernandez-Bellot E, Cullin C & Melki R (1999) Structural characterization of *Saccharomyces cerevisiae* prion-like protein Ure2. *J Biol Chem* **274**, 13666–13674.
35 Krzewska J & Melki R (2006) Molecular chaperones and the assembly of the prion Sup35p, an in vitro study. *EMBO J* **25**, 822–833.
36 Mädler S, Bich C, Touboul D & Zenobi R (2009) Chemical cross-linking with NHS esters: a systematic study on amino acid reactivities. *J Mass Spectrom* **44**, 694–706.
37 Laemmli UK (1970) Cleavage of structural proteins during the assembly of the head of bacteriophage T4. *Nature* **227**, 680–685.
38 Shevchenko A, Wilm M, Vorm O & Mann M (1996) Mass spectrometric sequencing of proteins silverstained polyacrylamide gels. *Anal Chem* **68**, 850–858.
39 Wenzel RJ, Kern S, Nazabal A & Zenobi R (2007) Quantitative comparison of sensitivity and saturation for MALDI-TOF detectors when measuring complex and high mass samples. Proceedings of the 55th ASMS Conference on Mass Spectrometry, Indianapolis, MP082.
40 Zimmer JS, Monroe ME, Qian WJ & Smith RD (2006) Advances in proteomics data analysis and display using

an accurate mass and time tag approach. *Mass Spectrom Rev* **25**, 450–482.

Supporting information

The following supplementary material is available:

Fig. S1. Analytical strategy for Ure2p–Ssa1p chemical cross-linking, cleavage and identification of the reaction products.

Fig. S2. Primary structure coverage obtained following tryptic and chymotryptic treatment of Ure2p (A) and Ssa1p (B).

Fig. S3. NanoLC-LTQ-Orbitrap chromatograms of the BS3 mono-linked peptide $W_{337}TK^{*}HMMR_{343}$ (double-charged ion peak at m/z 575 2820) produced by tryptic in-gel digestion.

Table S1. Molecular masses of NHS-ester cross-linker before and after reaction with lysine residues.

This supplementary material can be found in the online version of this article.

Please note: As a service to our authors and readers, this journal provides supporting information supplied by the authors. Such materials are peer-reviewed and may be re-organized for online delivery, but are not copy-edited or typeset. Technical support issues arising from supporting information (other than missing files) should be addressed to the authors.

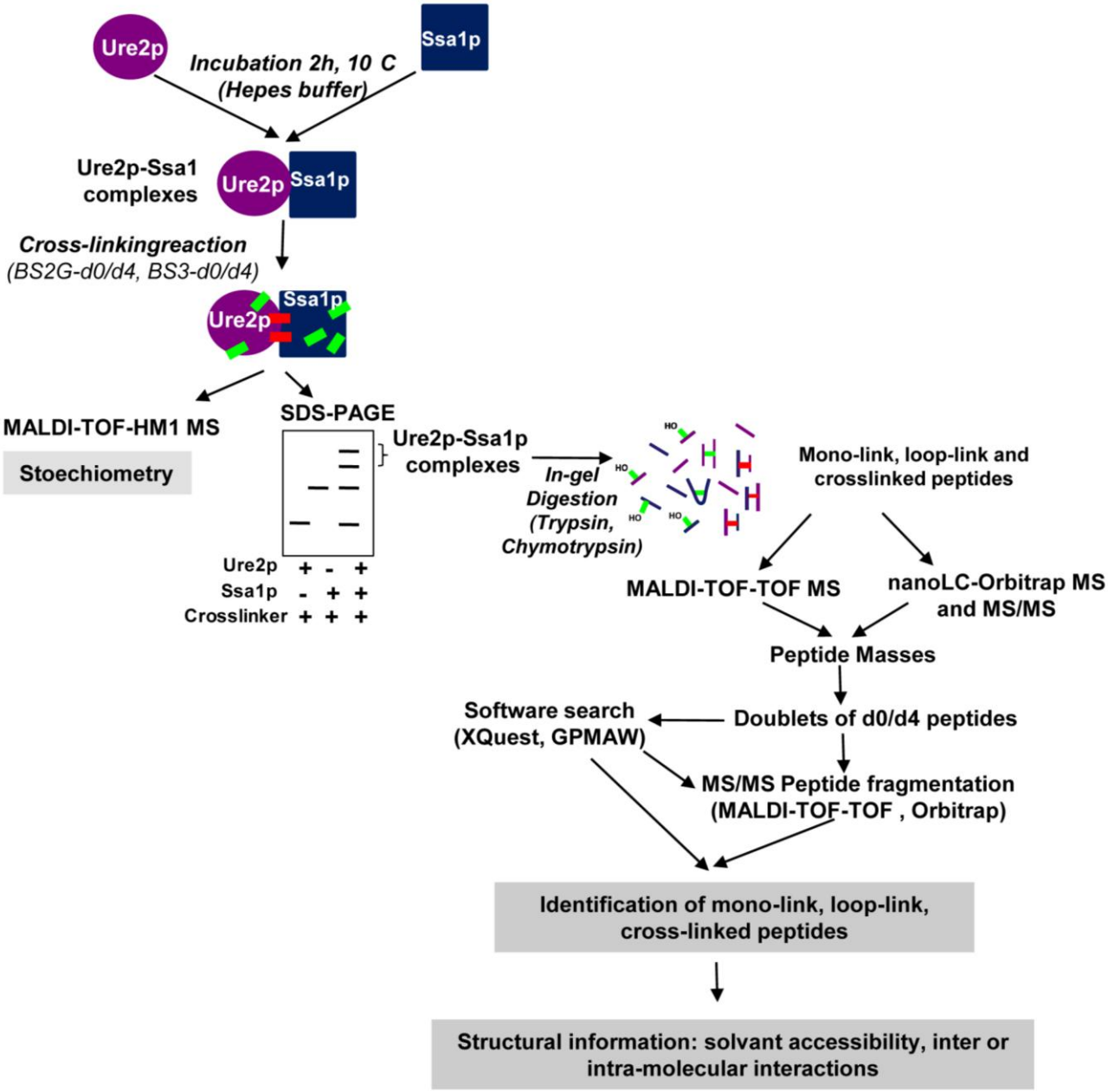

Figure S1: Analytical strategy for Ure2p-Ssa1p chemical cross-linking, cleavage and identification of the reaction products.

Ure2p was incubated with Ssa1p and the reaction products treated with a mixture of unlabeled and deuterated BS2G and BS3. The Ure2p-Ssa1p complexes were treated with a mixture of unlabeled and deuterated BS2G or BS3 following the incubation of Ure2p with Ssa1p. The reaction products were resolved by SDS-PAGE. Ure2p and Ssa1p stoichiometry were derived from high-mass MALDI-TOF MS measurements. The modified and cross-linked peptides were identified following in-gel tryptic and chymotryptic treatments. The digests were analyzed both by MALDI-TOF-TOF and nanoLC-LTQ-Orbitrap in the MS and MS/MS acquisition modes. In a first MS analysis, peptides of interest were detected using the d0/d4 mass tag and used to build a list of modified candidate peptides. From this list of peptides, mono-linked, loop-linked and cross-linked peptides were identified by MS/MS sequence information and software searches. These identifications give structural information on solvent accessibilities and inter and intra-molecular interactions.

Redeker et al. Figure S1

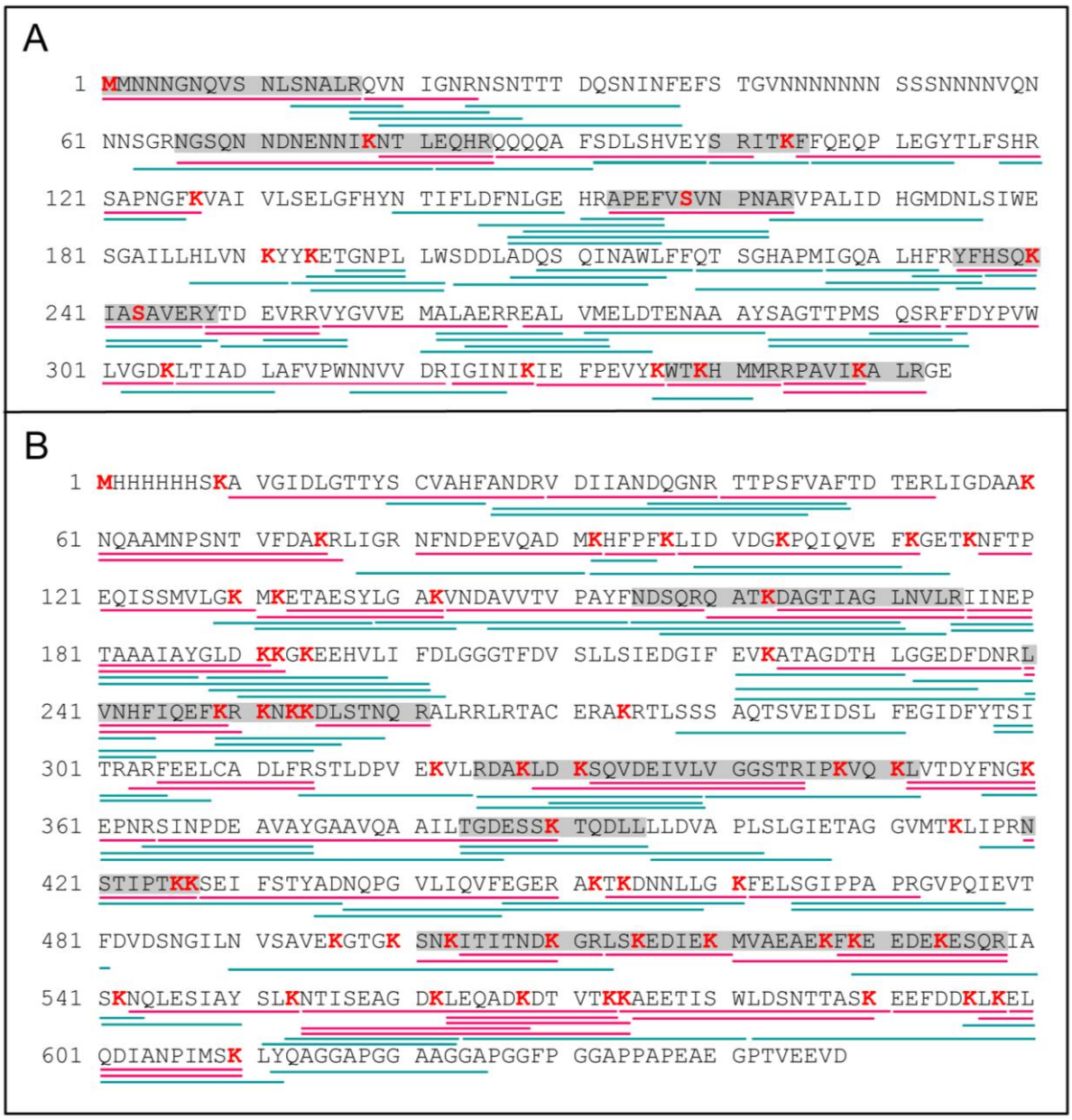

Figure S2: Primary structure coverage obtained following tryptic and chymotryptic treatment of Ure2p (A) and Ssa1p (B). The peptides were identified by MALDI-TOF-TOF and nanoLC-MS/MS analysis. The red and green segments correspond to tryptic and chymotryptic peptides, respectively. The stretches labeled in grey correspond to the mono-linked and loop-linked peptides identified in this work where the Lysine residues are in red. Ure2p sequence coverage was 57%, 70% and 86%, while that of Ssa1p was 77%, 76.4% and 84.7% upon trypsin, chymotrypsin and both treatments, respectively.

Redeker et al. Figure S2

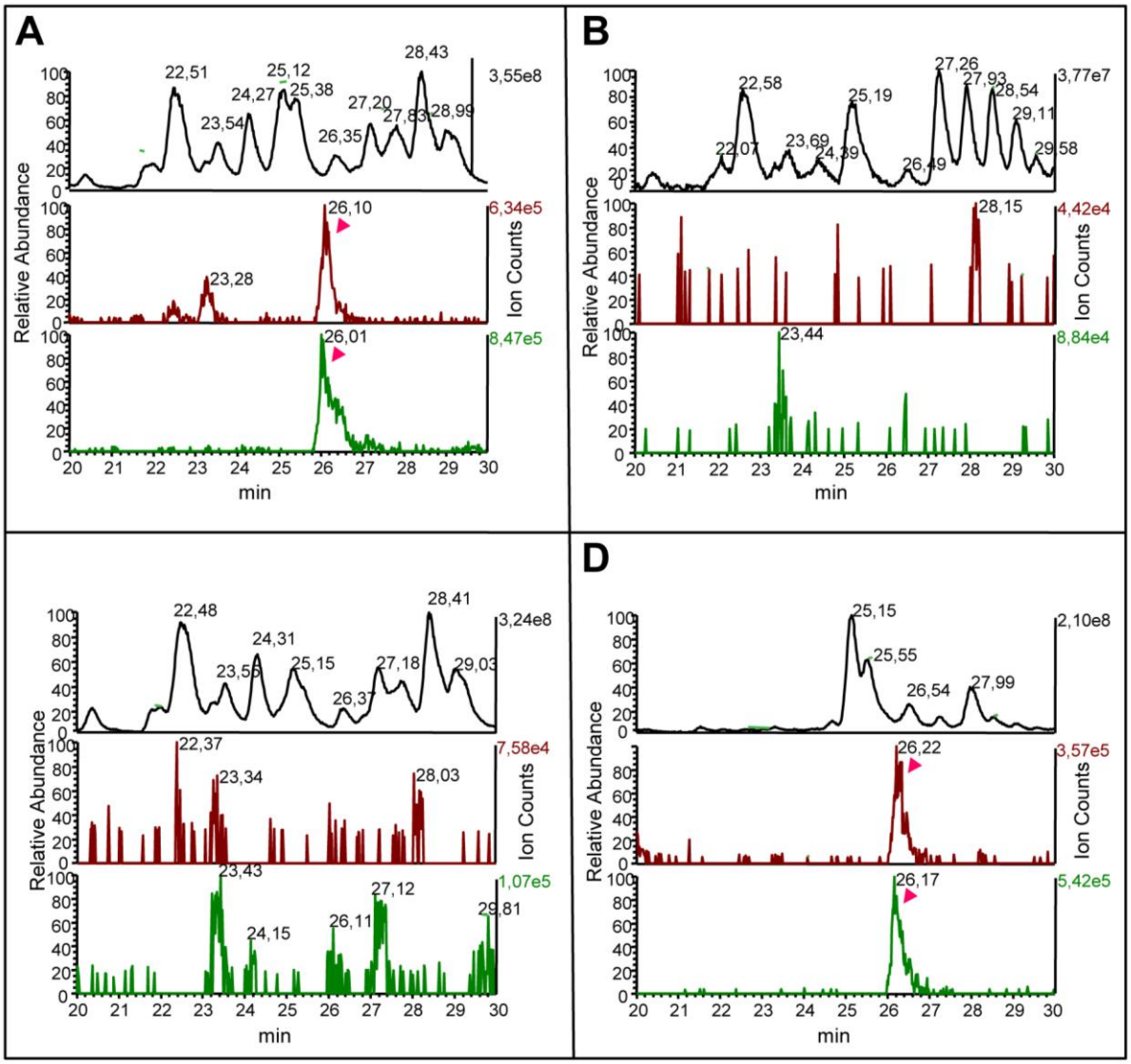

Figure S3 NanoLC-LTQ-Orbitrap chromatograms of the BS3 Mono-linked peptide $W_{337}TK^{*}HMMR_{343}$ (double charged ion peak at *m/z* 575,2820) produced by tryptic in-gel digestion. The peptides eluted between 20 and 30 min are shown. The total ion chromatogram is in black and the extracted ion chromatograms corresponding to the light precursor mass (552.2592) and the heavy precursor mass (554.2730) of peptide [337-343] are in red and green respectively. These chromatogramms are presented for the in-gel digested 160kDa Ure2p-Ssa1p complex (A), the 120kDa Ure2p-Ssa1p complex (B), the monomeric Ssa1p (C) and the monomeric Ure2p (D). The shifts in retention times between the different nanoLC separations are smaller than 0.5 min. Each spectrum is normalized to the most intense peak. Triangles in panels A and D show the light (red) and heavy (green) forms of the BS3 mono-linked peptide [337-343]. An overlap in elution time of the d0 and d4 peptides is observed, with the d4 peptide eluting slightly earlier, with less than 0.1 min difference.

Redeker et al. Figure S3

Cross-linker	MW	Spacer-Arm (Å)	Mass shift for mono-link	Mass shift for loop or cross-link	Mass of reporter ions of mono-link Lysine (MH+)
BS2-d0	530.35	7.7	114.0317	96.0211	198.14
BS2G-d4	534.38	7.7	118.056	100.046	202.16
BS3-d0	572.43	11.4	156.0786	138.0681	240.19
BS3-d4	576.45	11.4	160.103	140.093	244.21

Table S1: Molecular masses of NHS-ester cross-linker before and after reaction with Lysine residues. Multiple mass tags are used for cross-linked peptides: the d0/d4 mass difference is 4.0247 amu, the BS2G/BS3 mass difference is 42.0469 amu. The low mass reporter ions corresponding to mono-linked residues are indicated.

Redeker et al. Table S1

Bibliography

BIBLIOGRAPHY

Abeliovich, A., Y. Schmitz, et al. (2000). "Mice lacking alpha-synuclein display functional deficits in the nigrostriatal dopamine system." Neuron **25**(1): 239-52.

Aguzzi, A. and L. Rajendran (2009). "The transcellular spread of cytosolic amyloids, prions, and prionoids." Neuron **64**(6): 783-90.

Albanese, V., A. Y. Yam, et al. (2006). "Systems analyses reveal two chaperone networks with distinct functions in eukaryotic cells." Cell **124**(1): 75-88.

Alpers, M. P. (2008). "Review. The epidemiology of kuru: monitoring the epidemic from its peak to its end." Philos Trans R Soc Lond B Biol Sci **363**(1510): 3707-13.

Altschuler, E. (1999). "Aluminum-containing antacids as a cause of idiopathic Parkinson's disease." Med Hypotheses **53**(1): 22-3.

Angot, E. and P. Brundin (2009). "Dissecting the potential molecular mechanisms underlying alpha-synuclein cell-to-cell transfer in Parkinson's disease." Parkinsonism Relat Disord **15 Suppl 3**: S143-7.

Angot, E., J. A. Steiner, et al. (2010). "Are synucleinopathies prion-like disorders?" Lancet Neurol **9**(11): 1128-38.

Augusteyn, R. C. (2004). "alpha-crystallin: a review of its structure and function." Clin Exp Optom **87**(6): 356-66.

Auluck, P. K., H. Y. Chan, et al. (2002). "Chaperone suppression of alpha-synuclein toxicity in a Drosophila model for Parkinson's disease." Science **295**(5556): 865-8.

Bartels, T., J. G. Choi, et al. (2011). "alpha-Synuclein occurs physiologically as a helically folded tetramer that resists aggregation." Nature.

Bartlett, A. I. and S. E. Radford (2009). "An expanding arsenal of experimental methods yields an explosion of insights into protein folding mechanisms." Nat Struct Mol Biol **16**(6): 582-8.

Baxa, U., R. B. Wickner, et al. (2007). "Characterization of beta-sheet structure in Ure2p1-89 yeast prion fibrils by solid-state nuclear magnetic resonance." Biochemistry **46**(45): 13149-62.

Baylis, M. (2008). "Scrapie." Retrieved 23/08/2011, from http://accessscience.com/content/Scrapie/608000.

Berg, O. G. and P. H. von Hippel (1985). "Diffusion-controlled macromolecular interactions." Annu Rev Biophys Biophys Chem **14**: 131-60.

Besnoit C., M. C. (1898). "Note sur les lesions nerveuses de la tremblante du mouton." Rev. Vet **23**: 397-400.

Bonuccelli, U., P. Del Dotto, et al. (2009). "Role of dopamine receptor agonists in the treatment of early Parkinson's disease." Parkinsonism Relat Disord **15 Suppl 4**: S44-53.

Borbat, P., T. F. Ramlall, et al. (2006). "Inter-helix distances in lysophospholipid micelle-bound alpha-synuclein from pulsed ESR measurements." J Am Chem Soc **128**(31): 10004-5.

Bork, P., C. Sander, et al. (1992). "An ATPase domain common to prokaryotic cell cycle proteins, sugar kinases, actin, and hsp70 heat shock proteins." Proc Natl Acad Sci U S A **89**(16): 7290-4.

Bousset, L., H. Belrhali, et al. (2001). "Crystal structures of the yeast prion Ure2p functional region in complex with glutathione and related compounds." Biochemistry **40**(45): 13564-73.

Bousset, L., J. Bonnefoy, et al. (2010). "Structure and assembly properties of the N-terminal domain of the prion Ure2p in isolation and in its natural context." PLoS One **5**(3): e9760.

Bousset, L., F. Briki, et al. (2003). "The native-like conformation of Ure2p in fibrils assembled under physiologically relevant conditions switches to an amyloid-like conformation upon heat-treatment of the fibrils." J Struct Biol **141**(2): 132-42.

Bousset, L., N. H. Thomson, et al. (2002). "The yeast prion Ure2p retains its native alpha-helical conformation upon assembly into protein fibrils in vitro." EMBO J **21**(12): 2903-11.
Braak, H., R. A. de Vos, et al. (2006). "Gastric alpha-synuclein immunoreactive inclusions in Meissner's and Auerbach's plexuses in cases staged for Parkinson's disease-related brain pathology." Neurosci Lett **396**(1): 67-72.
Braak, H., K. Del Tredici, et al. (2002). "Staging of the intracerebral inclusion body pathology associated with idiopathic Parkinson's disease (preclinical and clinical stages)." J Neurol **249 Suppl 3**: III/1-5.
Braak, H., K. Del Tredici, et al. (2003). "Staging of brain pathology related to sporadic Parkinson's disease." Neurobiol Aging **24**(2): 197-211.
Braak, H., E. Ghebremedhin, et al. (2004). "Stages in the development of Parkinson's disease-related pathology." Cell Tissue Res **318**(1): 121-34.
Brocchieri, L., E. Conway de Macario, et al. (2008). "hsp70 genes in the human genome: Conservation and differentiation patterns predict a wide array of overlapping and specialized functions." BMC Evol Biol **8**: 19.
Brockwell, D. J. and S. E. Radford (2007). "Intermediates: ubiquitous species on folding energy landscapes?" Curr Opin Struct Biol **17**(1): 30-7.
Brown, P., R. G. Will, et al. (2001). "Bovine spongiform encephalopathy and variant Creutzfeldt-Jakob disease: background, evolution, and current concerns." Emerg Infect Dis **7**(1): 6-16.
Brown, R. (1828). "A brief account of microscopical observations made in the months of June, July and August, 1827, on the particles contained in the pollen of plants; and on the general existence of active molecules in organic and inorganic bodies." Phil. Mag **4**: 161-173.
Brundin, P., R. Melki, et al. (2010). "Prion-like transmission of protein aggregates in neurodegenerative diseases." Nat Rev Mol Cell Biol **11**(4): 301-7.
Burre, J., M. Sharma, et al. (2010). "Alpha-synuclein promotes SNARE-complex assembly in vivo and in vitro." Science **329**(5999): 1663-7.
Chandra, S., X. Chen, et al. (2003). "A broken alpha -helix in folded alpha -Synuclein." J Biol Chem **278**(17): 15313-8.
Chang, H. C., Y. C. Tang, et al. (2007). "SnapShot: molecular chaperones, Part I." Cell **128**(1): 212.
Chatellier, J., F. Hill, et al. (1998). "In vivo activities of GroEL minichaperones." Proc Natl Acad Sci U S A **95**(17): 9861-6.
Cheetham, M. E. and A. J. Caplan (1998). "Structure, function and evolution of DnaJ: conservation and adaptation of chaperone function." Cell Stress Chaperones **3**(1): 28-36.
Chu, Y. and J. H. Kordower (2010). "Lewy body pathology in fetal grafts." Ann N Y Acad Sci **1184**: 55-67.
Colby, D. W. and S. B. Prusiner (2011). "Prions." Cold Spring Harb Perspect Biol **3**(1): a006833.
Cotzias, G. C. and P. S. Papavasiliou (1969). "Autoimmunity in patients treated with levodopa." JAMA **207**(7): 1353-4.
Craig, E. A., P. Huang, et al. (2006). "The diverse roles of J-proteins, the obligate Hsp70 co-chaperone." Rev Physiol Biochem Pharmacol **156**: 1-21.
Creutzfeldt, H. G. (1989). "On a particular focal disease of the central nervous system (preliminary communication), 1920." Alzheimer Dis Assoc Disord **3**(1-2): 3-25.
Cuillé, J., Chelles P.L. (1936). "La tremblante du mouton est bien inoculable." C. R. Acad. Sci. **203**: 1552-1554.
Cuillé, J. and P. L. Chelles (1939). "Experimental transmission of trambling to the goat." Comptes Rendues des Séances de l'Académie des Sciences **208**: 1058-1160.
Daniel, S. E. and C. H. Hawkes (1992). "Preliminary diagnosis of Parkinson's disease by olfactory bulb pathology." Lancet **340**(8812): 186.

Danzer, K. M., W. P. Ruf, et al. (2010). "Heat-shock protein 70 modulates toxic extracellular alpha-synuclein oligomers and rescues trans-synaptic toxicity." FASEB J **25**(1): 326-36.
Daugaard, M., M. Rohde, et al. (2007). "The heat shock protein 70 family: Highly homologous proteins with overlapping and distinct functions." FEBS Lett **581**(19): 3702-10.
Davidson, W. S., A. Jonas, et al. (1998). "Stabilization of alpha-synuclein secondary structure upon binding to synthetic membranes." J Biol Chem **273**(16): 9443-9.
Davies, P., D. Moualla, et al. (2011). "Alpha-synuclein is a cellular ferrireductase." PLoS One **6**(1): e15814.
Davis, L. E. and J. C. Adair (1999). "Parkinsonism from methanol poisoning: benefit from treatment with anti-Parkinson drugs." Mov Disord **14**(3): 520-2.
de la Fuente-Fernandez, R., T. J. Ruth, et al. (2001). "Expectation and dopamine release: mechanism of the placebo effect in Parkinson's disease." Science **293**(5532): 1164-6.
Dedmon, M. M., J. Christodoulou, et al. (2005). "Heat shock protein 70 inhibits alpha-synuclein fibril formation via preferential binding to prefibrillar species." J Biol Chem **280**(15): 14733-40.
Dexter, D. T., A. Carayon, et al. (1991). "Alterations in the levels of iron, ferritin and other trace metals in Parkinson's disease and other neurodegenerative diseases affecting the basal ganglia." Brain **114 (Pt 4)**: 1953-75.
Dickson, D. W., H. Fujishiro, et al. (2009). "Neuropathology of non-motor features of Parkinson disease." Parkinsonism Relat Disord **15 Suppl 3**: S1-5.
Elbaz, A., J. Clavel, et al. (2009). "Professional exposure to pesticides and Parkinson disease." Ann Neurol **66**(4): 494-504.
Fahn, S. (2003). "Description of Parkinson's disease as a clinical syndrome." Ann N Y Acad Sci **991**: 1-14.
Falsone, S. F., A. J. Kungl, et al. (2009). "The molecular chaperone Hsp90 modulates intermediate steps of amyloid assembly of the Parkinson-related protein alpha-synuclein." J Biol Chem **284**(45): 31190-9.
Farooqui, T. and A. A. Farooqui (2011). "Lipid-mediated oxidative stress and inflammation in the pathogenesis of Parkinson's disease." Parkinsons Dis **2011**: 247467.
Forman, M. S., J. Q. Trojanowski, et al. (2004). "Neurodegenerative diseases: a decade of discoveries paves the way for therapeutic breakthroughs." Nat Med **10**(10): 1055-63.
Fredenburg, R. A., C. Rospigliosi, et al. (2007). "The impact of the E46K mutation on the properties of alpha-synuclein in its monomeric and oligomeric states." Biochemistry **46**(24): 7107-18.
Frost, B. and M. I. Diamond (2010). "Prion-like mechanisms in neurodegenerative diseases." Nat Rev Neurosci **11**(3): 155-9.
Gajdusek, D. C., C. J. Gibbs, Jr., et al. (1967). "Transmission and passage of experimenal "kuru" to chimpanzees." Science **155**(759): 212-4.
Galvin, J. E., V. M. Lee, et al. (1997). "Monoclonal antibodies to purified cortical Lewy bodies recognize the mid-size neurofilament subunit." Ann Neurol **42**(4): 595-603.
Georgieva, E. R., T. F. Ramlall, et al. (2008). "Membrane-bound alpha-synuclein forms an extended helix: long-distance pulsed ESR measurements using vesicles, bicelles, and rodlike micelles." J Am Chem Soc **130**(39): 12856-7.
Giasson, B. I., J. E. Duda, et al. (2000). "Oxidative damage linked to neurodegeneration by selective alpha-synuclein nitration in synucleinopathy lesions." Science **290**(5493): 985-9.
Gibbs, C. J., Jr., D. C. Gajdusek, et al. (1968). "Creutzfeldt-Jakob disease (spongiform encephalopathy): transmission to the chimpanzee." Science **161**(839): 388-9.
Glover, J. R. and S. Lindquist (1998). "Hsp104, Hsp70, and Hsp40: a novel chaperone system that rescues previously aggregated proteins." Cell **94**(1): 73-82.
Golbik, R., R. Zahn, et al. (1998). "Thermodynamic stability and folding of GroEL minichaperones." J Mol Biol **276**(2): 505-15.

Goldfarb, S. B., O. B. Kashlan, et al. (2006). "Differential effects of Hsc70 and Hsp70 on the intracellular trafficking and functional expression of epithelial sodium channels." Proc Natl Acad Sci U S A **103**(15): 5817-22.
Gorell, J. M., C. C. Johnson, et al. (1999). "Occupational exposure to manganese, copper, lead, iron, mercury and zinc and the risk of Parkinson's disease." Neurotoxicology **20**(2-3): 239-47.
Gorell, J. M., C. C. Johnson, et al. (1998). "The risk of Parkinson's disease with exposure to pesticides, farming, well water, and rural living." Neurology **50**(5): 1346-50.
Gorell, J. M., B. A. Rybicki, et al. (1999). "Occupational metal exposures and the risk of Parkinson's disease." Neuroepidemiology **18**(6): 303-8.
Gowers, W. R. (1886). A Manual of Diseases of the Nervous System. London, J. & A. Churchill.
Gribaldo, S., V. Lumia, et al. (1999). "Discontinuous occurrence of the hsp70 (dnaK) gene among Archaea and sequence features of HSP70 suggest a novel outlook on phylogenies inferred from this protein." J Bacteriol **181**(2): 434-43.
Griffith, J. S. (1967). "Self-replication and scrapie." Nature **215**(5105): 1043-4.
Gross, R. E., R. L. Watts, et al. (2011). "Intrastriatal transplantation of microcarrier-bound human retinal pigment epithelial cells versus sham surgery in patients with advanced Parkinson's disease: a double-blind, randomised, controlled trial." Lancet Neurol **10**(6): 509-19.
Hageman, G., J. van der Hoek, et al. (1999). "Parkinsonism, pyramidal signs, polyneuropathy, and cognitive decline after long-term occupational solvent exposure." J Neurol **246**(3): 198-206.
Hageman, J. and H. H. Kampinga (2009). "Computational analysis of the human HSPH/HSPA/DNAJ family and cloning of a human HSPH/HSPA/DNAJ expression library." Cell Stress Chaperones **14**(1): 1-21.
Hageman, J., M. A. van Waarde, et al. (2011). "The diverse members of the mammalian HSP70 machine show distinct chaperone-like activities." Biochem J **435**(1): 127-42.
Hansen, C., E. Angot, et al. (2010). "alpha-Synuclein propagates from mouse brain to grafted dopaminergic neurons and seeds aggregation in cultured human cells." J Clin Invest **121**(2): 715-25.
Hartl, F. U. (1996). "Molecular chaperones in cellular protein folding." Nature **381**(6583): 571-9.
Hartl, F. U. and M. Hayer-Hartl (2009). "Converging concepts of protein folding in vitro and in vivo." Nat Struct Mol Biol **16**(6): 574-81.
Hatcher, J. M., K. D. Pennell, et al. (2008). "Parkinson's disease and pesticides: a toxicological perspective." Trends Pharmacol Sci **29**(6): 322-9.
Hawkes, C. H., K. Del Tredici, et al. (2007). "Parkinson's disease: a dual-hit hypothesis." Neuropathol Appl Neurobiol **33**(6): 599-614.
Hawkes, C. H., K. Del Tredici, et al. (2009). "Parkinson's disease: the dual hit theory revisited." Ann N Y Acad Sci **1170**: 615-22.
Herrera, F., S. Tenreiro, et al. (2011). "Visualization of cell-to-cell transmission of mutant huntingtin oligomers." PLoS Curr **3**: RRN1210.
Hinault, M. P., A. F. Cuendet, et al. (2010). "Stable alpha-synuclein oligomers strongly inhibit chaperone activity of the Hsp70 system by weak interactions with J-domain co-chaperones." J Biol Chem **285**(49): 38173-82.
Hirsch, E. C., J. P. Brandel, et al. (1991). "Iron and aluminum increase in the substantia nigra of patients with Parkinson's disease: an X-ray microanalysis." J Neurochem **56**(2): 446-51.
Hohfeld, J., Y. Minami, et al. (1995). "Hip, a novel cochaperone involved in the eukaryotic Hsc70/Hsp40 reaction cycle." Cell **83**(4): 589-98.
Holstein, S. E., H. Ungewickell, et al. (1996). "Mechanism of clathrin basket dissociation: separate functions of protein domains of the DnaJ homologue auxilin." J Cell Biol **135**(4): 925-37.

Huang, C., H. Cheng, et al. (2006). "Heat shock protein 70 inhibits alpha-synuclein fibril formation via interactions with diverse intermediates." J Mol Biol **364**(3): 323-36.
Ii, K., H. Ito, et al. (1997). "Immunocytochemical co-localization of the proteasome in ubiquitinated structures in neurodegenerative diseases and the elderly." J Neuropathol Exp Neurol **56**(2): 125-31.
Ingolia, T. D. and E. A. Craig (1982). "Four small Drosophila heat shock proteins are related to each other and to mammalian alpha-crystallin." Proc Natl Acad Sci U S A **79**(7): 2360-4.
Iwai, A., E. Masliah, et al. (1995). "The precursor protein of non-A beta component of Alzheimer's disease amyloid is a presynaptic protein of the central nervous system." Neuron **14**(2): 467-75.
Jakes, R., M. G. Spillantini, et al. (1994). "Identification of two distinct synucleins from human brain." FEBS Lett **345**(1): 27-32.
Jakob, A. (1921). "Über eigenartige erkrankungen des zentralnervensystems mit bemerkenswertem anatomischem befunde. (Spastische pseudosklerose-encephalomyelopathie mit disseminierten degenerationsherden)." Z. ges. Neurol. Psychiatr. **64**: 147-228.
Jao, C. C., A. Der-Sarkissian, et al. (2004). "Structure of membrane-bound alpha-synuclein studied by site-directed spin labeling." Proc Natl Acad Sci U S A **101**(22): 8331-6.
Jao, C. C., B. G. Hegde, et al. (2008). "Structure of membrane-bound alpha-synuclein from site-directed spin labeling and computational refinement." Proc Natl Acad Sci U S A **105**(50): 19666-71.
Jo, E., J. McLaurin, et al. (2000). "alpha-Synuclein membrane interactions and lipid specificity." J Biol Chem **275**(44): 34328-34.
Kabani, M. and C. N. Martineau (2008). "Multiple hsp70 isoforms in the eukaryotic cytosol: mere redundancy or functional specificity?" Curr Genomics **9**(5): 338-248.
Kaganovich, D., R. Kopito, et al. (2008). "Misfolded proteins partition between two distinct quality control compartments." Nature **454**(7208): 1088-95.
Kampinga, H. H. and E. A. Craig (2010). "The HSP70 chaperone machinery: J proteins as drivers of functional specificity." Nat Rev Mol Cell Biol **11**(8): 579-92.
Kampinga, H. H., J. Hageman, et al. (2009). "Guidelines for the nomenclature of the human heat shock proteins." Cell Stress Chaperones **14**(1): 105-11.
Kastritis, P. L. and A. M. Bonvin (2010). "Are scoring functions in protein-protein docking ready to predict interactomes? Clues from a novel binding affinity benchmark." J Proteome Res **9**(5): 2216-25.
Kitada, T., S. Asakawa, et al. (1998). "Mutations in the parkin gene cause autosomal recessive juvenile parkinsonism." Nature **392**(6676): 605-8.
Klucken, J., Y. Shin, et al. (2004). "Hsp70 Reduces alpha-Synuclein Aggregation and Toxicity." J Biol Chem **279**(24): 25497-502.
Kopito, R. R. (2000). "Aggresomes, inclusion bodies and protein aggregation." Trends Cell Biol **10**(12): 524-30.
Kordower, J. H., T. B. Freeman, et al. (1995). "Neuropathological evidence of graft survival and striatal reinnervation after the transplantation of fetal mesencephalic tissue in a patient with Parkinson's disease." N Engl J Med **332**(17): 1118-24.
Krammer, C., H. M. Schatzl, et al. (2009). "Prion-like propagation of cytosolic protein aggregates: insights from cell culture models." Prion **3**(4): 206-12.
Krzewska, J. and R. Melki (2006). "Molecular chaperones and the assembly of the prion Sup35p, an in vitro study." EMBO J **25**(4): 822-33.
Kuzuhara, S., H. Mori, et al. (1988). "Lewy bodies are ubiquitinated. A light and electron microscopic immunocytochemical study." Acta Neuropathol **75**(4): 345-53.
Lang, A. E., S. Gill, et al. (2006). "Randomized controlled trial of intraputamenal glial cell line-derived neurotrophic factor infusion in Parkinson disease." Ann Neurol **59**(3): 459-66.
Lee, D., E. K. Lee, et al. (2001). "Self-oligomerization and protein aggregation of alpha-synuclein in the presence of Coomassie Brilliant Blue." Eur J Biochem **268**(2): 295-301.

Lee, H. J., C. Choi, et al. (2002). "Membrane-bound alpha-synuclein has a high aggregation propensity and the ability to seed the aggregation of the cytosolic form." J Biol Chem **277**(1): 671-8.
Lewy, F. H. (1912). Handbuch der Neurologie. Berlin, Springer.
Li, J., V. N. Uversky, et al. (2001). "Effect of familial Parkinson's disease point mutations A30P and A53T on the structural properties, aggregation, and fibrillation of human alpha-synuclein." Biochemistry **40**(38): 11604-13.
Lindvall, O. (1994). "Clinical application of neuronal grafts in Parkinson's disease." J Neurol **242**(1 Suppl 1): S54-6.
Lindvall, O., P. Brundin, et al. (1990). "In reply: fetal brain grafts and Parkinson's disease." Science **250**(4986): 1435.
Linstrom, F. D., G. Lieden, et al. (1977). "Dose-related levodopa-induced haemolytic anaemia." Ann Intern Med **86**(3): 298-300.
Liu, J., J. P. Zhang, et al. (2009). "Rab11a and HSP90 regulate recycling of extracellular alpha-synuclein." J Neurosci **29**(5): 1480-5.
Lo Bianco, C., J. Shorter, et al. (2008). "Hsp104 antagonizes alpha-synuclein aggregation and reduces dopaminergic degeneration in a rat model of Parkinson disease." J Clin Invest **118**(9): 3087-97.
Loquet, A., L. Bousset, et al. (2009). "Prion fibrils of Ure2p assembled under physiological conditions contain highly ordered, natively folded modules." J Mol Biol **394**(1): 108-18.
Luk, K. C., I. P. Mills, et al. (2008). "Interactions between Hsp70 and the hydrophobic core of alpha-synuclein inhibit fibril assembly." Biochemistry **47**(47): 12614-25.
Mall, M., M. Bleich, et al. (1998). "The amiloride-inhibitable Na+ conductance is reduced by the cystic fibrosis transmembrane conductance regulator in normal but not in cystic fibrosis airways." J Clin Invest **102**(1): 15-21.
Manning-Bog, A. B., A. L. McCormack, et al. (2002). "The herbicide paraquat causes up-regulation and aggregation of alpha-synuclein in mice: paraquat and alpha-synuclein." J Biol Chem **277**(3): 1641-4.
Marks, W. J., Jr., R. T. Bartus, et al. (2010). "Gene delivery of AAV2-neurturin for Parkinson's disease: a double-blind, randomised, controlled trial." Lancet Neurol **9**(12): 1164-72.
Masison, D. C. and R. B. Wickner (1995). "Prion-inducing domain of yeast Ure2p and protease resistance of Ure2p in prion-containing cells." Science **270**(5233): 93-5.
Matsui, H., B. R. Grubb, et al. (1998). "Evidence for periciliary liquid layer depletion, not abnormal ion composition, in the pathogenesis of cystic fibrosis airways disease." Cell **95**(7): 1005-15.
Maulucci, G., M. Papi, et al. (2011). "The thermal structural transition of alpha-crystallin inhibits the heat induced self-aggregation." PLoS One **6**(5): e18906.
McLean, P. J., H. Kawamata, et al. (2000). "Membrane association and protein conformation of alpha-synuclein in intact neurons. Effect of Parkinson's disease-linked mutations." J Biol Chem **275**(12): 8812-6.
McLean, P. J., H. Kawamata, et al. (2002). "TorsinA and heat shock proteins act as molecular chaperones: suppression of alpha-synuclein aggregation." J Neurochem **83**(4): 846-54.
Mendez, I., R. Sanchez-Pernaute, et al. (2005). "Cell type analysis of functional fetal dopamine cell suspension transplants in the striatum and substantia nigra of patients with Parkinson's disease." Brain **128**(Pt 7): 1498-510.
Mizuno, Y., N. Hattori, et al. (2001). "Familial Parkinson's disease. Alpha-synuclein and parkin." Adv Neurol **86**: 13-21.
Morar, A. S., A. Olteanu, et al. (2001). "Solvent-induced collapse of alpha-synuclein and acid-denatured cytochrome c." Protein Sci **10**(11): 2195-9.
Mougenot, A. L., S. Nicot, et al. (2011). "Prion-like acceleration of a synucleinopathy in a transgenic mouse model." Neurobiol Aging.
Munch, C. and A. Bertolotti (2011). "Self-propagation and transmission of misfolded mutant SOD1: Prion or Prion-like phenomenon?" Cell Cycle **10**(11).

Munch, C., J. O'Brien, et al. (2011). "Prion-like propagation of mutant superoxide dismutase-1 misfolding in neuronal cells." Proc Natl Acad Sci U S A **108**(9): 3548-53.
Nelson, R., M. R. Sawaya, et al. (2005). "Structure of the cross-beta spine of amyloid-like fibrils." Nature **435**(7043): 773-8.
Nikolaidis, N. and M. Nei (2004). "Concerted and nonconcerted evolution of the Hsp70 gene superfamily in two sibling species of nematodes." Mol Biol Evol **21**(3): 498-505.
Nollen, E. A., F. A. Salomons, et al. (2001). "Dynamic changes in the localization of thermally unfolded nuclear proteins associated with chaperone-dependent protection." Proc Natl Acad Sci U S A **98**(21): 12038-43.
Norris, E. H., B. I. Giasson, et al. (2004). "Alpha-synuclein: normal function and role in neurodegenerative diseases." Curr Top Dev Biol **60**: 17-54.
Olanow, C. W. and S. B. Prusiner (2009). "Is Parkinson's disease a prion disorder?" Proc Natl Acad Sci U S A **106**(31): 12571-2.
Opazo, F., A. Krenz, et al. (2008). "Accumulation and clearance of alpha-synuclein aggregates demonstrated by time-lapse imaging." J Neurochem **106**(2): 529-40.
Outeiro, T. F., J. Klucken, et al. (2006). "Small heat shock proteins protect against alpha-synuclein-induced toxicity and aggregation." Biochem Biophys Res Commun **351**(3): 631-8.
Pan-Montojo, F., O. Anichtchik, et al. (2010). "Progression of Parkinson's disease pathology is reproduced by intragastric administration of rotenone in mice." PLoS One **5**(1): e8762.
Pemberton, S., K. Madiona, et al. (2011). "Hsc70 interaction with soluble and fibrillar {alpha}-Synuclein." J Biol Chem.
Pemberton, S., Melki R (2012). "The interaction of Hsc70 protein with fibrillar α-Synuclein and its therapeutic potential in Parkinson's disease " Communicative and Integrative Biology **5**(1).
Peschanski, M., G. Defer, et al. (1994). "Bilateral motor improvement and alteration of L-dopa effect in two patients with Parkinson's disease following intrastriatal transplantation of foetal ventral mesencephalon." Brain **117 (Pt 3)**: 487-99.
Picard, D. (2002). "Heat-shock protein 90, a chaperone for folding and regulation." Cell Mol Life Sci **59**(10): 1640-8.
Piccini, P., D. J. Brooks, et al. (1999). "Dopamine release from nigral transplants visualized in vivo in a Parkinson's patient." Nat Neurosci **2**(12): 1137-40.
Prusiner, S. B. (1982). "Novel proteinaceous infectious particles cause scrapie." Science **216**(4542): 136-44.
Putcha, P., K. M. Danzer, et al. (2010). "Brain-permeable small-molecule inhibitors of Hsp90 prevent alpha-synuclein oligomer formation and rescue alpha-synuclein-induced toxicity." J Pharmacol Exp Ther **332**(3): 849-57.
Quinton, P. M. (2008). "Cystic fibrosis: impaired bicarbonate secretion and mucoviscidosis." Lancet **372**(9636): 415-7.
Ranson, N., T. Stromer, et al. (2006). "Insights into the architecture of the Ure2p yeast protein assemblies from helical twisted fibrils." Protein Sci **15**(11): 2481-7.
Redeker, V., J. Bonnefoy, et al. (2010). "A region within the C-terminal domain of Ure2p is shown to interact with the molecular chaperone Ssa1p by the use of cross-linkers and mass spectrometry." FEBS J **277**(24): 5112-23.
Redeker, V., F. Halgand, et al. (2007). "Hydrogen/deuterium exchange mass spectrometric analysis of conformational changes accompanying the assembly of the yeast prion Ure2p into protein fibrils." J Mol Biol **369**(4): 1113-25.
Rekas, A., C. G. Adda, et al. (2004). "Interaction of the molecular chaperone alphaB-crystallin with alpha-synuclein: effects on amyloid fibril formation and chaperone activity." J Mol Biol **340**(5): 1167-83.
Rekas, A., L. Jankova, et al. (2007). "Monitoring the prevention of amyloid fibril formation by alpha-crystallin. Temperature dependence and the nature of the aggregating species." Febs J **274**(24): 6290-304.

Remy, I. and S. W. Michnick (2006). "A highly sensitive protein-protein interaction assay based on Gaussia luciferase." Nat Methods **3**(12): 977-9.
Ren, P. H., J. E. Lauckner, et al. (2009). "Cytoplasmic penetration and persistent infection of mammalian cells by polyglutamine aggregates." Nat Cell Biol **11**(2): 219-25.
Riederer, P., E. Sofic, et al. (1989). "Transition metals, ferritin, glutathione, and ascorbic acid in parkinsonian brains." J Neurochem **52**(2): 515-20.
Roodveldt, C., C. W. Bertoncini, et al. (2009). "Chaperone proteostasis in Parkinson's disease: stabilization of the Hsp70/alpha-synuclein complex by Hip." EMBO J **28**(23): 3758-70.
Rudiger, S., A. Buchberger, et al. (1997). "Interaction of Hsp70 chaperones with substrates." Nat Struct Biol **4**(5): 342-9.
Rybicki, B. A., C. C. Johnson, et al. (1993). "Parkinson's disease mortality and the industrial use of heavy metals in Michigan." Mov Disord **8**(1): 87-92.
Sarradet, M. (1883). "Un cas de tremblante sur un boeuf." Rev. Med. Vet. **3**: 310-312.
Savistchenko, J., J. Krzewska, et al. (2008). "Molecular chaperones and the assembly of the prion Ure2p in vitro." J Biol Chem **283**(23): 15732-9.
Schreiber, G. and A. R. Fersht (1996). "Rapid, electrostatically assisted association of proteins." Nat Struct Biol **3**(5): 427-31.
Segrest, J. P., M. K. Jones, et al. (1992). "The amphipathic helix in the exchangeable apolipoproteins: a review of secondary structure and function." J Lipid Res **33**(2): 141-66.
Seidler, A., W. Hellenbrand, et al. (1996). "Possible environmental, occupational, and other etiologic factors for Parkinson's disease: a case-control study in Germany." Neurology **46**(5): 1275-84.
Selkoe, D. J. (2003). "Folding proteins in fatal ways." Nature **426**(6968): 900-4.
Sharma, D., C. N. Martineau, et al. (2009). "Function of SSA subfamily of Hsp70 within and across species varies widely in complementing Saccharomyces cerevisiae cell growth and prion propagation." PLoS One **4**(8): e6644.
Shimshek, D. R., M. Mueller, et al. (2010). "The HSP70 molecular chaperone is not beneficial in a mouse model of alpha-synucleinopathy." PLoS One **5**(4): e10014.
Shin, H. J., E. K. Lee, et al. (2000). "Eosin interaction of alpha-synuclein leading to protein self-oligomerization." Biochim Biophys Acta **1481**(1): 139-46.
Shoup, D. and A. Szabo (1982). "Role of diffusion in ligand binding to macromolecules and cell-bound receptors." Biophys J **40**(1): 33-9.
Stutts, M. J., C. M. Canessa, et al. (1995). "CFTR as a cAMP-dependent regulator of sodium channels." Science **269**(5225): 847-50.
Tang, Y. C., H. C. Chang, et al. (2007). "SnapShot: molecular chaperones, Part II." Cell **128**(2): 412.
Tanner, C. M. (2003). "Is the cause of Parkinson's disease environmental or hereditary? Evidence from twin studies." Adv Neurol **91**: 133-42.
Taylor, J. P., J. Hardy, et al. (2002). "Toxic proteins in neurodegenerative disease." Science **296**(5575): 1991-5.
Territo, M. C., R. W. Peters, et al. (1973). "Autoimmune hemolytic anemia due to levodopa therapy." JAMA **226**(11): 1347-8.
Thual, C., A. A. Komar, et al. (1999). "Structural characterization of Saccharomyces cerevisiae prion-like protein Ure2." J Biol Chem **274**(19): 13666-74.
Trexler, A. J. and E. Rhoades (2009). "Alpha-synuclein binds large unilamellar vesicles as an extended helix." Biochemistry **48**(11): 2304-6.
Ubeda-Banon, I., D. Saiz-Sanchez, et al. (2010). "alpha-Synucleinopathy in the human olfactory system in Parkinson's disease: involvement of calcium-binding protein- and substance P-positive cells." Acta Neuropathol **119**(6): 723-35.
Ungewickell, E., H. Ungewickell, et al. (1995). "Role of auxilin in uncoating clathrin-coated vesicles." Nature **378**(6557): 632-5.

Uryu, K., C. Richter-Landsberg, et al. (2006). "Convergence of heat shock protein 90 with ubiquitin in filamentous alpha-synuclein inclusions of alpha-synucleinopathies." Am J Pathol **168**(3): 947-61.
Uversky, V. N. and D. Eliezer (2009). "Biophysics of Parkinson's disease: structure and aggregation of alpha-synuclein." Curr Protein Pept Sci **10**(5): 483-99.
Uversky, V. N., J. Li, et al. (2002). "Synergistic effects of pesticides and metals on the fibrillation of alpha-synuclein: implications for Parkinson's disease." Neurotoxicology **23**(4-5): 527-36.
Uversky, V. N., J. Li, et al. (2001). "Evidence for a partially folded intermediate in alpha-synuclein fibril formation." J Biol Chem **276**(14): 10737-44.
Uversky, V. N., J. Li, et al. (2001). "Metal-triggered structural transformations, aggregation, and fibrillation of human alpha-synuclein. A possible molecular NK between Parkinson's disease and heavy metal exposure." J Biol Chem **276**(47): 44284-96.
Uversky, V. N., J. Li, et al. (2001). "Pesticides directly accelerate the rate of alpha-synuclein fibril formation: a possible factor in Parkinson's disease." FEBS Lett **500**(3): 105-8.
Van Den Eeden, S. K., C. M. Tanner, et al. (2003). "Incidence of Parkinson's disease: variation by age, gender, and race/ethnicity." Am J Epidemiol **157**(11): 1015-22.
Walker, L. C. and H. LeVine (2000). "The cerebral proteopathies: neurodegenerative disorders of protein conformation and assembly." Mol Neurobiol **21**(1-2): 83-95.
Wanamaker, W. M., S. J. Wanamaker, et al. (1976). "Thrombocytopenia associated with long-term levodopa therapy." JAMA **235**(20): 2217-9.
Warrick, J. M., H. Y. Chan, et al. (1999). "Suppression of polyglutamine-mediated neurodegeneration in Drosophila by the molecular chaperone HSP70." Nat Genet **23**(4): 425-8.
Wasmer, C., A. Schutz, et al. (2009). "The molecular organization of the fungal prion HET-s in its amyloid form." J Mol Biol **394**(1): 119-27.
Wells, G. A., A. C. Scott, et al. (1987). "A novel progressive spongiform encephalopathy in cattle." Vet Rec **121**(18): 419-20.
Wenning, G. K., P. Odin, et al. (1997). "Short- and long-term survival and function of unilateral intrastriatal dopaminergic grafts in Parkinson's disease." Ann Neurol **42**(1): 95-107.
Werner-Washburne, M., D. E. Stone, et al. (1987). "Complex interactions among members of an essential subfamily of hsp70 genes in Saccharomyces cerevisiae." Mol Cell Biol **7**(7): 2568-77.
Will, R. G., J. W. Ironside, et al. (1996). "A new variant of Creutzfeldt-Jakob disease in the UK." Lancet **347**(9006): 921-5.
Wine, J. J. and N. S. Joo (2004). "Submucosal glands and airway defense." Proc Am Thorac Soc **1**(1): 47-53.
Wolfe, L. S., M. F. Calabrese, et al. (2010). "Protein-induced photophysical changes to the amyloid indicator dye thioflavin T." Proc Natl Acad Sci U S A **107**(39): 16863-8.
Wolozin, B. and C. Behl (2000). "Mechanisms of neurodegenerative disorders: Part 1: protein aggregates." Arch Neurol **57**(6): 793-6.
Young, J. C., J. M. Barral, et al. (2003). "More than folding: localized functions of cytosolic chaperones." Trends Biochem Sci **28**(10): 541-7.
Zahn, R., A. M. Buckle, et al. (1996). "Chaperone activity and structure of monomeric polypeptide binding domains of GroEL." Proc Natl Acad Sci U S A **93**(26): 15024-9.
Zayed, J., S. Ducic, et al. (1990). "[Environmental factors in the etiology of Parkinson's disease]." Can J Neurol Sci **17**(3): 286-91.
Zhou, Y., G. Gu, et al. (2004). "Analysis of alpha-synuclein-associated proteins by quantitative proteomics." J Biol Chem **279**(37): 39155-64.
Zhu, X., X. Zhao, et al. (1996). "Structural analysis of substrate binding by the molecular chaperone DnaK." Science **272**(5268): 1606-14.
Zourlidou, A., M. D. Payne Smith, et al. (2004). "HSP27 but not HSP70 has a potent protective effect against alpha-synuclein-induced cell death in mammalian neuronal cells." J Neurochem **88**(6): 1439-48.

◆ **Résumé:**

Cette thèse caractérise l'interaction de l'α-synucléine avec deux protéines chaperons : Hsc70 de l'Homme et Ssa1p, son équivalent, chez la levure. La formation et dépôt de fibres d'α-synucléine dans le cerveau humain est à l'origine de la maladie de Parkinson. Nous montrons que les protéines chaperons étudiées inhibent l'assemblage de l'α-synucléine en fibres, ce qui pourrait ouvrir la voie à des applications thérapeutiques.

Mot clés: chaperons moléculaires; co-chaperons; protéine de choc thermique ; maladie de Parkinson ; assemblage des protéines ; repliement des protéines ; α-Synucléine ; fibres ; Hsc70 ; oligomères ; Ssa1p.

◆ ***Summary:***

This thesis characterises the interaction of α-Synuclein with two molecular chaperones: human Hsc70 and the yeast equivalent Ssa1p. The formation and deposition of α-Synuclein fibrils in the human brain is at the origin of Parkinson's disease. We show that the chaperones studied inhibit the assembly of α-Synuclein into fibrils, which could have therapeutic significance.

Key words: *Molecular chaperones; Co-chaperones; Heat shock protein; Parkinson's disease; Protein assembly; Protein folding; α-Synuclein; Fibrils; Hsc70; Oligomers; Ssa1p.*

◆ **Laboratoire de rattachement :**

Laboratoire d'Enzymologie et Biochimie Structurales
CNRS, 1 Avenue de la Terrasse, 91198, Gif-sur-Yvette Cedex, France.

PÔLE : INGÉNIERIE DES PROTÉINES ET CIBLES THÉRAPEUTIQUES

UNIVERSITÉ PARIS-SUD 11
UFR « FACULTÉ DE PHARMACIE DE CHATENAY-MALABRY »
5, rue Jean Baptiste Clément
92296 CHÂTENAY-MALABRY Cedex